UNIVERSIDADE DE LISBOA
FACULDADE DE CIÊNCIAS
DEPARTAMENTO DE QUÍMICA E BIOQUÍMICA

MODULATION OF FATTY ACID SYNTHASE AND PLASMA MEMBRANE MICRODOMAINS BY HYDROGEN PEROXIDE

Ana Isabel Ayres de Mendonça Cardoso Matias

Tese orientada pela
Prof. Doutora Helena Susana Marinho e pelo Prof. Doutor Fernando Antunes

DOUTORAMENTO EM BIOQUÍMICA
(ESPECIALIDADE BIOQUÍMICA)

2011

Contents

Figure Index

Table Index

Acknowledgments

A realização deste trabalho apenas foi possível graças à colaboração das seguintes instituições e pessoas a quem expresso os meus sinceros agradecimentos:

À Fundação para a Ciência e a Tecnologia pelo financiamento da minha bolsa de doutoramento (SFRH/BD/41421/2007) que permitiu a realização deste trabalho.

Ao Centro de Reitoria das Universidades Portuguesas, que através do financiamento concedido pela Acção Integrada Luso-Espanhola E-16/05 permitiu o desenvolvimento de parte do trabalho no Departament de Ciències Mèdiques Bàsiques, Universitat de Lleida.

Ao Instituto de Investigação Científica Bento da Rocha Cabral por ter concedido financiamento extraordinário para realização deste trabalho.

Ao Centro de Química e Bioquímica da Faculdade de Ciências da Universidade de Lisboa, a instituição de acolhimento onde foi realizada a maior parte do trabalho experimental apresentado nesta tese.

Ao Grupo de Bioquímica dos Oxidantes e Antioxidantes que apostou em mim e me acolheu.

Aos meus orientadores, Doutor Fernando Antunes e Doutora Susana Marinho, que foram fundamentais para o desenvolvimento desta tese, guiando-me ao longo do trabalho experimental mas dando-me sempre a liberdade para o meu crescimento enquanto investigadora. À Doutora Luísa Cyrne que, não sendo oficialmente orientadora deste trabalho, me deu todo o seu apoio e aconselhamento ao longo destes anos.

Ao Doutor Enrique Herrero por me ter recebido no seu laboratório, onde tive oportunidade de desenvolver parte do trabalho apresentado nesta tese; ao Doutor Rui Malhó pela preciosa ajuda dada no trabalho de microscopia; ao Doutor Rodrigo Almeida pela orientação dada no campo da biofísica.

Ao Nuno, Vanderlei, Daniela, Sara, André, Francisco, Xana, Juan, Verônica e todos os colegas que passaram pelo laboratório e que sempre ajudaram a que o ambiente de trabalho fosse o melhor. Um agradecimento especial à Virgínia, uma amiga que ganhei e com quem pude partilhar os melhores e os piores momentos do seu e do meu trabalho, celebrando as vitórias e ultrapassando os momentos mais complicados com um sorriso.

A todos os meus amigos que sempre me apoiaram e me ajudaram a finalizar esta etapa da minha vida.

À minha família, em especial aos meus pais, que sempre me apoiaram nas minhas decisões e me transmitiram os valores que hoje são fundamentais na minha vida. Sem eles nunca teria sido possível deenvolver este trabalho.

Ao Antero, o meu porto de abrigo sempre presente, que me ensinou a enfrentar os obstáculos, a rir das adversidades e me deu sempre o seu apoio incondicional.

List of Publications

Published

Ana C. Matias, H. Susana Marinho, Luísa Cyrne, Enrique Herrero, Fernando Antunes. Biphasic modulation of fatty acid synthase by hydrogen peroxide in Saccharomyces cerevisiae. Arch.Biochem.Biophys 515:1-2 (2011) 107-111

Ana C. Matias, Nuno Pedroso, Nuno Teodoro, H. Susana Marinho, Antunes F., Nogueira J.M., Herrero E., Cyrne L. *Fatty acid synthase down-regulation increases the resistance of Saccharomyces cerevisiae cells to H_2O_2*. Free Radical Biology & Medicine 43 (2007) 1458–1465

Nuno Pedroso, Ana C. Matias, Luísa Cyrne, Fernando Antunes, Carlos Borges, Rui Malhó, Rodrigo F.M. de Almeida, Enqrique Herrero, H. Susana Marinho. *Modulation of plasma membrane lipid profile and microdomains by H_2O_2 in Saccharomyces cerevisiae*. Free Radical Biology & Medicine 46 (2009) 289-298

Vanderlei Folmer, Nuno Pedroso, Ana C. Matias, Sílvia C.D.N. Lopes, Fernando Antunes, Luísa Cyrne, H. Susana Marinho. *H_2O_2 induces rapid biophysical and permeability changes in the plasma membrane of Saccharomyces cerevisiae.* Biochimica et Biophysica Acta 1778:4 (2008) 1141-1148

In preparation

Ana C. Matias, Fernando Antunes, Luísa Cyrne, Rui Malhó, Rodrigo F.M. de Almeida, Enrique Herrero, H. Susana Marinho. *Fatty acid synthase expression levels modulate plasma membrane lipid composition and organization in Saccharomyces cerevisiae.*

Resumo

O peróxido de hidrogénio (H_2O_2) é a espécie reactiva de oxigénio mais abundante em organismos aeróbios, uma vez que é produzido intracelularmente de forma contínua. As suas características fisico-químicas, juntamente com a facilidade de difusão através das membranas celulares fazem com que o H_2O_2 seja uma importante molécula sinalizadora em diversos processos celulares. Porém, a regulação precisa dos níveis intracelulares de H_2O_2 é crucial, uma vez que a exposição a diferentes doses de H_2O_2 pode levar a respostas tão diferentes como proliferação celular, senescência, adaptação, apoptose ou necrose.

Em *Saccharomyces cerevisiae*, a exposição a doses baixas de H_2O_2 (150 μM) leva à adaptação das células, tornando-as mais resistentes a uma exposição posterior a uma dose letal deste mesmo agente. Esta adaptação ao H_2O_2 deve-se não só a um aumento da actividade dos principais enzimas que catalisam a redução do H_2O_2 (catalase e citocromo c peroxidase), mas também a uma diminuição da permeabilidade da membrana plasmática ao H_2O_2, impedindo a sua difusão para o interior das células. O mecanismo reponsável por estas alterações permanece ainda desconhecido porém, estudos anteriores mostraram que a adaptação ao H_2O_2 leva a alterações na composição lipídica e organização da membrana plasmática, sendo este muito provavelmente responsável pelas alterações de fluidez e permeabilidade ao H_2O_2 detectadas. Estudos anteriores mostraram que, após uma curta exposição a uma dose adaptativa de H_2O_2, há um aumento dos níveis de esqualeno (intermediário na via de síntese do ergosterol), uma alteração na composição relativa dos principais fosfolípidos e uma reorganização dos microdomínios rígidos da membrana plasmática, enriquecidos em ergosterol e esfingolípidos. Neste estudo observaram-se também alterações nos níveis de expressão de genes envolvidos no metabolismo de lípidos, nomeadamente, de genes envolvidos na via biosintetica do ergosterol (*ERG1*, *ERG3*, *ERG7* and *ERG25*) e do metabolismo de ácidos gordos (os genes *ELO1*, *ELO*2 and *ELO3*, envolvidos na enlongação de ácidos gordos, o gene *OLE1* envolvido na desaturação de ácidos gordos e nos genes *FAS1* e *FAS2* codificantes para as duas sub-unidades do sintase de ácidos gordos). Uma vez que os ácidos gordos são um dos principais componentes das membranas, o sintase de ácidos gordos surgiu como um candidato interessante para o estudo das alterações celulares na adaptação ao H_2O_2.

Neste trabalho fez-se então uma abordagem ao mecanismo de adaptação centrada nas alterações observadas no sintase de ácidos gordos (Fas), pretendendo-se compreender de que modo o H_2O_2 altera a actividade de Fas e de que modo as alterações na actividade

deste enzima alteram, por si, a resistência celular ao H_2O_2 e a composição e organização da membrana plasmática.

Um dos principais resultados obtidos foi o de que a exposição de células de *Saccharomyces cerevisiae* a doses adaptativas de H_2O_2, que leva a uma diminuição da expressão do gene *FAS1,* levando consequentemente a uma diminuição da actividade de Fas. Porém, foi observada uma variação dos efeitos celulares do H_2O_2 num intervalo curto de concentrações de H_2O_2. Este resultado demonstra que é essencial que haja um controlo estrito da concentração de H_2O_2 a que as células estão expostas de modo a ter uma reprodutibilidade de resultados. A exposição em estado estacionário demonstrou ser a mais adequeada a este tipo de estudos, uma vez que permite a exposição prolongada a uma dose constante de H_2O_2, aproximando-se mais das condições fisiológicas. A sobre-expressão de *FAS1* (conseguida através da construção de uma estirpe contendo o gene sob influência de um promotor regulável) levou por si a uma diminuição da capacidade de sobreviver a doses letais de H_2O_2, sendo esta reestabelecida com a diminuição da expressão de *FAS1*.

A importância do gene *FAS1* no mecanismo de adaptação ao H_2O_2 foi reforçada pela observação de que uma estirpe *fas1*Δ, com uma diminuição em aproximadamente 50 % dos níveis de expressão do gene *FAS1* e consequente diminuição da actividade de Fas, apresenta por si uma maior resistência a doses letais de H_2O_2. Os níveis de actividade dos principais enzimas responsáveis pela remoção de H_2O_2 intracelular (catalase e citocromo *c* peroxidase) não aumentaram com a diminuição da expressão de *FAS1* em 50 %. Os níveis de citocromo *c* peroxidase mostraram até ser inferiores na estirpe *fas1*Δ, o que demonstra que a maior resistência celular ao H_2O_2 nestas células não se deve a um aumento da capacidade de eliminação de H_2O_2. Estudos de integridade da parede celular (estrutura que poderia também actuar como barreira de entrada ao H_2O_2) mostraram não existirem alterações a nível da parede que possam justificar a diferente resistência ao H_2O_2. Deste modo a membrana plasmática, que já demonstrou no mecanismo de adaptação ao H_2O_2 ser uma estrutura dinâmica que sofre alterações de modo a limitar a difusão de H_2O_2 para o interior da célula, foi considerada como a principal responsável pela resistência acrescida ao H_2O_2 nas células *fas1*Δ.

Efectivamente, a membrana plasmática da estirpe *fas1*Δ apresentou um aumento da razão PC/PE. Devido às suas características biofísicas, esta alteração leva por si a um aumento da rigidez da membrana plasmática. A membrana plasmática da estirpe *fas1*Δ apresentou também um aumento acentuado dos níveis de ácido lignocérico (C24:0) (40 %) e ácido cerótico (C26:0) (50 %), sugerindo que as alterações na composição da membrana plasmática em ácidos gordos de cadeia muito longa (VLCFA) estão envolvidas neste

processo. Em concordância estão os estudos de fluorescência com ácido trans-parinárico que revelaram que a repressão de Fas leva a um aumento quantitativo e aumento da rigidez dos domínios gel da membrana plasmática. Também os estudos de microscopia com marcação dos princípais microdomínios da membrana plasmática de *S. cerevisiae* (MCC-microdomains occupied by Can1 e MCP – microdomains occupied by Pma1) mostraram que as alterações na actividade de Fas levam a uma reorganização destes domínios lipídicos na membrana plasmática. A diminuição da actividade de Fas não provoca alterações significativas na distribuição dos domínios MCP (ao contrário do acontece na adaptação), observando-se, porém, um pequeno aumento dos níveis de Pma1p na membrana plasmática, embora não tão significativo como o observado no processo de adaptação ao H_2O_2. As maiores alterações foram observadas ao nível dos domínios MCC, que sofreram não só uma reorganização na membrana como um aumento em número na membrana plasmática das células da estirpe *fas1*Δ. As alterações nos MCC poderão estar associadas às restantes alterações observadas na membrana plasmática das células *fas1*Δ, uma vez que estes domínios se encontram normalmente associados aos eisossomas, estruturas organizadoras da membrana plasmática.

Foram também efectuados alguns estudos preliminares em Jurkat mostraram que a exposição a uma dose não letal de H_2O_2 por tempos curtos leva a uma diminuição da fluidez da membrana plasmática acompanhada por uma alteração da sensibilidade à digitonina e por uma reorganização dos microdomínios da membrana plasmática. Não foi porém ainda possível estabelecer uma ligação entre estas alterações e a sintase de ácidos gordos.

Em conclusão, este trabalho revela o papel fundamental de Fas na modulação da permeabilidade da membrana plasmática ao H_2O_2 durante o processo de adaptação e sugere que a repressão de Fas é um dos mecanismos moleculares pelos quais o H_2O_2 estimula a formação de jangadas lipídicas em *S. cerevisiae*. O proteína Fas é aqui apresentada pela primeira vez como um novo candidato na resposta ao *stress* oxidativo em *S. cerevisiae*.

Palavras-chave: Membrana plasmática; adaptação ao H_2O_2; sintase de ácidos gordos; ácidos gordos de cadeia muito longa; jangadas lipídicas

Abstract

Adaptation of *Saccharomyces cerevisiae* cells to hydrogen peroxide (H_2O_2) decreases plasma membrane permeability, slowing H_2O_2 diffusion into cells and turning cells more resistant to H_2O_2. The mechanism responsible for this change remains largely unknown. Here this mechanism was addressed revealing that fatty acid synthase (Fas) plays a key role during the cellular response of *S. cerevisiae* to H_2O_2: Adaptation to H_2O_2 was associated with a decrease in both Fas expression and activity. However, cellular effects of H_2O_2 were shown to vary over a narrow range of concentrations. Therefore, a tight control of H_2O_2 exposure is essential for cellular studies of H_2O_2-dependent redox regulation. The importance of Fas in adaptation was reinforced by the observation that the decrease of Fas activity by 50 % through deletion of one of the *FAS1* alleles increases the resistance to lethal doses of H_2O_2. The plasma membrane of *fas1*Δ cells presented a large increase lignoceric acid (C24:0) (40%) and cerotic acid (C26:0) (50%) levels, suggesting that alterations in the plasma membrane composition of very-long-chain fatty acids (VLCFA) occur with Fas down-regulation. Through interdigitation or by modulating formation of lipid rafts, VLCFA may decrease the overall or localized plasma membrane permeability to H_2O_2, respectively, thus conferring a higher resistance to H_2O_2. In agreement, fluorescence studies with *trans*-parinaric acid showed that both H_2O_2 adaptation and Fas downregulation increase the formation of lipid domains in the plasma membrane. Also, microscopy studies revealed that changes in Fas activity lead to the reorganization of plasma membrane domains. Preliminary studies in Jurkat T cells showed a decrease in plasma membrane fluidity, alteration to digitonin sensitivity and reorganization of membrane microdomains after exposure to a non-lethal H_2O_2 dose for 4 h. However, no relation between these changes and fatty acid synthase activity could be established. In conclusion, these results reveal the key role of Fas in the modulation of plasma membrane permeability to H_2O_2 during adaptation in *S. cerevisiae* and suggest that downregulation of *FAS1* is the molecular mechanism by which H_2O_2 leads to the reorganization of the plasma membrane by remodelling specific membrane microdomains.

Keywords: Plasma membrane**;** H_2O_2 adaptation; Fatty acid synthase; Very-long-chain fatty acids; Fluidity; Lipid rafts

Abbreviation List

acetyl-CoA – Acetyl coenzyme A

acyl-CoA – Acyl coenzyme A

ACP – Acyl carrier protein

APS - Ammonium persulfate

ATP – Adenosine triphosphate

BSA – Bovine serum albumine

C16:0 – Hexadecanoic acid or palmitic acid

C16:1Δ^9 – *cis*-Δ^9–hexadecanoic acid or palmitoleic acid

C17:0 – Heptadecanoic acid or margaric acid

C18:0 – Octadecanoic or stearic acid

C18:1Δ^9 – *cis*-Δ^9–octadecanoic acid or oleic acid

C20:0 – Eicosanoic or arachidic acid

C22:0 – Docosanoic or behenic acid

C24:0 – Tetracosanoic or lignoceric acid

C26:0 – Hexacosanoic or cerotic acid

CCP – Cytochrome *c* peroxidase

CDP-DAG – Cytydine diphosphate-diacylglycerol

$CO_2^{\bullet -}$ - Carbon dioxide

$CO_3^{\bullet -}$ - Carbonate anion

Cys – Cysteine

DCFH- Dichlorofluorescein

DCFH-DA - 2',7'–dichlorofluorescein–diacetate

DMSO - Dimethyl sulfoxide

DNA – Desoxyribonucleic acid

DPH – Diphenylhexatriene

DRM – Detergent resistant membranes

DTPA - Diethylene triamine pentaacetic acid

DTT – Dithiothreitol

EDTA - Ethylenediamine tetraacetic acid

ER – Endoplasmatic reticulum

Fas – Fatty acid synthase; acyl-CoA:malonyl-CoA C-acyltransferase (decarboxylating, oxoacyl- and enoyl-reducing and thioester-hydrolysing) EC 2.3.1.85

FITC - Fluorescein isothiocyanate

GC/MS – Gas chromatography/Mass spectrometry

GPI – Glycophosphatidylinositol

GPx – Glutathione peroxidase

GFP – Green fluorescent protein

GSH – Glutathione

GSSG – Oxidized gluthatione

$HO^{\cdot}$ - Hydroxyl radical

$HO_2^{\cdot}$ - Hydroperoxyl radical

HOBr - Hypobromous acid

HOCl - Hypoclorous acid

H_2O_2 – Hydrogen peroxide

$HOOCO_2^-$ - Peroxomonocarbonate anion

IPC – Inositolphosphoceramide

LB – Liquid broth

LCB – Long-chain base

LCFA – Long-chain fatty acid

MCC – Membrane compartments occupied by Can1

MCP – Membrane compartments occupied by Pma1

MIPC – Mannosyl- inositolphosphoceramide

M(IP)2C – Inositolphosphoryl - mannosyl- inositolphosphoceramide

MOPS – 3-(N-morpholino)propanesulfonic acid

mRNA – Messenger Ribonucleic acid

$NADP^+$ - Nicotinamide adenine dinucleotide phosphate

NADPH – Reduced nicotinamide adenine dinucleotide phosphate

NF-κB – Nuclear factor-κappa B

NOX – NADPH oxidase

O_2 – Molecular oxygen

$O_2^{\cdot -}$ - Superoxide radical

O_3 – Ozone

OD – Optical density

$ONOO^-$ - Peroxynitrite

O_2NOO^- - Peroxynitrate anion

ONOOH - Peroxynitrous acid

$ONOOCO_2^-$ - Nitrosoperoxycarbonate anion

ORF – Open reading frame

PA - Phosphatidic acid

PBS – Phosphate buffer saline

PC – Phosphatidylcholine

PDGF – Platelet-derived growth factor

PE – Phosphatidylethanolamine

PI – Phosphatidylinositol

PMSF - Phenylmethylsulphonyl fluoride

PS – Phosphatidylserine

Prx - Peroxiredoxin

RBS – Reactive bromine species

RCS – Reactive chlorine species

RNA – Ribonucleic acid

RNS – Reactive nitrogen species

$RO^{\cdot}$ - Alkoxyl radical

$RO_2^{\cdot}$ - Peroxyl radical

ROOH - Organic peroxides

ROS – Reactive oxygen species

SC – Synthetic complete medium

Sc - Sacharomyces cerevisiae

S. cerevisiae – Sacharomyces cerevisiae

SDS - Sodium dodecyl sulphate

SOD – Superoxide dismutase

SOOH – Sulfinic acid

SOR – Superoxide reductase

TBARS - Thiobarbituric acid reactive substances

TEMED – Tetramethylethylenediamine

TLC – Thin-layer chromatography

TNF-α – Tumor necrosis factor alpha

t-PnA – *Trans*-parinaric acid

Trx – Thioredoxin

TSCPC - Time-correlated single-photon counting

ura – Uracil

VLCFA – Very-long-chain fatty acid

wt – Wild type

YNB – Yeast nitrogen base

YPD - Yeast peptone D-glucose

1 Introduction

1.1 Hydrogen peroxide and other reactive oxygen species (ROS)

1.1.1 Reactive Oxygen Species

Reactive oxygen species (ROS) are a variety of chemically reactive molecules derived from dioxygen (O_2), one of the main constituents of atmospheric air on earth (approximately 21 %) [1] and essential for the survival of aerobic life forms. Dioxygen appeared in significant amounts over 2.2 billion years ago, mainly due to the evolution of photosynthesis in cyanobacteria [2]. O_2 is essential for the efficient production of energy by the electron transport chain in living organisms. However, it can also damage organisms, due to the oxidation of essential cellular components [3]. The first theory of oxygen toxicity stating the importance of partially reduced forms of oxygen was published in 1954 by Gerschman and her co-workers [4]. Dioxygen in the ground state is in a triplet state, containing two unpaired electrons in the outer shell. Since these two electrons have the same spin, oxygen in this state it is not very reactive. However, if one of the two unpaired electrons is excited (with a consequent spin change), the resulting singlet state dioxygen becomes very reactive.

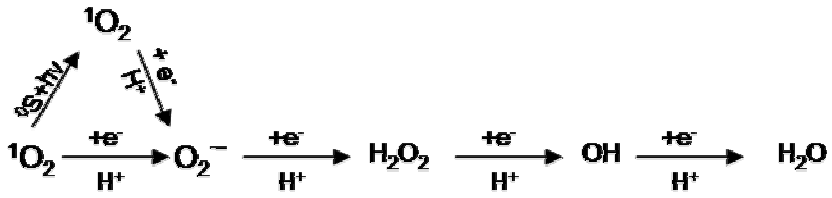

Figure 1. Pathways in the univalent reduction of oxygen to water leading to generation of various intermediate reactive oxygen species (ROS).

Care should be taken when classifying these oxidant molecules, since ROS is a collective term that includes not only oxygen radicals but also some non-radical derivatives of O_2. Hence, all oxygen radicals are ROS, but not all ROS are oxygen radicals [5]. Table1 briefly summarizes the known radical and non-radical ROS species:

Table 1. Nomenclature of reactive oxygen species. Adapted from [5]**.**

Free radicals		Non-radicals	
Name	**Chemical Formula**	**Name**	**Chemical Formula**
Superoxide	$O_2^{\cdot -}$	Hydrogen peroxide	H_2O_2
Hydroxyl	$HO^{\cdot}$	Hypobromous acid	HOBr
Hydroperoxyl	$HO_2^{\cdot}$	Hypoclorous acid	HOCl
Carbonate	$CO_3^{\cdot -}$	Ozone	O_3
Peroxyl	$RO_2^{\cdot}$	Singlet oxygen	$^1O_2$
Alkoxyl	$RO^{\cdot}$	Organic hydroperoxides	ROOH
Carbon dioxide	$CO_2^{\cdot -}$	Peroxynitrite	$ONOO^-$
Nitrogen oxide	$NO^{\cdot}$	Peroxynitrate	O_2NOO^-
Nitrogen dioxide	$NO_2^{\cdot}$	Peroxynitrous acid	ONOOH
Nitrogen trioxide	$NO_3^{\cdot}$	Nitrosoperoxycarbonate	$ONOOCO_2^-$
		Peroxomonocarbonate	$HOOCO_2^-$

The term oxidative stress was defined by Sies in 1985 [6] as *a disturbance in the prooxidant-antioxidant balance in favour of the former, leading to potential damage*. The damage caused to the cell by oxidant species is designed as oxidative damage. Cells and organisms are said to be sustaining oxidative stress when an imbalance between ROS generation and detoxification or repair leads to an increase in the level of ROS-dependent damage.

ROS are generated intracellularly by several pathways as by-products of aerobic metabolism. The major sites of cellular reactive oxygen species generation include the mitochondrial electron transport chain (Mito-ETC), the endoplasmic reticulum (ER) and the NADPH oxidase (NOX) complex, being superoxide ($O_2^{\cdot -}$) the main initial free radical species formed. Although several oxidases can generate H_2O_2 (e.g. xanthine oxidase, urate oxidase, coproporphyrinogen III oxidase, glucose oxidase, lysyl oxidase, monoamine oxidase and D-aminoacid oxidases) [5], it is mainly produced by the dismutation of $O_2^{\cdot -}$ catalyzed by the superoxide dismutases (SODs). This dismutation can occur in mitochondria, peroxisomes, cytosol and plasma membrane, as well as extracellularly [7].

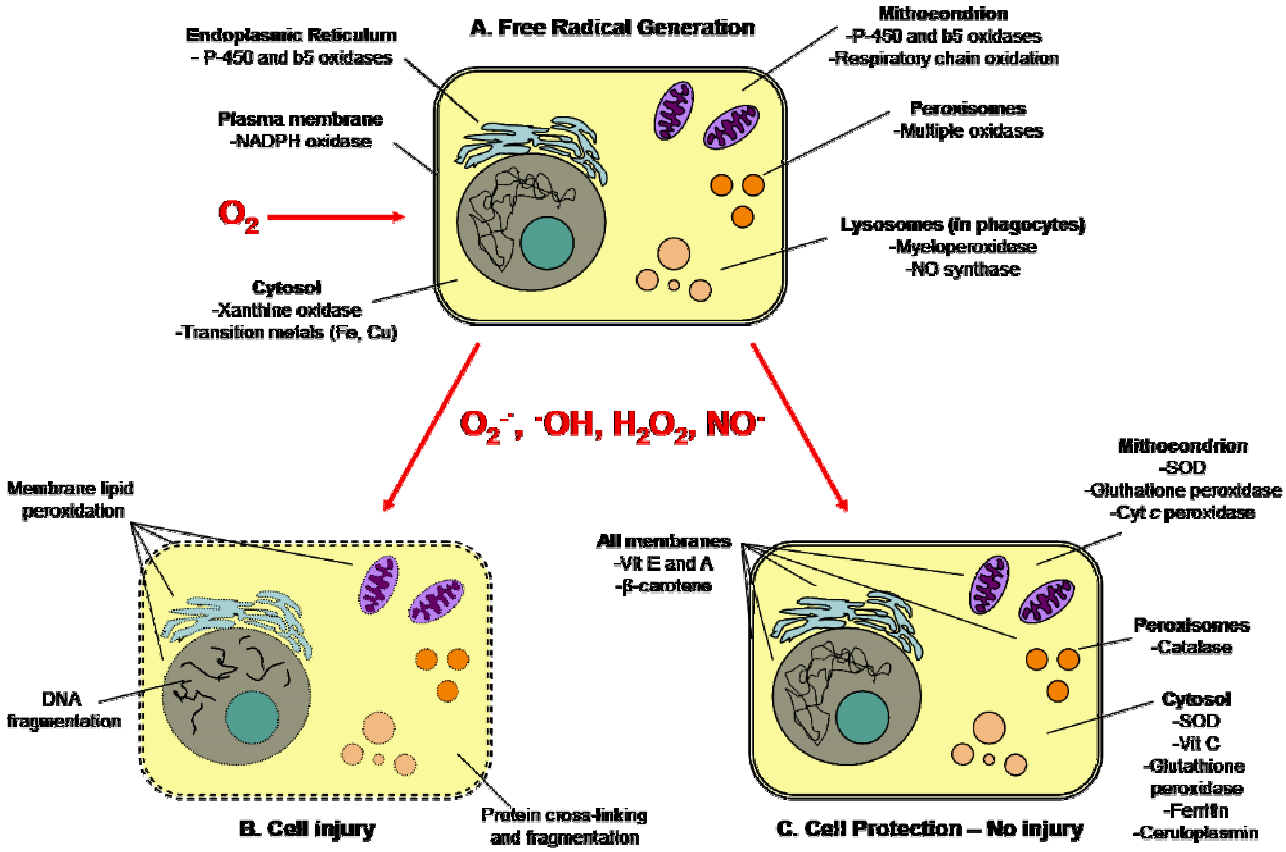

Figure 2. Intracellular formation and scavenging of reactive oxygen species. The maintenance of the balance between ROS generation (A) and elimination (C) is crucial to in order to avoid oxidative damage of cell components (B).Figure adapted from [8].

The mitochondrial electron transport chain has been described as one of the major cellular generators of ROS [7, 9] since, as electron flow down the respiratory chain, there is some electron leakage forming intermediate radicals (like the ubisemiquinone radical) that, eventually, upon reaction with O_2 form $O_2^{\cdot-}$ [10, 11]. Microsomal metabolism and the respiratory burst produced by phagocytes also lead to the production of $O_2^{\cdot-}$, which, although not strongly reactive, is able to directly induce oxidative damage in some proteins [12]. In the presence of transition metal ions (such as Fe^{2+}), H_2O_2 can be converted to hydroxyl radical ($HO^{\cdot}$), which is highly reactive and can cause damage to lipids, proteins and DNA. Nitric oxide (NO) is a reactive radical produced from arginine by nitric oxide synthase (NOS). Nitric oxide can react with superoxide to form peroxynitrite ($ONOO^-$), a non-radical species that is capable of modifying the structure and function of proteins [13]. Figure 2 illustrates the main ROS production sites and scavenging enzymes that, together with other redox systems, guarantee the maintenance of the cellular redox homeostasis.

A big interest in ROS has developed since it has been established that mitochondrial ROS production can be involved in ageing and age-related diseases. The mitochondrial free radical theory of aging (MFRTA) proposes that aging is caused by the toxicity of ROS through a vicious cycle in which ROS damage to the constituents of mitochondria leads to the generation of more ROS. This theory integrates numerous observations about the generation, toxicity and detoxification of ROS, as well as about how these parameters change with the physiological state of cells and organisms and with chronological age [14]. Moreover, ROS have been related with cancer, not only because it was observed that exposure to oxidants favours cancer initial development, but also due to observations suggesting that cancer cells, contrary to normal cells, are under increased oxidative stress associated with oncogenic transformation, and show alterations in metabolic activity and increased generation of reactive oxygen species. One of the major findings related to the involvement of ROS in cancer is that over-expression of NOX1 in NIH-3T3 cells or prostate cancer cell lines increases $O_2^{\bullet -}$ formation, which is followed by an increase in cell proliferation and the development of some features of malignancy [15]. Although many questions still need to be clarified in order to reach a real application, research on the oxidative stress and regulation mechanisms of the cellular redox state rose as one of the areas to explore in order to discover new potential therapeutic solutions.

1.1.2 Mechanisms of cellular protection against ROS

The term antioxidant is becoming a common sense word in everyday life, mainly due to the propaganda by the pharmaceutical and food industry, which offers us countless supplements that promise protection against the continuous threat of oxidants. However, the exact scientific definition for an antioxidant is not always easy. Halliwell and Gutteridge proposed a simplified definition of an antioxidant as any *substance that delays, prevents or removes oxidative damage to a target molecule, when present at lower concentrations than that target* [5].

Antioxidant systems are essential to the normal functioning of the cell in aerobic organisms since, as already referred, ROS are inevitable in aerobic living organisms, since they are continuously produced during normal cellular metabolism and energy production. The maintenance of a redox homeostasis and control of ROS toxicity is therefore guaranteed by the balance between the production of oxidant molecules and its elimination by antioxidant systems. This elimination is achieved by a complex network of non-enzymatic antioxidants, which include non-thiol compounds, essentially vitamins (ascorbate, tocopherol) and polyphenols; sulfhydryl-containing compounds, such as glutathione (GSH) and thioredoxin

(Trx); and enzymes, such as superoxide dismutases (SOD), catalase, cytochrome c peroxidase (CCP), glutathione peroxidases (GPx), and peroxiredoxins (Prx) [16]. Table 2 briefly summarizes the main enzymatic antioxidant cell defences.

Table 2. Main antioxidant enzymes found in eukaryotic and prokaryotic cells. [a] electron donor. Table constructed from information synthesised from [5].

	Localization	**Catalysed Reaction**
Cupper-zinc SOD (CuZnSOD)	Mostly in cytosol but also in lysosomes, nucleus, mythocondria, peroxisomes and periplasmic space of bacteria	$O_2^{\cdot -} + O_2^{\cdot -} + 2H^+ \rightarrow H_2O_2 + O_2$
Manganese SOD (MnSOD)	Mainly in mithocondria but rare cases in cytosol	$O_2^{\cdot -} + O_2^{\cdot -} + 2H^+ \rightarrow H_2O_2 + O_2$
Iron SOD (FeSOD)	Cytosol and chloroplasts	$O_2^{\cdot -} + O_2^{\cdot -} + 2H^+ \rightarrow H_2O_2 + O_2$
Nickel SOD (NiSOD)	Some cyanobacteria and *Streptomyces* cytosol	$O_2^{\cdot -} + O_2^{\cdot -} + 2H^+ \rightarrow H_2O_2 + O_2$
Extracellular SOD	Extracellular fluids (eukaryotic tissues)	$O_2^{\cdot -} + O_2^{\cdot -} + 2H^+ \rightarrow H_2O_2 + O_2$
Superoxide reductase (SOR)	Cytosol of anaerobic bacteria	$O_2^{\cdot -} + 2H^+ + X^a \rightarrow H_2O_2 + X\ (ox)$
Catalase	Mainly in peroxisomes. In the cytosol of yeast.	$2H_2O_2 \rightarrow 2H_2O + O_2$
Glutathione peroxidase (GPx)	Cytosol, plasma and extracellular fluids of mammals. Less common in plants and bacteria.	$H_2O_2 + 2GSH \rightarrow GSSG + 2H_2O$
Cytochrome *c* peroxidase (CCP)	Cytosol and *S.cerevisiae* mitochondria inner membrane space	$CCP + H_2O_2 + 2$ ferrocytochrome $c + 2H^+ \rightarrow CCP + 2H_2O + 2$ ferricytochrome c
Thioredoxins (Trx)	Cytosol	$ProteinS_2 + Trx(SH)_2 \rightarrow Protein(SH)_2 + TrxS_2$
Thioredoxin reductase (TrxRs)	Cytosol	$TrxS_2 + NADPH + H^+\ Trx(SH)_2 + NADP^+$
Peroxiredoxins (Prx)	Cytosol and mitochondria	$H_2O_2 + Prx(SH)_2 \rightarrow 2H_2O + PrxS_2$

Some of the enzymes included in Table 2 (especially the ones involved in H_2O_2 metabolism) will be further explored in this introduction. As mentioned above, additionally to enzymatic antioxidant defences, there are also some non-enzymatic molecules that protect the cell against ROS, with glutathione (GSH) as the most important of them. In addition of being a GPx cosubstrate, GSH is by itself an antioxidant, being able to react *in vivo* with $HO^{\cdot}$, HOCl, $ONOO^-$, $RO^{\cdot}$, $RO_2^{\cdot}$, $CO_3^{\cdot -}$, $NO_2^{\cdot}$, carbon-centered radicals and $^1O_2$ [5]. Glutathione (GSH) is so central to detoxification that the ratio of GSH to GSSG (oxidized glutathione) is commonly used as a good indicator of the redox status of the cell. The concentration of GSH in the cytoplasm lies within the 1–10 mM range, with over 99% existing as the reduced GSH form. *S. cerevisiae* mutant cells that lack glutathione were shown to be hypersensitive to H_2O_2 [17].

1.1.3 H_2O_2 metabolism and signalling

Hydrogen peroxide (H_2O_2) is the most abundant ROS in aerobic organisms, since it is continuously produced intracellularly, presenting a steady-state concentration of 10^{-7} to 10^{-9} M inside cells [7]. H_2O_2 has a distinctive set of features compared to other ROS: I) it has no charge; II) it is not a radical; III) it possesses an intermediate oxidation number; IV) it is relatively stable under physiological conditions [18]. Table 3 resumes some of the features of H_2O_2, superoxide (the two most abundant ROS present intracellularly) and hydroxyl radical (the most reactive).

Table 3. Biological features of the main ROS formed intracellularly.

	Physiological concentration (M) [19]	**Half-life time (s) [19, 20]**	**Diffusion distance (μm) [20, 21]**
H_2O_2	10^{-7}	10^{-3} - 10^{-5}	6.3
$O_2^{\cdot}$	10^{-10}	10^{-5} - 10^{-6}	0.4
$HO^{\cdot}$	10^{-15}	10^{-9} – 10^{-10}	1.7 x 10^{-3}

The NADPH oxidases (Nox) are a family of ROS-generating enzymes. Nox4 is one of the isoforms present in the ER membrane that produce primarily H_2O_2 and is involved in cell signalling [22]. Many evidences suggest that various growth factors and cytokines (e.g. insulin, agiotensin and TNF-α) generate hydrogen peroxide in target cells by stimulating the activation of NADPH oxidases [23, 24]. The β-oxidation of fatty acids is the most important

metabolic process contributing to the formation of H_2O_2 in the peroxisome [25], with FAD as a co-factor, since the high-potential electrons formed by FAD oxidation are transferred to O_2, yielding H_2O_2 [25]. SODs produce H_2O_2 from dismutation of superoxide and are essential for cell protection. Their physiological relevance has been illustrated by several experiments in SOD knock-out mice. When *SOD2* was not expressed, the mice died several days after birth since they could not protect themselves against oxidative injury [26]. The lack of *SOD1* originated the development of several pathologies, among them hepatocellular carcinoma [27], acceleration of age-related muscle mass loss [28], earlier incidence of cataracts and a reduced lifespan.

The major antioxidant enzymes involved in the removal and maintenance of the H_2O_2 steady-state in mammalian cells are peroxidases, mainly catalase and GSH peroxidases and also peroxiredoxins [29]. In yeast cells, a cytochrome *c* peroxidase (CCP) is also present, which together with cytosolic catalase are the main enzymes responsible for H_2O_2 removal. The cytochrome *c* peroxidase, GSH peroxidases and peroxiredoxins pathways of H_2O_2 elimination are illustrated in Figure 3.

Catalase was the first H_2O_2-removing enzyme to be discovered and it is present in all types of cells in the peroxisomes, where H_2O_2 levels are high. However, it can also be found in the cytosol (*S. cerevisiae* cells express both a peroxisomal catalase (encoded by the *CTA1* gene) [30] and a cytosolic catalase (encoded by the *CTT1* gene) [31]) and in the mitochondrial matrix (in *S. cerevisiae* cells [32] and in rat heart [33]). Catalases catalyse the dismutation of H_2O_2 to O_2 and H_2O and the deletion of the gene expressing this enzyme (usually designed as acatalasemia) leads to cells which are both more sensitive to H_2O_2 or H_2O_2-generating toxins, and to phagocytic killing. The acatalasemia state frequently does not lead to clinical symptoms, although it has been suggested as a being a risk factor for the development of diabetes [34], higher susceptibility to ischemia-reperfusion injury and to cancer development [35]. In yeast, catalase is not essential to cell survival in the exponential phase of growth (possibly due to the existence of other H_2O_2-removing systems), but deletion of both genes encoding for cytosolic and peroxisomal catalase is crucial for yeast cells growing in the stationary-phase and also for yeast cells during adaptation to H_2O_2 (in which catalase is over-expressed) [36].

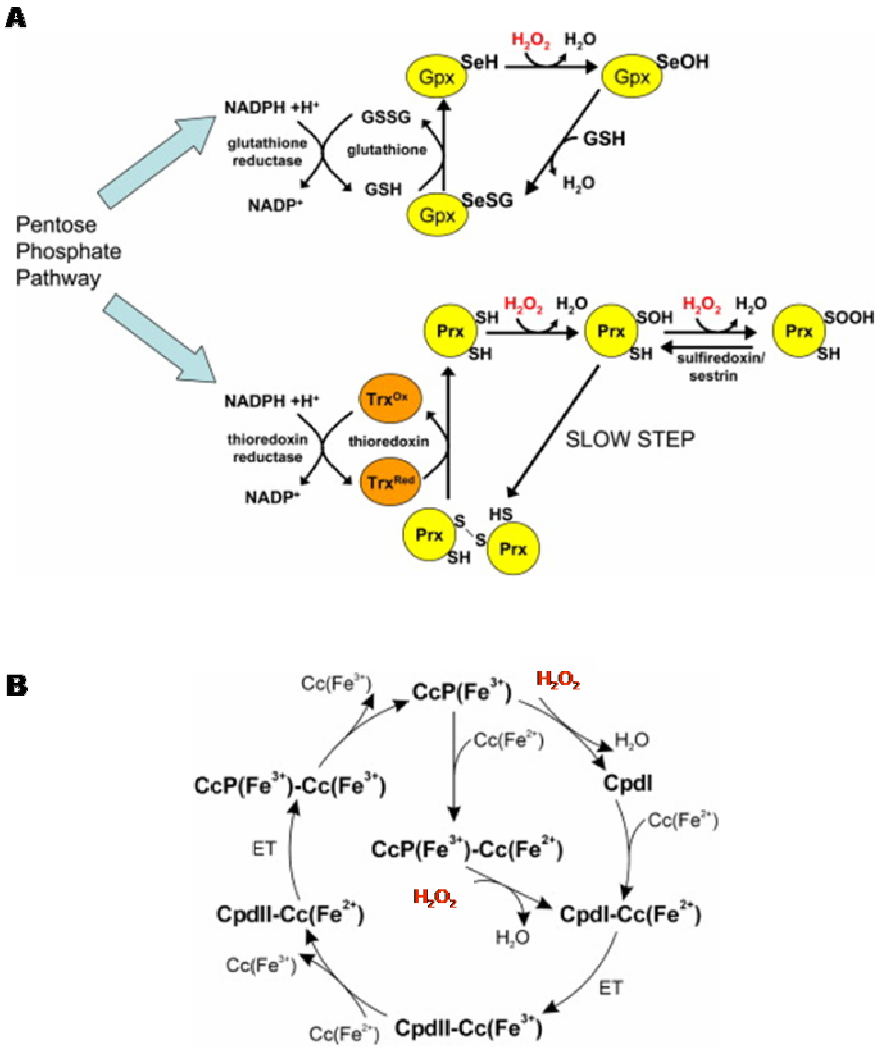

Figure 3. The redox-cycling reactions involved in the catalytic removal of H_2O_2 by glutathione peroxidases and peroxiredoxins (A) and cytochrome *c* peroxidase (B). Cytochrome *c* peroxidase, together with catalase, are the two major H_2O_2 removing enzymes in yeast. Since yeast cells do not contain she, the specific activity of GPx is much lower than the one observed in mammalian cells. GPx, glutathione peroxidase; Trx^{Ox}, oxidized thioredoxin peroxidase; Trx^{Red}, reduced thioredoxin peroxidase; Prx, peroxiredoxin; SeH, selenocysteine (not present in yeast); SH, cysteine; GSH, reduced glutathione; GSSG, oxidized glutathione; SOH, sulfenic acid; SOOH, sulfinic acid; ET, electron transfer. Figure adapted from [24] and [37].

Another major group of H_2O_2-removing enzymes are the GSH peroxidases, the most important in higher eukaryotic cells, and peroxiredoxins. In *S. cerevisiae*, the major role played by GSH peroxidases in H_2O_2 removal is replaced by CCP. Although CCP it is not essential for cell survival, it is up-regulated, together with catalase, in cells exposed to H_2O_2 [38]. The catalytic reduction of hydrogen peroxide by GPxs and Prxs involves the oxidation of catalytic selenyl groups on the selenocysteine (SeH) residues in GSH peroxidases and sulphydryl groups (SH) in cysteine residues of peroxiredoxins (in yeast the GPx activity is much lower than in mammalian cells since yeast GPxs does not contain selenocysteine

residues [39]). The recycling of oxidized peroxidase enzymes involves oxidation of reduced glutathione (GSH) or thioredoxin (TRx) and the reduction by NADPH of oxidized glutathione and oxidized thioredoxin catalysed by glutathione reductase or thioredoxin reductase, respectively. The pentose phosphate pathway provides the NADPH needed for the reduction, and hence the cellular antioxidant capacity is also linked to cellular metabolism [24]. There are also membrane-associated GPxs (phospholipid hydroperoxide GPxs, PHGPxs), considered one of the main lipid peroxidation repairing enzymes [5].

The peroxiredoxin class 2-Cys Prx contains two highly-conserved cysteine residues that are involved in the thioredoxin-coupled catalytic reduction of H_2O_2. In the first step the cysteine residue is oxidized to sulfenic acid (SOH), and then a disulfide bond is formed with a cysteine residue on the partner protein thus preventing further oxidation. However, disulfide bond formation in eukaryotic cells is slow and, as a result, the SOH form of the peroxidatic cysteine residue is sensitive to further oxidation to a sulfinic acid (SOOH) derivative which can be reduced by either sulfiredoxin or sestrin enzymes [24]. As the studies on peroxiredoxins extend, the knowledge about the involvement of these H_2O_2-removing enzymes in redox signalling cascades has increased. It has been observed that cells stimulated either with PDGF or TNF-α and over-expressing Prx have a lower increase of intracellular H_2O_2 levels [40]. Also, over-expression of Prx leads to an inhibition of NF-κB activation by TNF-α [41] and blocks induction of apoptosis by ceramide [42]. In yeast, peroxiredoxins participate in the most important yeast H_2O_2-regulated pathways: the *S. cerevisiae* Yap1p and *Schizosaccharomyces pombe* Pap1p and Sty1p pathways [43]. *S.cerevisae* cells respond to oxidative stress by altering their transcriptional program in a complex way. At the transcriptional level, two factors are mainly involved Yap1p and Skn7p, which participate cooperatively in the peroxide response [44]. Yap1p functions as a redox sensor as it is rapidly activated after exposure to H_2O_2 [45] by oxidation of two Cys residues and the formation of an intermolecular disulfide bond, which changes the conformation of Trx2 and leads to its activation [46].

The tight regulation of H_2O_2 levels in the cells is crucial, since, the interaction with transition metal ions (Fe^{2+} ou Cu^{+}) by the Fenton reaction can lead to the formation of the hydroxyl radical ($HO^{\cdot}$), which reacts with most metabolites and macromolecules. Moreover, the cell response to H_2O_2 is highly dependent of the dose to which they are exposed to. The consequences of oxidative stress are highly variable, depending on the dose of ROS to which cells are exposed to, the type of cells exposed and the conditions of growth. Therefore, exposure to ROS has been described as causing different cell responses like cell proliferation, adaptation, cell injury, senescence or cell death by apoptosis or necrosis [5].

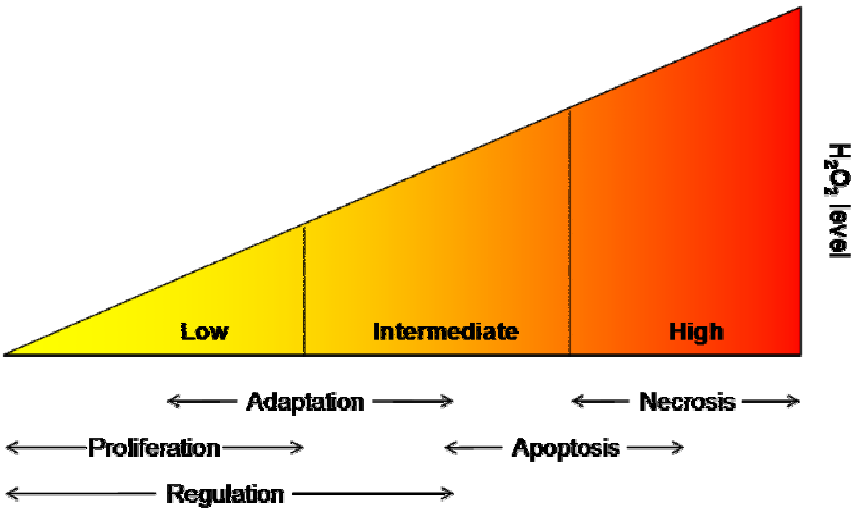

Figure 4. The cellular effects of H_2O_2 are highly dependent on its intracellular concentration. Low levels of H_2O_2 can induce proliferation of cell and adaptation to H_2O_2, turning cells more resistant to lethal doses of this agent. Low levels of H_2O_2 can also have regulatory effects in cells. High levels of H_2O_2 can induce cell death by apoptosis or even necrosis. The H_2O_2 concentration considered as a "low" or "high" is highly variable depending on the cells in question and other external and internal factors, such as cell density, carbon source and the presence of other stress inducing factors. Figure adapted from [47].

H_2O_2 seems to be the most important ROS acting a signalling molecule. Furthermore, in recent years H_2O_2 has become established as an important regulator of eukaryotic signal transduction, being generated in response to various stimuli, including cytokines and growth factors. It has also been established that H_2O_2 is involved in regulating biological processes as diverse as the immune cell activation and vascular remodelling in mammals and stomatal closure and root growth in plants [24]. In addition, since H_2O_2 is relatively stable and can diffuse across membranes (although this diffusion rate-limits its catabolism, since H_2O_2 gradients are formed across biomembranes [48]), it can diffuse out of the mitochondria into the cytoplasm, where it can trigger signalling events [24]. However, its sphere of influence is restricted by its short half-life (in the range of milliseconds). Although H_2O_2 by itself is not very reactive, it can directly react with specific proteins, mainly the ones containing deprotonated SH groups in their cysteine residues. The specificity of this signalling is very important and it is achieved due to the fact that not many proteins possess a cysteine residue that is vulnerable to oxidation by H_2O_2 in cells [49]. Tyrosine phosphatases, highly conserved molecules that play a central role in signal transduction from cell surface receptors to the nucleus [50] are one example of proteins that can be directly oxidized by H_2O_2. Also, H_2O_2 down-regulates several transcription factors like p53, Jun and Fos [51]. Recent work showed that H_2O_2, in moderate and steady-state doses, has a synergistic effect on the TNF-α-dependent p65 subunit of NF-κB translocation to the nucleus, thereby up-

regulating several NF-κB-dependent genes [52]. In yeast, the Yap1 transcription factor is an essential regulator of the H_2O_2 adaptive response [53]. In response to H_2O_2, Yap1 is activated by oxidation and deactivated by enzymatic reduction with Yap1-controlled thioredoxins, thus providing a mechanism for autoregulation [46].

Cell adaptation is a process by which cells react to non-lethal levels of an agent, up-regulating the adequate protection systems and becoming more resistant to subsequent exposure to lethal levels of this agent. Exposure to low to mild concentrations of oxidative agents can lead to adaptation, where cells up regulate their protection systems in order to protect cells against oxidative damage. Adaptation to oxidative stress is a complex phenomenon, involving several pathways, including induction of antioxidant and heat-shock enzymes [54], repair mechanisms [55] and proteasomal and lysosomal activation [56]. Recent studies showed that, in *S.cerevisiae* cells, the plasma membrane also plays a crucial role in the adaptation to H_2O_2 [57], acting has a barrier for the entrance of H_2O_2 into the cell. More detail of the changes in plasma membrane composition and organization occurring during adaptation to H_2O_2 will be addressed in section 1.3 of this introduction.

1.1.4 The steady-state delivery of H_2O_2

Most studies on regulation by H_2O_2 use an exogenous bolus addition of this agent. This is made by a unique addition of H_2O_2 to the growth medium. Since H_2O_2 will be rapidly consumed by growing cells due to the presence of H_2O_2-removing enzymes, when using a bolus addition of H_2O_2, it is necessary to add a high initial H_2O_2 concentration in order to see some effect in cells [58]. Since in the bolus addition it is very difficult to control the concentration of H_2O_2 to which cells are exposed along the time of the experience, it is harder to interpret the observed results. Also, the need for a high initial H_2O_2 concentration means that, frequently, lethal H_2O_2 doses are used for regulation and adaptation studies [17, 59-61]. Usually, a bolus addition constitutes a shock to the cell, possibly leading to a deregulation of cellular homeostasis, accompanied by irreversible structural alterations [58]. An alternative method of H_2O_2 delivery to cells is the steady-state approach. This method allows the maintenance of a constant concentration of H_2O_2 along time, since glucose oxidase is added to the cell medium in order to compensate for the cellular consumption of H_2O_2. More specifically, H_2O_2 is added initially to the cell medium (at the desired concentration for the undergoing study) together with an amount of glucose oxidase that produces an amount of H_2O_2 that matches the H_2O_2 cellular consumption observed under the specific conditions of the experiment. This approach is much closer to what occurs *in vivo*, where H_2O_2 homeostasis is maintained by regulation of H_2O_2-producing and H_2O_2–

scavenging systems. It also enables the use of much lower H_2O_2 concentrations, allowing a more accurate titration of biological responses to physiological concentrations of this oxidizing agent and avoiding misinterpretation of results.

1.2 The Plasma membrane

The plasma membrane is the main protective barrier of the cell since it separates the intracellular from the extracellular environment and mediates the transport of solutes and other molecules between the cell and the exterior. Moreover, it plays a very important role in stress sensing [62]. In 1972, Singer and Nicolson proposed the fluid mosaic model, in which the plasma membrane was described as a lipid bilayer interspersed with proteins (Figure 5), behaving like a fluid because of its hydrophobic integral components such as lipids and membrane proteins that move laterally or sideways throughout the membrane [63].

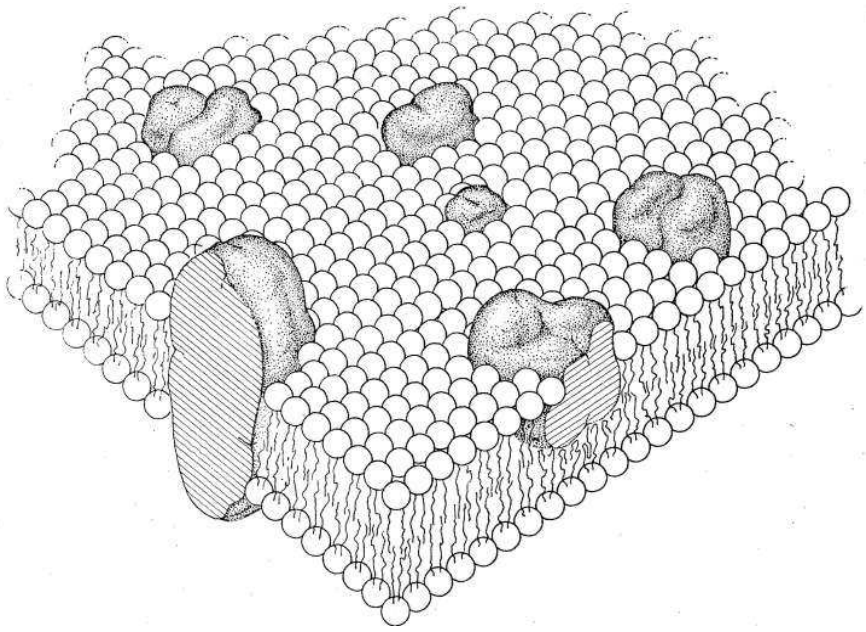

Figure 5. The fluid mosaic model of membranes. Original picture from Singer and Nicholson (1972) showing a membrane cross section with integral proteins in the phospholipid bilayer mosaic [63].

The understanding of the plasma membrane has developed enormously since 1972, and further details in the way lipids and proteins organize have been discovered. The main evolution comprise the description of a high heterogeneity of the membrane due to its

organization in microdomains enriched in particular proteins and/or lipids that act as important structures for cell protection, metabolism, signalling and transport.

1.2.1 Plasma membrane composition

1.2.1.1 Phospholipids

Phospholipids are the main components of the plasma membrane. All membranes (indeed even each leaflet of the bilayer) in a tissue can have a distinctive phospholipid composition that is in some way related to their function. Phospholipids are usually divided in two classes, depending on their composition: I) glycerophospholipids for glycerol-containing phospholipids and II) sphingolipids.

The glycerophospholipid structure is based on a glycerol-3-phosphate backbone in which fatty acyl groups are esterified to positions 1 and 2. The fatty acid composition of each phospholipid is also highly variable between cell type and organisms. Considering this heterogeneity in the major categories of phospholipids with respect to acyl chain diversity and that mammalian cells have a big complexity of fatty acids, mammalian cells are considered to have a huge diversity of phospholipids [64]. The same is true for all the other lipid categories, and mammalian cells are estimated to have a thousand or more lipid species [65]. Yeast contains a much lower diversity of lipids, being widely used as a model in lipidomic studies.

The main phospholipids in the yeast plasma membrane are phosphatidylcoline (PC), phosphatidyletanolamine (PE), phosphatidylserine (PS), phosphatidylinositol (PI) and phosphatidic acid (PA) [66]. Figure 6 gives a schematic view of phospholipid synthesis pathways in yeast. These pathways are generally common to those found in higher eukaryotic organisms. The fatty acid composition of the yeast *S. cerevisiae* is also quite simple in comparison to other organisms and consists mainly of palmitic- (C16:0), palmitoleic- (C16:1Δ^9), stearic- (C18:0) and oleic (C16:1Δ^9) acids [67]. Also smaller amounts of arachidic acid (C20:0), behenic acid (C22:0), lignoceric acid (C24:0) and cerotic acid (C26:0) are detected as part of the backbone of glycerophospholipids and sphingolipids [66].

S.cerevisiae cells do not contain polyunsaturated fatty acids, since their only fatty acyl desaturase is the acyl-CoA 9-desaturase [68, 69]. For this reason, the lipids of the plasma membrane of *S.cerevisiae* are almost insensitive to peroxidation [70]. Yeast strains transformed with the acyl-CoA Δ12-desaturase and, therefore, capable of synthesising

polyunsaturated fatty acids, became more sensitive to H_2O_2, probably due to a gain of susceptibility to lipid peroxidation [71]. The membrane composition in phospholipids and the respective associated fatty acids is highly variable upon yeast strain, growth media, temperature, pH and other conditions of growth [72]. The fatty acid biosynthetic pathway will be further addressed in section 1.4 of this introduction.

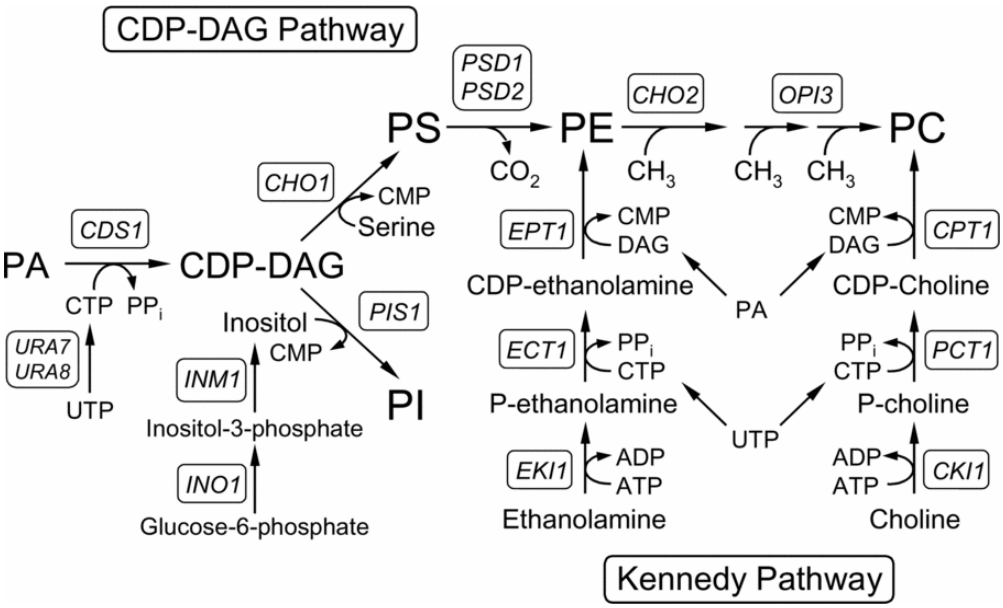

Figure 6. Schematic representation of phospholipid metabolism in *S. cerevisiae*. All major phospholipids are derived from phosphatidic acid (PA), which is partitioned between CDP-diacylglycerol (CDP-DAG) and diacylglycerol (DAG). The major phospholipids are primarily synthesized from PA via CDP-DAG (i.e., CDP-DAG pathway). Phosphatidylinositol (PI) and phosphatidylcholine (PC) can also be synthesised from ethanolamine and choline (obtained from growth medium supplementation or from the phospholipase D-mediated turnover of the PE or PC synthesized via CDP-DAG) via the Kennedy pathway. PA, phosphatidic acid; CDP-DAG, cytidine diphosphate-diacylglycerol; PS, phosphatidylserine; PE, phosphatisylethanolamine; PC, phosphatidylcholine; PI, phosphatidylinositol; PSS, PS synthase; PSD, PS decarboxylase; PEMT, PE methyltransferase; PLMT, phospholipid methyltransferase**;** EK, ethanolamine kinase; ECT, phosphoethanolamine cytidylyltransferase; EPT, ethanolaminephosphotransferase; CK, choline kinase; CCT, phosphocholine cytidylyltransferase; CPT, cholinephosphotransferase**;** IPS, inositol phosphate synthase; IPP, inositol phosphate phosphatase; PIS, PI synthase; DPP, DGPP phosphatase; PAP, PA phosphatase; DGA, DG acyltransferase; CTPS, CTP synthetase. Figure from [77].

As the major components of the plasma membrane, phospholipids influence plasma membrane intrinsic characteristics like permeability, curvature and fluidity. The polar heads of phospholipids induce changes in plasma membrane flexibility and curvature according to their size and shape [73]. The fatty acid tails directly affect the fluidity of the membrane, according to their carbon chain size and saturation degree. A longer carbon chain and lower

insaturation degree lead to a less fluid membrane [72]. Also, the asymmetric distribution of phospholipids between the two leaflets of the plasma membrane is important in the maintenance of its function. The exoplasmic leaflet is enriched in PC, while the cytoplasmic leaflet is enriched in PS and PE [74]. The maintenance of this distribution is guaranteed by flipase proteins, which were shown to be involved in a variety of vesicle transport pathways in *S.cerevisiae* [75].

The expression of genes codifying for proteins involved in phospholipid synthesis is controlled by multiple factors, including carbon source, nutrient availability, growth stage, pH and temperature [76]. Alterations in cellular zinc concentration (by altered expression of zinc transporters) regulate phospholipid synthesis, leading to alterations in the plasma membrane phospholipid composition, mainly PE and PI [77]. An increase in plasma membrane PS levels leads to an increase in ethanol tolerance in *S. cerevisae* [78]. It has also been observed an increase in PI levels and in the PC/PE ratio upon entrance in the stationary phase of growth [79]. Phospholipid membrane composition (regarding PC fatty acid saturation levels, PI and PA content) was also related to changes in furfural, phenol and acetic acid tolerance in *S.cerevisiae* [80] and to alterations in sugar transportation dynamics due to changes in function of membrane coupled proteins [81]. Phospholipid composition of cellular membranes has also influences the intracellular trafficking of some transporters, since strains with alterations in phospholipid synthesis presented defects in Arn1 trafficking (an integral membrane protein that mediates the uptake of ferrichrome, an important nutritional source of iron, in *S. cerevisiae*) [82].

Sphingolipids comprise a complex range of lipids in which fatty acids are linked via amide bonds to a long-chain (or sphingoid) base. Glycosphingolipids contain a sugar chain as polar head group, while sphingomyelin has a phosphocholine instead. Complex sphingolipids have a hydrophobic residue (ceramide) that consists of sphingosine and fatty acids. Sphingolipids comprise approximately 10 % of the plasma membrane, being usually associated with sterols and forming membrane microdomains, which will be further explored in section 1.2.2 of this introduction. Moreover, sphingolipids have been identified as second messengers in signal transduction pathways controlling essential cellular processes as differentiation, migration, programmed cell death and inflammation, playing essential roles in diseases like cancer, diabetes, microbial infections and neurological disorders [83]. Like phospholipids, sphingolipid distribution in the two leaflets of the plasma membrane is not homogeneous, with sphingolipids almost entirely present in the outer leaflet of the membrane [84].

As it happens for glycerophospholipids, the yeast *S. cerevisiae* presents also a simplified sphingolipid composition, comprising inositolphosphoceramides (IPCs), mannosyl- IPCs

(MIPCs) and inositolphosphoryl-MIPCs [$M(IP)_2Cs$] [85]. Once again, the complexity in polar headgroups and fatty acids in mammalian cells leads to a huge diversity of sphingolipids, turning studies in these cells much more difficult. Yeast, as a model organism containing a simpler lipidome, but highly conserved pathways (containing many genes orthologues to the ones involved in mammalian sphingolipid metabolism [86]) may help to understand the much more complex processes of sphingolipid metabolism and composition in mammalian cells [87]. Yeast sphingolipids contain mannose and inositol residues and present differences in the polar group and ceramide type when compared to human sphingolipids. They also do not contain sphingosine, the unsaturated long chain base (LCB) present in mammals [72]. Moreover, contrarily to humans that synthesise sphingolipids containing long-chain fatty acids (LCFAs) that are formed by carbon chains with 18 and 16 carbons, yeast only synthesises sphingolipids containing VLCFAs (with carbon chains no shorter than 20 carbons) [88, 89]. Figure 7 shows a schematic representation of yeast sphingolipid metabolism.

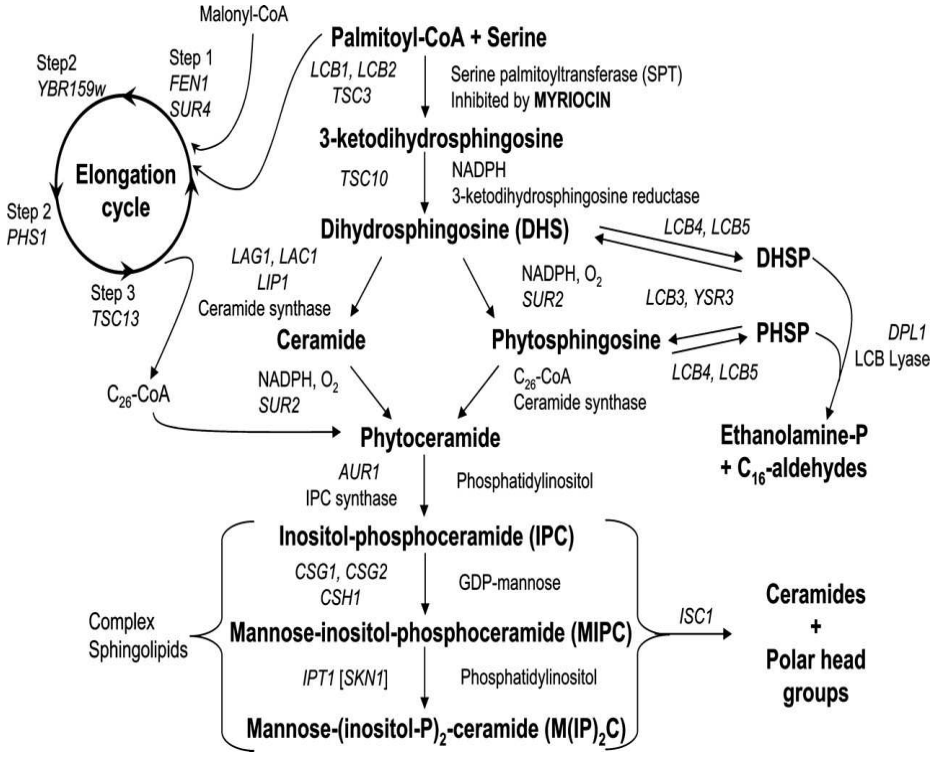

Figure 7. Sphingolipid metabolism in *Saccharomyces cerevisiae*. The first, rate-limiting step in sphingolipid metabolism involves the condensation of serine and palmitoyl-CoA in the endoplasmic reticulum (ER) by serine palmitoyl transferase. After the initial condensation of serine and palmitoyl-CoA into 3-keto dihydrosphingosine, it is converted to dihydrosphingosine by the enzyme 3-keto reductase. Then, dihydrosphingosine is hydroxylated into phytosphingosine, which is acylated to phytoceramide. Finally, ceramides are incorporated in complex sphingolipids. Metabolic intermediates and complex sphingolipids are shown in bold, genes are indicated by italics, and enzyme names are in regular lettering. Figure from [83].

1.2.1.2 Sterols

Sterols are another of the most abundant components of the plasma membrane, consisting on a polar four-ring structure and an aliphatic hydrocarbon tail. Sterols are the product of a complex biosynthetic pathway with more than 20 distinct reactions (Figure 8**)**. Just as sphingolipids differ in structure between fungi and mammals, the sterols differ too. Ergosterol, the main sterol in fungi, is distinct from the mammalian cholesterol by three structural modifications, two in the side chain and one in the B ring. The structure of the plant phytosterols is intermediate between that of the fungal ergosterol and the mammalian cholesterol [90]. Figure 8 schematizes the biosynthetic pathway of sterol synthesis in different organisms.

In membranes, sterols intercalate with phospholipids, maintaining their hydroxyl groups close to the polar head groups of phospholipids. When cells sense a lowering in temperature, cholesterol amount in the membrane increases, intercalating with the increasingly ordered phospholipid bilayers in order to prevent membranes from freezing [91]. Studies in CHO cells showed that roughly 60-70 % of the plasma membrane cholesterol is located in the inner leaflet, which probably has important implications in cholesterol transport since, this way, it is readily available for the cytosolic carrier involved in the non-vesicular pathway of cholesterol transport [92]. This localization can also provide mechanisms to organize liquid ordered domains in the cytosolic leaflet that exist concomitantly with ordered domains of the outer leaflet [93]. Overall, sterols confer important properties to the plasma membrane through their interactions with phospholipids and sphingolipids and play an essential role in the stability of membranes *in vivo* by affecting their rigidity [94, 95], permeability [96], tensile properties [97], phase separation and curvature of liquid-ordered phase [98].

Once again yeast showed to be a very useful model for the study of sterol metabolism, since the ease to obtain mutants deficient in enzymes participating in the ergosterol biosynthetic pathway helped to further elucidate how sterol molecular properties influence different pathways in the cell. A recent study showed that the non-lethal ergosterol mutant *erg6*Δ, which accumulates ergosterol precursors, is highly sensitive to hydric perturbations when compared to the wild-type strain due to changes in basic plasma membrane properties that protect cells against osmotic stress [99]. Also the analysis of *erg*Δ cells that accumulate different sterol intermediates showed that sterols play a role in the early stages of endocytosis and also in the later stages of vesicle trafficking [100]. Sterols are also responsible for yeast resistance to several anti-micotic drugs (either due to changes in plasma membrane permeability to the drugs or to altered activity in membrane transporters due to changes in the lipid environment where they are inserted) [101]. *S. cerevisiae* cells

grown in the presence of ethanol presented modifications in membrane composition. A decrease of plasma membrane sterol content leads to an increased cell tolerance to ethanol-induced stress (which is very important for industrial applications of yeast) [102].

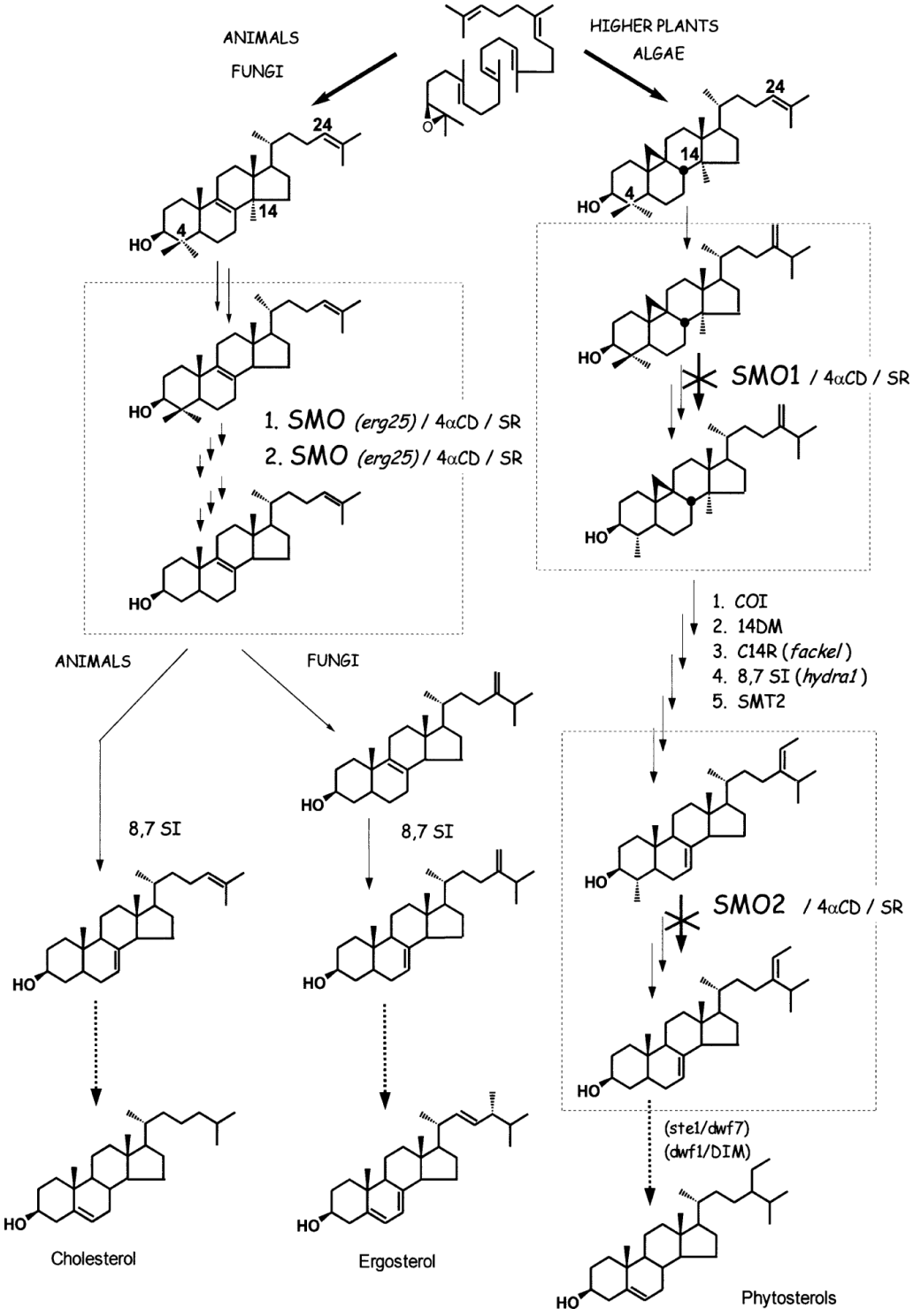

Figure 8. Simplified sterol biosynthetic pathways in different organisms. Full arrows represent distinct enzymes and arrows with broken lines represent several biosynthetic steps. The boxes represent C-4-demethylation multienzymatic complexes, including SMO, 4a-CD and SR. COI, cycloeucalenol isomerase; 14DM, obtusifoliol 14-demethylase; C14R, D8,14-sterol C-14-reductase; 8,7 SI, D8-sterol 8,7-isomerase; SMT2, sterol methyltransferase 2. Figure from [103].

1.2.1.3 Proteins

The plasma membrane protein profile is still a target of studies, since many technical limitations in isolation and analysis of these proteins are only now being outdated. The proteins on the plasma membrane play crucial roles in cell function including intercellular communication, cellular development, cell migration and drug resistance, and include several functions as transporters, receptors, anchors and enzymes. Moreover, membrane proteins are pointed as participating in organizing and stabilizing functional domains of the membrane association with the lipids in their surroundings [104]. Environmental changes leads to rapid changes in the dynamic lipid and proteomic composition of membranes and comparative proteomics is with no doubt a powerful approach when screening for alterations in protein levels and post-translational modifications associated with diseases, environmental changes, stress and many other processes.

The type of interaction between membrane proteins and membrane lipids is variable. Some proteins are intrinsic to the membrane, being largely contained within the bilayers, while others can have large structures outside the lipid region, creating stearic contacts and other interactions with the environment outside the bilayer [105]. Other proteins interact with the membrane through lipid fatty acid anchors or single helices. That is the case of GPI-anchored proteins, characteristic of plasma membrane microdomains in *S. cerevisiae*.

Plasma membrane proteins in *S.cerevisiae* are encoded by only about 4 % of the yeast genome, being estimated as a total of 240 proteins [106]. The H^+-ATPase Pma1p is located in plasma membrane lipid rafts of *S.cerevisiae* and is often used as a marker protein of the plasma membrane and rafts in this organism. Recent work in *S.cerevisiae* cells showed that there is a rapid plasma membrane proteome modulation regarding protein levels and organization after a short (10 minutes) treatment under mild salt stress [106]. Also adaptation to H_2O_2 led to several changes in membrane-associated proteins with functions as variable as transport, biosynthesis/degradation, cellular organization, stress response, metabolism, distribution and vesicular transport and signalling [107].

1.2.2 Plasma membrane organization: Lipid rafts and other membrane microdomains

The existence of lipid domains in cell membranes was suggested for the first time in 1982 by Karnovsy and his co-workers [108]. It is now well established that there is a high heterogeneity in the distribution of lipid and protein components of membranes, which are not distributed homogeneously, ocurring in selectively enriched regions designed as

microdomains. The mechanism by which membrane domains are formed is not yet fully understood and, probably, a variety of factors are involved. These include strong interactions between the trans-membrane proteins and certain lipid species and lipid-lipid interactions. One commonly accepted hypothesis is the formation of protein-directed lipid domains [109]. Specific lipids are accumulated around the protein because of favourable lipid–protein interactions. This variation of the local lipid composition causes other proteins to be recruited to the domain, thus inducing further lipid reorganization. Then, the cluster is amplified, since every lipid interacts with several near neighbours, finally leading to domain formation [109].

Lipid rafts, the most common type of microdomains, are formed by the lateral association and tight packing of sterols and the long fatty acids constituents of sphingolipids, in association with specific proteins [110]. Lipid rafts have been implicated in the organization of membrane trafficking and cell signalling in mammalian cells and protein sorting in yeast [111]. Rafts have been proposed as signalling platforms for the interaction of receptors, coupling factors, effector proteins and substrates [112] acting like an entrance point for viruses [113], bacteria [114] and toxins [115] which can use these regions to enter or interact with the host cell.

The formation of lipid rafts represents a phase separation in the fluid lipid bilayer, described as being in the liquid ordered phase, which segregates from the bulk liquid disordered phase of the plasma membrane [116]. In addition to sterols and sphingolipids, lipid rafts can also contain small amounts of other glycerophospholipids that contain an higher amount of saturated fatty acids, contributing to their higher rigidity [111, 112]; for example, PE plays an important role in the stability of *S. cerevisiae* microdomains [117]) Recent studies using fluorescent probes revealed for the first time the existence of gel domains in *S. cerevisiae* plasma membrane [118]. These domains were shown not to be ergosterol-enriched, being mainly composed of sphingolipids, (possibly inositolphosphorylceramide), and containing GPI-anchored proteins, suggesting an important role in membrane traffic and signalling, and interactions with the cell wall [118]. In spite of these observations, not much is yet known about plasma membrane organization and microdomains, which can vary extensively in size, organization and composition.

Small (50-100 nm), flask-shaped invaginations have been observed in the plasma membrane of mammalian cells. This specific type of lipid raft domains is organized due to the insertion of a protein denominated caveolin and, therefore, these microdomains are denominated caveolae [119]. Once formed, caveolae domains are very stable, immobile structures, maintained by the interaction of the GPI anchor of the protein with cholesterol, being caveolae internalization stimulated by exogenous cholesterol and glycosphingolipid addition

[120, 121]. Caveolae have the ability to transport molecules across endothelial cells and constitute an entire membrane system with multiple functions essential for the cell [119]. Studies in cultured endothelial cells showed that lipid rafts mediate H_2O_2 prosurvival affects, suggesting that plasma membrane compartments rich in cholesterol participate in signal transduction pathways activated by oxidative stress [122]. In T lymphocytes the assembly of lipid rafts is promoted by ROS, probably as a mechanism of T-cell activation. Moreover, the treatment of these cells with ROS scavengers leads to a decrease in raft formation [123].

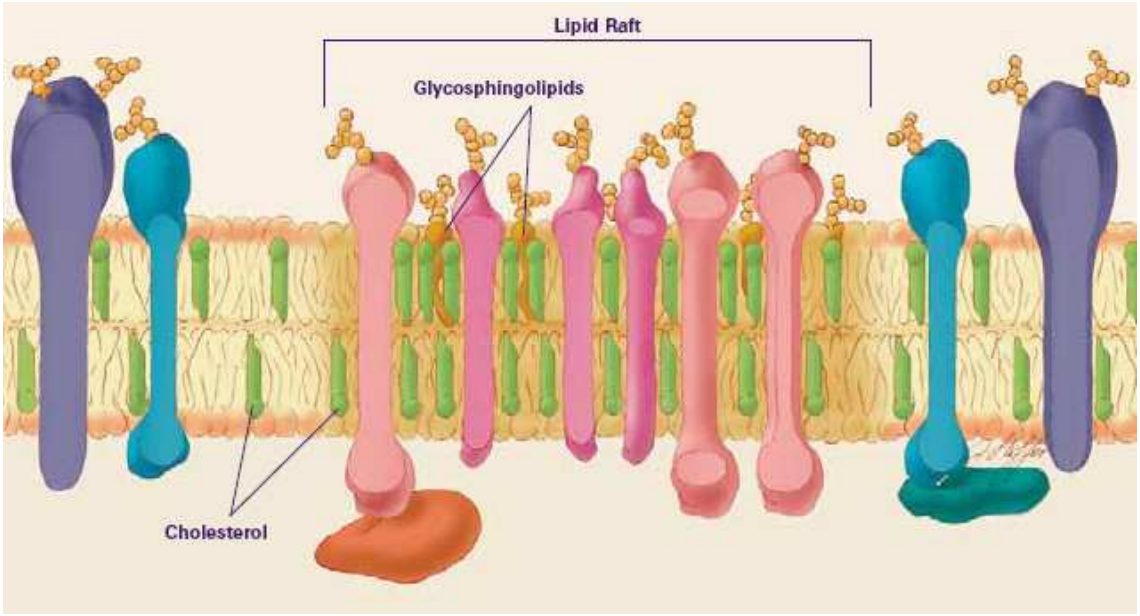

Figure 9. Schematic representation of a lipid raft. Lipid rafts consist in domains enriched in sterols (represented in green) and sphingolipids (represented in orange) associated with membrane integral proteins (represented in pink). Figure from [124].

In *S. cerevisiae* different types of plasma membrane domains, with different lipid and protein composition, have been identified: I) the membrane compartment occupied by Pma1p (MCP); II) the membrane compartment occupied by Can1p (MCC) and III) the membrane compartment occupied by *TOR*C2 (MCT).

The MCC domains accommodate not only the arginine/H^+ -symporter Can1p, which gives name to the compartment [125], but also the uracil/H^+ -symporter Fur4p and Sur7p, a protein presumably involved in endocytosis [126]. MCC domains are stable over time and likely to be enriched in ergosterol, since they co-localize with membrane domains stained by filipin, a fluorescent marker that binds to sterols [126]. It is not yet clear if MCCs represent raft-like structures in *Saccharomyces cerevisiae* [125] or are distinct structures since they reflect a

stable lateral membrane compartment rather than a compartment that freely dislocates in the membrane (characteristic of rafts) [127]. The MCP domains contain the H^+-ATPase Pma1p and occupy a mesh-shaped compartment that spreads between the discrete patches formed by MCC [128]. MCP domains are probably enriched in sphingolipids, since it was observed that Pma1p does not form oligomers in mutant cells containing lower levels of sphingolipids [129]. Administration of agents that disturb lipid rafts in the plasma membrane of yeast abolished the antifungal action and accumulation of miconazole, as well as miconazole-induced stabilization of the actin cytoskeleton and ROS accumulation [130]. It was also observed that Nce102p, a protein localized in MCC domains, functions as a possible sphingolipid sensor in the membrane, reinforcing the role of these domains in signalling [131]. The MCT compartment contains the Tor Complex 2 (*TOR*C2), one of the cell complexes containing rapamycin kinases [132]. The lipid composition of this compartment is not yet known.

Exposure of cells to mild osmotic stress induced a global reorganization of the plasma membrane by internalization of Pma1p and increased expression of Pil1p and Lsp1p. Pil1p and Lsp1p are the two main components of the eisosomes [106], immobile protein assemblies located underneath the plasma membrane sites involved in endocytosis, which have a profound role in regulating plasma membrane architecture. Eisosomes possibly function as a signalling platform by clustering lipids and/or proteins together at the membrane, thereby facilitating their interaction. [133]. Eisosomes interact with the MCC domain, since Lsp1p and Pil1p co-localize with the MCC marker Sur7p [133]. Moreover, the deletion of the *PIL1* gene leads to a collapse of the MCC patchy fluorescence signal to a uniform plasma membrane signal [133].

1.3 Plasma membrane modulation by H_2O_2

The misleading concept that H_2O_2, being a small non-charged molecule, diffuses freely across biomembranes has been counteracted by the measurement of H_2O_2 gradients when the H_2O_2 source is separated from the site of H_2O_2 removal by a membrane. H_2O_2 gradients were originally measured across the plasma membrane of Jurkat T-cells [48] and, subsequently, gradients have been measured in *Escherichia coli* [134], *S. cerevisiae* (in exponential phase and stationary phase [57, 135]), MCF-7 cells [52], and HeLa cells [136]. Table 4 resumes the gradient values measured in the different types of cells.

Table 4. H_2O_2 gradients measured in different cell types.

Cell type	Gradient
Jurkat T-cells	7 [48]
E. coli	5-9 [134]
S. cerevisiae (exponential phase)	2 [57]
S. cerevisiae (stationary phase)	18 [135]
MCF-7	2 [52]
HeLa	7 [136]

Moreover, in *S. cerevisiae*, the plasma membrane permeability to H_2O_2 is modulated both during adaptation to H_2O_2 [57] and upon entrance in the stationary phase of growth [135], limiting diffusion of H_2O_2 into cells and thus acting as a protective mechanism against H_2O_2. So, the plasma membrane acts as a dynamic barrier against the entrance of H_2O_2.

Originally it was suggested that the decrease of plasma membrane permeability in H_2O_2-adapted cells could be related to changes in ergosterol content, since *erg3*Δ and *erg6*Δ cells presented higher H_2O_2 consumption rates and a higher susceptibility to lethal doses of H_2O_2 [57]. Subsequent analysis of the plasma membrane composition during adaptation to H_2O_2 did not confirm this hypothesis, since adaptation did not induce changes in the levels of ergosterol, and H_2O_2-adapted cells had only increased levels of the sterol precursor squalene when compared with control cells [66]. In spite of founding no changes in the ergosterol levels, Pedroso et al [66] found that ergosterol-rich domains were redistributed along the plasma membrane during the H_2O_2 adaptation process [66]. These observations, together with the measurement of an increased fluorescence intensity of *trans*-parinaric acid (t-PnA) [66], a fluorescent probe that partitions preferentially into liquid ordered domains rich in sphingolipids, suggested an involvement of plasma membrane microdomains in the membrane reorganization occurring during adaptation to H_2O_2.

H_2O_2 also induces rapid biophysical changes in the plasma membrane of *S. cerevisiae* H_2O_2-adapted cells [95]. Biophysical studies with fluorescent probes showed a decreased fluidity of the plasma membrane after 30 minutes of exposure to adaptive doses to H_2O_2 [95], suggesting that changes in plasma membrane rigidity are related to the decreased plasma membrane permeability.

Previous studies showed alterations in plasma membrane phospholipid composition, in the content of plasma membrane proteins and in the expression of genes involved in lipid metabolism in H_2O_2-adapted *S. cerevisiae* cells [66, 107]. After 15 minutes of exposure to an adaptive dose of H_2O_2, several gene of ergosterol biosynthesis were down-regulated (*ERG1*, *ERG3*, *ERG7* and *ERG25*). Also several genes involved in fatty acid metabolism were down-regulated (*ELO1*, *ELO2* and *ELO3*, involved in fatty acid elongation, *OLE1* involved in fatty acid desaturation and *FAS1* and *FAS2* involved in fatty acid biosynthesis) [107]. Since fatty acids are important constituents of membranes, the *FAS1* gene (codifying for the β-subunit of fatty acid synthase) appeared as an interesting candidate for further studies in adaptation to H_2O_2, since changes in the initial steps of fatty acid synthesis may lead to important alterations in plasma membrane properties. Therefore, the main objective of this thesis is to understand how H_2O_2 modulates fatty acid synthase and how alterations in Fas activity levels may lead by itself to changes in plasma membrane.

1.4 Fatty acid synthase

Fatty acids are essential metabolites for all organisms (with the only exception of *Archaea*), being structural components of membrane lipids, the major storage form of metabolic energy and components of post-translationaly modified proteins. The reaction mechanisms involved in fatty acid synthesis are highly conserved among different types of cells. Fatty acid synthase (Fas) is a multifunctional enzyme, comprising several enzymatic activities involved in *de novo* fatty acid biosynthesis. The mammalian Fas consist of two identical multifunctional polypeptides separated by a core region. The N-terminal section contains the catalytic domains ketoacyl synthase, malonyl/acetyl transferase and dehydrase and the C-terminal domains contain the catalytic domains enoyl reductase, ketoacyl reductase , acyl carrier protein and thioesterase [137]. In fungi, Fas is a barrel shaped multienzymatic protein, containing six copies of eight independent functional domains in an α6β6 molecular complex of 2.6 MDa (Figure 10) [138]. The α subunits comprise the acyl-carrier domain and three independent enzymatic functions: 3-ketoreductase, 3-ketosynthase and phosphopantetheinyl transferase [139, 140], while the β subunits comprise four independent enzymatic functions: acetyltransferase, enoyl reductase, dehydratase, and malonyl/palmitoyl-transferase [141].

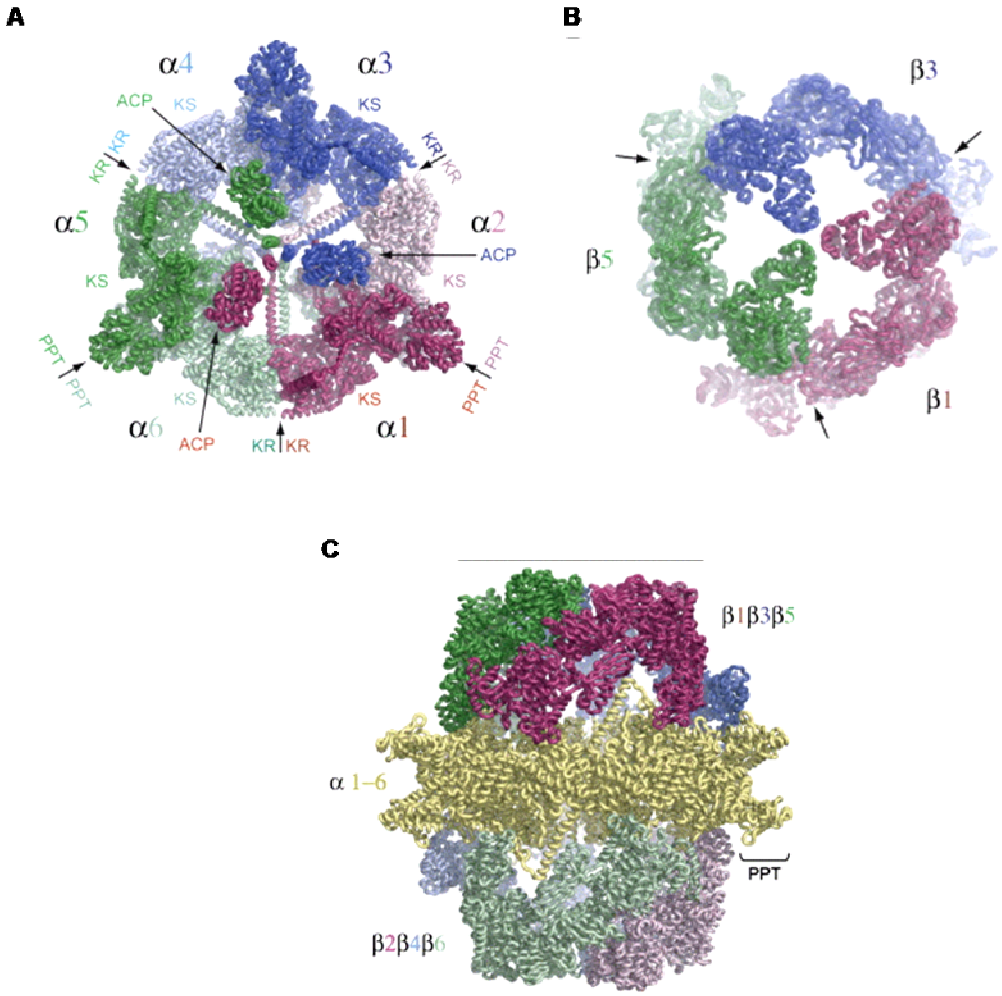

Figure 10. Overall structure of yeast fatty acid synthase. A - The α subunit hexamer viewed from the top; B - The top view of the β subunit trimer, showing that it is formed by interactions between its N-terminal domains at the center and by interactions between neighbouring subunits (arrows); C- The barrel-shaped structure of FAS has two domes composed of β subunit trimers (green, pink, and blue) and an equatorial wheel composed of α subunits (yellow). ACP – acyl-carrier protein; KS - ketosynthase; KR - ketoreductase; PPT - phosphopantetheinyl transferase. Figure adapted from [142].

De novo synthesis of fatty acids in several organisms is a highly-conserved chemical pathway. However, during evolution, a number of functionally differentiated Fas variants, as well as large family of Fas-related enzymes have developed a diversity of Fas systems regarding structural features and organization of their catalytic units, being divided into two types: Fas I and Fas II systems [143]. Type I fatty acid synthases (Fas I) are present in the cytoplasm of yeast, fungi and animals, but also in some bacteria like corynebacteria and mycobacteria while type II fatty acid synthases (Fas II) are present in prokaryotes, plants and in the mitochondria of animal cells and yeast. The fundamentally different architectures of mammalian and fungal Fas are an example of convergent evolution resulting in multienzymes with increased catalytic efficiency owing to high local concentrations of

substrates between catalytic sites, compartmentalization and easier regulation of gene expression [144].

The first step of fatty acid synthesis consists in the acetyl-CoA carboxylation to malonyl-CoA mediated by acetyl-CoA carboxylase. This carboxylation reaction requires biotin as a cofactor and consumes ATP [145]. Activated acyl and malonyl substrates are then transferred from coenzyme A to the phosphopantetheine prosthetic group of the acyl carrier protein. In animals, the substrates are loaded by a double specific malonyl/acetyl transferase while in fungi by two separate enzyme domains, the acetyl transferase and the malonyl/palmitoyl transferase [143]. The substrates are then condensed by the ketoacyl reductase domain of the enzyme, where malonyl is decarboxylated to acetoacetyl-acyl carrier protein, which is further modified at the β-carbon position by ketoacyl reductase, dehydratase and enoyl reductase domains in order to yield butyryl-ACP. Each of these cycles introduces two carbon units in the newly synthesised fatty acyl chain, until a length of 16 to 18 carbons is reached. In fungi, the palmitoyl residue is then transferred onto coenzyme A by the malonyl/palmitoyl transferase subunit of the fungal enzyme, while, in animals, the enzyme releases the free fatty acid by thioesterase mediated hydrolytic cleavage of palmitoyl-ACP [146]. Figure 11 resumes the main catalytic reaction pathways for fatty acid synthesis by type I Fas enzymes in animals (a) and fungi (b).

Most human tissues have a low Fas activity and, therefore, low fatty acid synthesis, using preferentially dietary fatty acids [148]. By contrast, in cancer cells, *de novo* fatty-acid synthesis is frequently increased in order to produce new membranes. This high activity of Fas (mainly by over-expression of *FASN*) leads directly to cellular fatty-acid accumulation and affects fundamental cellular processes, including signal transduction and gene expression. Increased expression of *FASN* has been detected in a wide range of epithelial cancers, including breast, prostate, ovary, lung, colon, endometrium, stomach, tongue, oral cavity and esophagus [149, 150]. Fas was related with synthesis of phospholipids partitioning into detergent-resistant domains in cancer cells, being therefore probably linked to the control of lipid composition of these microdomains, and responsible for deregulating membrane composition and functioning in tumour cells which could have impact in processes such as signal transduction, intracellular trafficking or cell polarization and enhance tumour development and progression [149]. Therefore, *FASN* inhibitors have been pointed out as potential molecules for cancer therapy.

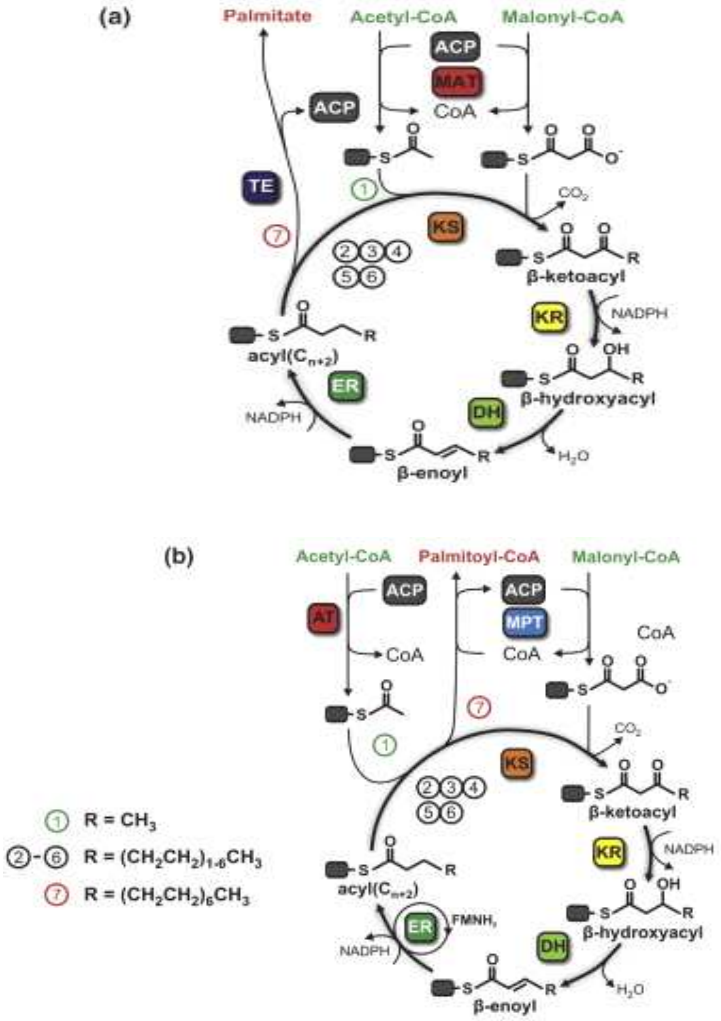

Figure 11. Catalytic reaction cycles of (a) animal and (b) fungi fatty acid synthase. ACP, acyl-carrier protein; MAT, malonyl/acetyl transferase; KS, ketoacyl synthase; KR, ketoacyl reductase; DH, dehydratase; ER, enoyl reductase; TE, thiosterase; AT, acetyl transferase; MPT, malonyl/palmitoyl transferase; CoA, coenzyme A. Figure from [144].

S. cerevisiae Fas is an enzyme complex responsible both for the synthesis of fatty acids with a chain length up to 20 carbons [143] and, by interaction with elongation enzymes (Elo), mediation of the synthesis of fatty acids up to C26 [151]. Fas is composed by two subunits (α and β) whose synthesis is regulated by two genes, *FAS2* and *FAS1*, respectively. The expression of these genes is regulated by an upstream activating sequence (UAS) usually designated as inositol/choline responsive element (ICRE) [152], since it is repressed in the presence of the phospholipid precursors inositol and choline [153]. Although the presence of inositol alone is enough to trigger repression, enhanced repression is observed when choline is also present, suggesting that these two precursors affect a common signal in an additive fashion [154]. Many genes codifying for enzymes essential for phospholipid metabolism (like *INO1* and *CHO1*) also contain a regulatory UAS_{INO} region [155, 156]. This regulation

mechanism requires the participation of the helix-loop-helix transcription factors, Ino2p and Ino4p (gene products from the *INO2* and *INO4* genes) as well as the participation of the Opi1p negative regulator of transcription. When cells are grown in the absence of inositol and choline in the growth medium, the transcriptional heterodimeric complex composed by Ino2p and Ino4p binds to the conserved *cis*-acting upstream activating sequence ICRE, activating the expression of genes regulated by this promoter region [157]. When exogenous inositol and/or choline are present, there is a decrease in phosphatidic acid levels, which is directly sensed by Opi1p, a component of the endoplasmic reticulum (ER) lipid sensing complex, causing it to dissociate from the ER and translocate to the nucleus, where it participates in the repression of the target genes [158]. The Opi1p repressor, consisting on a basic leucine zipper motif [158], directly interacts with the Ino2p activator, leading to its deactivation [159] and with the pleiotropic repressor Sin3p, a histone deacetylase that functions as a global transcriptional repressor [159]. Figure 12 schematizes the regulatory circuit of inositol-choline mediated gene expression.

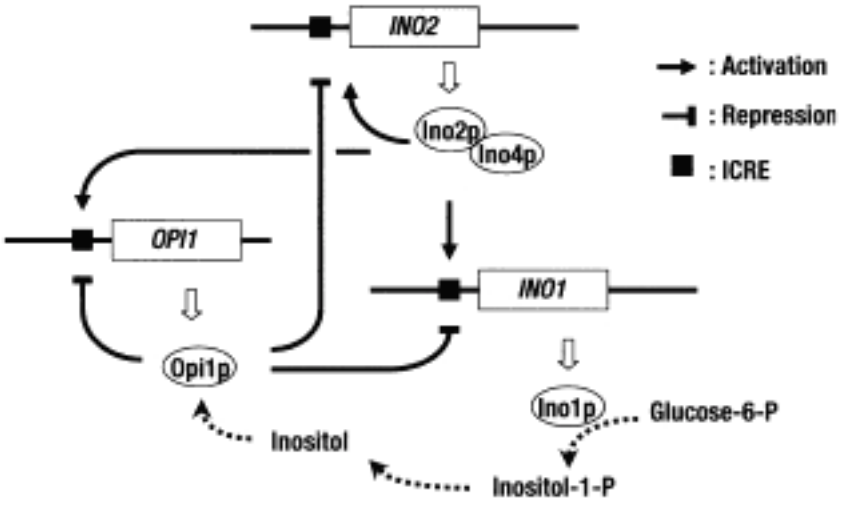

Figure 12. Schematic representation of the regulatory circuit of inositol-choline mediated gene expression. The complex Ino2p/Ino4p binds to the consensus sequences ICRE activating the expression of the genes under the action of the regulator sequence. On the other hand Opi1p acts as a repressor in the presence of inositol and choline. Figure from [160].

In addition to UAS elements influenced by phospholipid precursors, *FAS* promoters are also activated by binding sites of the essential transcription factor Rap1p, Abf1p and Reb1p. These constitutive activating motifs ensure the maintenance of housekeeping fatty acid biosynthesis, even under conditions of inositol/choline repression [161].

Another regulating sequence has been identified as responsible for the auto regulation of the *FA*S genes. The stoichiometry of the two subunits is tightly regulated and determined by the expression of *FAS1*. *FAS1* over-expression results in a concomitant increase in *FAS2* m*RNA* levels and, conversely, a decrease in *FAS2* m*RNA* is observed in *fas1*Δ cells. However, *FAS1* expression is independent of the level of *FAS2* (or *ACC1*) expression [162]. Although the mechanism responsible for *FAS* auto regulation is not fully understood, it is known that the *FAS1*-dependent regulation of *FAS2* is due to the presence of a auto regulatory *cis*-acting sequence downstream repression site (DRS) located within the coding sequence of *FAS2* [162]. This mechanism is independent of ICRE motifs and of constitutive motifs of transcription, being mediated by the *FAS1* gene product, which may function as an indirect positive factor, leading to deactivation of an unknown repressor (Figure 13). In order to maintain balance in the levels of Fas subunits, they also undergo post-transcriptional regulation and the Fas1p subunit present in excess in cells lacking the Fas2p subunit is rapidly degraded by the vacuolar proteases, Pep4p and Prb1p [152, 163]. Similarly, Fas2p in excess is ubiquitinated and subsequently subjected to proteasomal degradation [164].

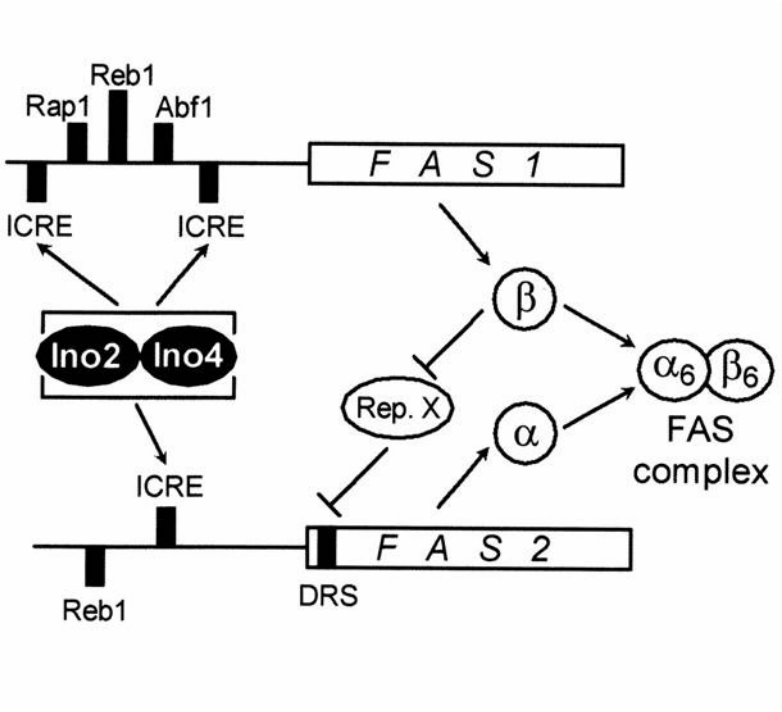

Figure 13. Coordinate control of *FAS* genes by Fas1-dependent anti-repression of *FAS2* gene expression. In the absence of non-complexed Fas1 (β-subunit), the *FAS2* control region (including downstream sequence) is substantially weaker than the *FAS1* promoter. An excess of free β-subunit may directly or indirectly deactivate the repressor leading to maximal *FAS2* expression. ICRE – inositol/choline responsive element; DRS – downstream repression site; Rep X- unknown repressor. Figure adapted from [162].

Recent studies showed that over expression of *FAS1* in *S.cerevisiae*, resulting in increased Fas activity, reduced α-synuclein (a protein that, in the presence of oxidizing agents, forms stable oligomers [165] involved in neurodegenerative disorders and lethal to *S. cerevisiae*) effects on cell growth, whereas its partial inhibition by cerulenin increased α-synuclein toxicity [166]. The mutant cells synthesising α-synuclein also presented increased levels of ROS and lipid droplet accumulation.

Fatty acid synthesis is also an interesting target for development of new antibacterial agents [167]. The rapid emergence of resistance to the most commonly used antibiotics (which mainly exert their effects on bacterial cell wall synthesis, protein synthesis, and DNA replication) led to the need of search for drugs which target other cellular pathways. Since fatty acid synthesis is essential to cell survival, either natural based or chemically synthesised Type II Fas inhibitors are promising antibacterial molecules [167].

Human cells preferentially use exogenous lipids; therefore fatty acid synthase activity and *FASN* expression are usually low in most tissues [168]. The liver and adipose tissues are an exception, where Fas produces fatty acids in order to store energy in the form of triacylglycerols [150]. A wide range of epithelial cancers (including carcinomas of the ovary, breast, prostate, colon and endometrium,) present an up-regulated *FASN* in order to guarantee their elevated need of supply for fatty acids [149]. This increased activity occurs very early in cancer development and suggested Fas as a potential therapeutic target for cancer treatment [150]. In hormone-sensitive cancers Fas over expression is more pronounced as the tumour progresses towards a more advanced stage [149]. Fatty acid synthase increased activity in tumour cells is mainly due to a transcriptional regulation of *FASN* [169]. The low pH, hypoxia and nutrient starvation usually present in tumour cells in order to promote malignant progression, induce *FASN* expression by up-regulating SREBP-1, the major transcriptional regulator of this gene [170]. In prostate cancer cells Fas is also regulated at a posttranscriptional level by interaction with isopeptidase USP2a (ubiquitin-specific-protease-2a), stabilizing the protein. This observation suggests that Fas is subject of regulation at multiple levels in cancer cells [171]. Development in this field is promising, since many studies already show that inhibition of Fas effectively and selectively kills cancer cells, with minimal side effects to normal cells [172].

2 Objectives and outline

The plasma membrane is a dynamic barrier that protects the cells from the entrance of damaging extracellular agents, like H_2O_2. Previous studies revealed that the plasma membrane is modulated during adaptation to H_2O_2 (an important biological mechanism, by which cells pre-exposed to non-lethal doses of H_2O_2 become more resistant to lethal doses of H_2O_2), becoming less permeable to this oxidizing agent [57]. Moreover, mutant strains in the ergosterol biosynthetic pathway showed to be more sensitive to H_2O_2 than wt cells [57]. Further, biophysical studies showed that this permeability alteration is accompanied by a decrease in plasma membrane fluidity, reinforcing the role of the plasma membrane in the adaptation process [95]. Plasma membrane lipid composition is altered during adaptation to H_2O_2 [66]. Among the changes that occur, there is a decrease in oleic acid and in 2-hydroxy-C26:0 fatty acid levels, a decrease in the ratio between unsaturated and saturated long chain fatty acids and an accumulation of squalene in the plasma membrane [66]. Although ergosterol content was unaltered by adaptation to H_2O_2, there was also a reorganization of the ergosterol-rich domains of the plasma membrane in adaptation to H_2O_2 [66]. These changes were probably due a reprogramming of gene expression. In fact, rapid changes in the expression of genes involved in lipid metabolism were detected [66]. One of the genes down-regulated was the *FAS1* gene, which codifies for the β sub-unit of fatty acid synthase and regulates the levels of this protein in the cell. Since fatty acids are major constituents of the plasma membrane and interfere directly in its fluidity, it is essential to understand if modulation of the *FAS1* gene is involved in adaptation to H_2O_2 and the related changes in plasma membrane permeability to H_2O_2. Thus, the main objective of this work was to study how the modulation of Fas affects the plasma membrane properties and cell resistance to H_2O_2 and if the regulation of Fas can be one of the main mechanisms by which H_2O_2 adaptation induces alterations in the plasma membrane.

The results obtained were divided into chapters 4, 5, 6 and 7. In chapter 4 the studies of Fas modulation by H_2O_2 are presented. Mainly, how Fas activity and *FAS1* expression are altered by exposing cells to non-lethal H_2O_2 concentrations and how the control of the used dose is crucial for the interpretation of the observations. Chapter 5 describes studies obtained using yeast strains with artificial constructs that allow regulation of Fas activity. The effect of down- and up regulated expression of *FAS1* in yeast resistance to H_2O_2 and in plasma membrane permeability to H_2O_2 was studied. In chapter 6, the effect of different Fas expression levels on the yeast plasma membrane composition and biophysical properties are presented. The results obtained clarify how the yeast plasma membrane reorganizes in response to adaptive

doses of H_2O_2. Finally, in chapter 7 preliminary results obtained in Jurkat T cells with the aim to find whether the plasma membrane of mammalian cells undergoes changes similar to those found in the yeast upon exposure to non-lethal doses of H_2O_2 and whether fatty acid synthase is involved in these changes. Chapter 8 consists of an overall discussion of the results obtained, in order to put forward a hypothesis for the mechanism(s) by which Fas is involved in plasma membrane modulation by H_2O_2.

3 Materials and Methods

3.1 Materials

All the strains were obtained from EUROSCARF (Frankfurt, Germany). Table 1 summarizes genotypic details of the strains used.

Table 5. Strains used in the experimental work.

Strain name	Genotype	Source
BY4741 (hwt)	MATa; his3Δ1; leu2Δ0; met15Δ0; ura3Δ0	EUROSCARF
BY4743 (wt)	MATa/MATα; his3Δ0/his3Δ0; leu2Δ /leu2Δ0; met15Δ0/MET15; LYS2/lys2Δ0; ura3Δ0/ura3Δ0	EUROSCARF
*fas1*Δ	BY4743; YKL182w::kanMX4/YKL182w	EUROSCARF
*ctt1*Δ	BY4743; YGL088w::kanMX4/YGL088w::kanMX4	EUROSCARF
*fas1*Δ- p*FAS1*	BY4743; YKL182w::kanMX4/YKL182w pCM189-*FAS1*	This work
*fas1*Δ-pCM189	BY4743; YKL182w::kanMX4/YKL182w pCM189	This work
wt-Can1GFP	BY4743; CAN1::GFP::URA3 (YIp211)	This work
*fas1*Δ-Can1GFP	BY4743; YKL182w::kanMX4/YKL182w; CAN1::GFP::URA3 (YIp211)	This work

For over-expression studies, a strain containing the *FAS1* gene under control of a tetracycline-regulatable promoter system was constructed from the *fas1*Δ strain by transformation with a construct plasmid (See 3.2.11). Table 6 summarizes the nomenclature used for this set of strains.

Table 6. Transformant strains used in the experimental work.

strain name	Autonomously replicating plasmid
*fas1*Δ- p*FAS1*	p*FAS1*
*fas1*Δ-pCM189	pCM189

Jurkat T cells were obtained from American Type Culture Collection (Manassas, VA, USA). Yeast extract, peptone, yeast nitrogen base (YNB) and agar were from Difco (Detroit, MI, USA). Yeast media amino acids, bovine liver catalase, glucose oxidase from *Aspergillus niger*, digitonin, fatty acid and phospholipid standards, glass beads for cell disruption (425-600µm), Sephadex G25, benzamidin, leupeptin, pepstatin, phenylmethylsulphonyl fluoride (PMSF) and dithiothreitol (DTT), diethylene triamine pentaacetic acid (DTPA), bovine heart cytochrome *c*, dimethyl sulfoxide (DMSO) and Folin's reagent were obtained from Sigma Aldrich (St Louis, MO, USA). RPMI 1640 medium, antibiotics and fetal bovine serum were obtained from Cambrex, Verviers, Belgium. Nitrocellulose membranes for Western and Northern blot were from Schleider and Schnell (Dassel, DE). The primary antibodies anti-Pma1p (Sc-57978) and anti-Fas (Sc-48357) and secondary antibody anti-mouse (Sc-2005) were obtained from Santa Cruz Biotechnology (Delaware, CA, USA). RNA RiboPure-yeast extraction kit was from Ambion (Austin, TX, USA). Glucose, hydrogen peroxide (H_2O_2), Tween 20, ethylenediamine tetraacetic acid (EDTA) and glycin were obtained from Merck (Whitehouse station, NJ, USA). Tetramethylethylenediamine (TEMED) and ammonium persulfate (APS) were from Promega (Madison, WI, USA). Diphenylhexatriene (DPH), *trans*-parinaric acid (t-PnA) and Alamar Blue were from Invitrogen (Leiden, The Netherlands). Acrylamide was from Fluka (St.Louis, MO, USA). Sodium dodecyl sulphate (SDS) was obtained from Gibco (Barcelona, Spain). Tris base was obtained from Riedel-de-Haën (Seelze, Alemanha). 3 MM paper was from Whatman (Maidstone, UK). ECL Enhanced chemiluminescence kit (ECL) was obtained from GE Healthcare (Chalfont St. Giles, UK).Yeast Lytic Enzyme (from *Arthrobacter luteus*) was obtained from ICN Biomedicals (Aurora, OH, USA).

3.2 Methods

3.2.1 Yeast media and growth conditions

For yeast cell stock maintenance and cell survival count experiences cells were inoculated in yeast peptone D-glucose (YPD) solid medium plates. YPD medium contained 1 % (w/v) yeast extract, 2 % (w/v) peptone and 2 % (w/v) glucose and was supplemented with 2 % agar (w/v) for solid medium.

In most experiences yeast cells were grown in liquid synthetic complete (SC) media, composed by 6.8 % (w/v) yeast nitrogen base (YNB), 2 % (w/v) glucose, 0.002 % (w/v) arginine, 0.002 (w/v) methionine, 0.003 % (w/v) tyrosine, 0.003 % (w/v) isoleucine, 0.003 %

(w/v) lisine, 0.005 % (w/v) phenylalanine, 0.01 % (w/v) glutamic acid, 0.015 % (w/v) valine, 0.01 % (w/v) aspartic acid, 0.0025 % (w/v) adenine, 0.04 % (w/v) serine, 0.01 % (w/v) leucine, 0.005 % (w/v) triptophan, 0.01 % (w/v) histidine, 0.02 % (w/v) threonine and 0.0025 % (w/v) uracil.

Before every experience a small volume of SC medium was inoculated from the YPD stock plate and grown overnight until the stationary phase of growth. This pre-culture was then diluted in fresh medium at a known concentration of cells. For every experience yeast cells were cultured at 30 ºC and 160 rpm until the mid exponential phase of growth with, at least, two cell division cycles before harvesting. By analysis of the growth curves of the used strains an optical density of 0.6 OD/mL was established as mid-exponential phase. Cell growth was followed by measuring optical density of the culture at 600 nm (OD_{600}), being that 1 OD_{600}=2-3x10^7 cells [57].

3.2.2 Cell Culture

Jurkat T Cells were grown in RPMI 1640 medium supplemented with 10 % fetal bovine serum, penicillin 100 U/mL, streptomycin 100 µg/mL and 2 mM L-glutamine. Cells were kept at 10^5-10^6 cells/mL and the medium was changed every 2-3 days. All experiments were performed with a cell density of 10^6 cells/mL and the growth medium was always replaced by fresh medium 24 h before the beginning of the experiment.

3.2.3 Exposure to H_2O_2 exposition – steady state

Adaptation of *S. cerevisiae* cells to H_2O_2 was achieved by exposing yeast cells to 150 µM steady-state H_2O_2 for 90 min as described in [57]. Jurkat T cells were exposed to 5 µM steady-state H_2O_2 for 1-4 h. This method guarantees that cells are exposed to a constant concentration of H_2O_2 along time, since an initial concentration of H_2O_2 is added to the culture together with glucose oxidase. Glucose oxidase (GO) catalyses the oxidation of glucose with the concomitant production of H_2O_2 (eq, 1), and it is added to the culture medium at an amount enough to have a production of H_2O_2 that balances the H_2O_2 consumption by the cells. Equation 1 described the reaction catalyzed by glucose oxidase.

$$\beta\text{-D-glucose} + \text{GO-FAD} \rightleftharpoons \text{GO-FADH}_2 + \delta\text{-D-glucolactone}$$
$$\text{GO-FADH}_2 + O_2 \longrightarrow \text{GO-FAD} + H_2O_2 \qquad \text{(Equation 1)}$$

H_2O_2 and glucose oxidase were added to yeast cultures in mid-exponential phase and H_2O_2 concentration was measured every 20 min in the oxygen electrode as described in 3.2.4. To establish the dose that induces adaptation (or sub-lethal dose), yeast cells were exposed to different H_2O_2 steady-state concentrations in the range 0.15 to 1 mM for 90 min and a 150 µM H_2O_2 dose was chosen [57]. In Jurkat cells H_2O_2 and glucose oxidase were added to cultures at a cell density of 10^6 cells/mL. The growth medium was replaced by fresh medium 24 h before the addition.

3.2.4 H_2O_2 consumption and determination of H_2O_2-permeability constant

The plasma membrane permeability toward H_2O_2 was determined according to [48, 57]. Yeast cells in mid exponential phase were harvested by centrifugation at 5000 **g** for 5 min, washed twice in 0.1 M potassium phosphate buffer, pH 6.5 and ressuspended in the same buffer to a concentration of 0.5 OD_{600}/mL. This suspension was divided in two samples, one used for measurement of consumption in intact cells and the other for measurement in permeabilized cells. Intact cells were incubated for 20 min with 300 µM H_2O_2 in order to oxidize all the reducing equivalents before starting the measurement of H_2O_2 consumption. This H_2O_2 concentration was optimized for diploid cells and differs from the one used in the original protocol for haploid cells (BY4741). It was determined using the diploid mutant strain *ctt1*Δ, which lacks the H_2O_2-removing enzyme cytosolic catalase. This technique stands in the principle that the H_2O_2 consumption measured with the oxygen electrode is only due to catalase activity and not cytochrome *c* peroxidase since all the reducing equivalents were oxidized before starting the measurements. The concentration of H_2O_2 and time of exposure required for this was determined as the one in which no more H_2O_2 consumption was measured in intact *ctt1*Δ cells. Yeast cell were permeabilized by incubating them for 10 min with 100 µg/mL digitonin (using a freshly made solution of purified digitonin in water).

To measure H_2O_2 consumption, aliquots were taken from cell culture and put in an oxygen electrode chamber (Hansatech Instruments Ltd., Norfolk, UK). H_2O_2 was measured as O_2 release after the addition of catalase (typically 59 U as defined by the manufacturer). H_2O_2 concentrations were related to electrode response by constructing a calibration curve with H_2O_2 stock solutions of known concentration determined spectrophotometrically at 240 nm (ε= 43.4 $M^{-1}cm^{-1}$).

Plasma membrane permeability constant (k_{perm}) was calculated using equation 2,

$$\frac{[H_2O_2]_{in}}{[H_2O_2]_{out}} = \frac{k_{perm}}{k_{perm} + k_{catabolism}} \quad \text{(Equation 2)}$$

where $k_{catabolism}$ refers to the first-order rate constant describing the intracellular consumption of H_2O_2 by catalase (*i.e.* catalase activity); $k_{intact\ cells}$ to the constant for H_2O_2 consumption by intact cells, i.e. the apparent activity of catalase, and $k_{catabolism}$ to the rate constant for H_2O_2 consumption by permeabilized cells [48].

3.2.5 Determination of survival fractions

(a) *S. cerevisiae*

Yeast cells were cultured until mid-exponential phase and exposed to steady-state concentrations of H_2O_2 if adaptation was required. Culture aliquots were sequentially diluted were then serially diluted (10-fold dilution factor) to a 10^{-5} concentration and 100 µL were plated on YPD plates or SC ura$^-$ plates (without uracil) if working with transformant strains. The cultures were divided in two and a lethal dose of H_2O_2 (between 0.750 and 6 M) was added to one of the vials, being the other the control where no lethal dose of H_2O_2 was added. Liquid cultures were incubated for 60 min at 30 ºC, 160 rpm, after which an aliquot was plated in solid medium. Plates were incubated at 30 ºC for 48 h and cell colonies were counted [173]. The survival rates obtained were normalized against the survival rate of the appropriate control samples (plated before exposure to H_2O_2 and plated after 60 min, but not exposed to a lethal dose of H_2O_2).

(b) Jurkat T cells

100 µL of control or H_2O_2-exposed cells at a density of approximately 10^6 cells/mL were mixed with 10 µL of alamar blue in a 96-well plate and incubated at 37 ºC for at least 1 h. Fluorescence was read with excitation at 560 nm and emission at 590 nm. A blank sample not containing cells and one with no alamar blue were always performed simultaneously.

3.2.6 Total protein extraction

(a) Yeast

For total protein extraction 50 mL of culture were harvested by centrifugation at 1000 **g** for 5 minutes and washed once with 0.1 M potassium phosphate buffer, pH 7.4. Cells were centrifuged and the pellet ressuspended in 250 µL of the same buffer with 100 mM PMSF. The same volume of glass beads was added to the tube and cell lysis was obtained using a bench vortex 7 times for 1 min at maximum speed, with pauses of 1 min in ice. Glass beads and cell debris were pelleted by centrifugation at 530 **g** for 20 min at 4ºC and the supernatant containing the total protein extract was transferred to a new tube.

(b) Jurkat T Cells

Approximately 10^7 cells were harvested by centrifugation 900 **g** for 5 minutes, washed with PBS and ressuspended in 100 µL of lysis buffer (50 mM Tris-HCl pH 8, 150 mM NaCl, 1% Triton X-100) with protease inhibitors (100 mM PMSF, 1 mg/mL leupeptine, 0.15 mg/mL benzamidine and 0.1 mg/mL pepstatine). One small scoop of glass beads was added to the tube and the mixture was subjected to vortex for 40 seconds at medium speed. After adding 500 µL of lysis buffer and mixing well, the tubes were centrifuged for 5 min at 10 000 **g** and the supernatant containing the total protein extract was recovered to a new tube. All steps were performed at 4ºC and all tubes and solutions were kept on ice.

3.2.7 Protein quantification

Protein concentrations were determined by a modified Lowry method [174]. For the calibration curve bovine serum albumin (BSA) was used as a standard in concentrations between 10 and 50 µg/mL.

To 100 µL of diluted protein 1 mL of copper-tartarate reagent [1 volume of a solution of 0.1 % (m/v) $CuSO_4.5H_2O$, and 0.2 % (m/v) sodium tartarate; 2 volumes 5 % (m/v) SDS; 1 volume 0.8 M NaOH) was added, mixed and left for 10 min at room temperature. 0.5 mL of Folin reagent diluted 1/7 (v/v) was then added and mixed by vortex. After 1 h at room temperature the amount of protein was determined spectrophotometrically at 750 nm.

3.2.8 Determination of enzymatic activities

For the determination of all enzymatic activities total protein was extracted as described in 3.2.6.

3.2.8.1 Fas Activity

Fas activity in yeast was determined based on the protocol described in [175] with modifications in substrate concentrations since it was observed that the rate measured was not maximum when using the described concentrations. A mix of 2.5 mM EDTA, 10 mM cysteine, 0.3 mg/mL BSA, 0.24 mM acetyl-CoA, 0.15 mM NADPH, 20 µL of total protein extract, potassium phosphate buffer 0.1 M, pH 6.5 (to 1 mL final volume) was made in a 1 mL spectrophotometry cuvette. After mixing, absorbance at 340 nm was measured for 1 min at 25 ºC for blank determination since some residual decreased of absorbance was always measured. Afterwards 0.28 mM malonyl-CoA was added and absorbance at 340 nm was again followed for 1 min at 25 ºC. One unit of Fas activity is the quantity of enzyme that catalyses the reduction of 1 µmol of $NADP^+$/min at 25ºC and pH 6.5.

3.2.8.2 Catalase activity

For the determination of catalase activity a mix of 20 µL total protein extract and 880 µL of 0.05 M potassium phosphate buffer pH 7 with 1 mM DTPA was made in a spectrophotometer cuvette and absorbance at 240 nm was calibrated to zero. 10 mM H_2O_2 were added to the cuvette and the decrease of absorbance at 240 nm (ε_{H2O2} =43.4 $M^{-1}cm^{-1}$) was measured for 2 min at 25 ºC [176]. Data were plotted in a semi-logarithmic graphic and the activity (first-order rate constant) was obtained by the slope of the graph.

3.2.8.3 Cytochrome *c* peroxidase activity

Reduced cytochrome *c* was obtained by mixing oxidized cytochrome c with sodium dithionite in 100 mM sodium phosphate buffer pH 7.0 [177]. The reduced cytochrome *c* was then passed through a Sephadex G-100 chromatography column equilibrated with 0.25 mM phosphate buffer pH 7.4 with 1 mM DTPA (saturated in N_2) in order to remove all the excess dithionite. .The reduced cytochrome fractions were saturated with nitrogen and kept at -20 ºC until use. The concentration of reduced cytochrome *c* in each fraction was determined spectrophotometrically at 550 nm (ε =29 $mM^{-1}cm^{-1}$). For cytochrome c activity determination

20 µM cytochrome *c* were mixed with approximately 0.6 mg of total protein extract in 0.25 M phosphate buffer, pH 7.4, 1 mM DTPA [177]. The reaction was initiated by the addition of 50 µM H_2O_2 and followed spectrophotometrically at 550 nm for 4 min at 25 ºC. One unit is defined as the amount of enzyme needed for catalysis of the oxidation of 1 µmol of cytochrome *c* per min at 25 ºC and pH 7.4.

3.2.9 Western blot

Electrophoretical separation of proteins was made using a denaturating polyacrylamide gel with SDS (SDS-PAGE) using the BIORAD Mini-Protean II system [178]. For all studied proteins a 5 % acrylamide concentration gel [5% (m/v) acrylamide; 0.14 % (m/v) bis-acrylamide; 0.06 Tris-HCl pH 6.8; 0.1 % (m/v) SDS; 0.1 % (v/v) TEMED; 0.1 % (m/v) PSA] and a 8 % acrilamide resolution gel [8 % (m/v) acrylamide; 0.1 % (m/v) bis-acrylamide; 0.04 M Tris-HCl pH 8.8; 0.1 % (m/v) SDS; 0.05 % (v/v) TEMED; 0.05 % (m/v) PSA] were used. After quantification of total protein in extracts, the volume corresponding to 50 µg (for Pma1p studies in yeast) or 100 µg protein (for Fas studies in Jurkat T cells) was transferred to a new tube and water was added to a final volume of 60 µL. 15 µL of loading buffer 5x were added to a final concentration of 1 % (m/v) SDS; 5 % (v/v) glycerol and 0.08 M Tris-HCl pH 6.8; 0.002 % (m/v) bromophenol blue; 5 % (v/v) β-mercaptoethanol and the samples were heated to 100ºC for 5 min (except for studies of Pma1p, since this protein is temperature sensitive, samples were only heated to 30 ºC for 5 min) and the sample was applied to the gel. The separation was made using 0.025 M Tris base, 0.192 M glycine and 0.1 % (m/v) SDS as electrophoresis buffer with a current of 50 mA/gel. Proteins were transferred to a nitrocellulose membrane using a semi-dry electroblotting system and the membrane was stained with Ponceau S red. The membrane was blocked with 5 % nonfat dry milk in PBS, followed by immunoblotting using anti-Fas (Sc-57978; 1:1000) or anti-Pma1p (Sc-48357; 1:500) primary antibody and a secondary anti-mouse antibody conjugated to horseradish peroxidase (sc-2005; 1:2000). Incubation was performed overnight at 4ºC for primary antibodies and 1 h at room temperature for the secondary antibody. Signals were developed using the ECL chemiluminescence system and immunoblot films were digitalized and analysed with the ImageJ software [179]. Control of protein loading was performed by analysis of the membrane stained with Ponceau S red.

3.2.10 Gene expression analysis

3.2.10.1 Total RNA extraction from *S. cerevisiae*

Control and H_2O_2-adapted yeast cells were harvested in mid-exponential phase of growth (0.5 OD/mL) by centrifugation at 1000 **g** for 2 minutes washed once, ressuspended in 1 mL of distilled water and transferred to *Eppendorf* tubes. The cells were spun down and, the supernatant discarded, and the pellet was frozen in liquid nitrogen. Cells were kept at -80 ºC until usage. Total RNA was extracted using the Pure-yeast Ambion kit according to the manufacturer instructions. RNA concentration was determined by UV spectroscopy ($1A_{260nm}$~40 µg/ml single-stranded RNA). Protein contamination was checked by the ratio $A_{260nm}/A_{280nm.}$ Highly pure RNA should have $1.8< A_{260nm}/A_{280nm}<2$ [180]. The overall quality of RNA was assessed by electrophoresis in a denaturating agarose gel. Typically, for *Saccharomyces cerevisiae* high quality RNA, two bands should be seen corresponding to the 18S (migrating as ~1800 nt) and 28S (migrating as ~3000 nt) ribosomal RNA (rRNA). The intensity of the 28S band should be about twice that of the 18S band. Smaller RNAs as tRNA and 5S rRNA are seen as smaller and more diffuse bands and genomic DNA contamination appear as a high molecular weight smear.

3.2.10.2 RNA probe synthesis

Synthesis of probes for the detection of the *FAS1* gene product was performed by random priming PCR with digoxigenin-dUTP labelling mixture as described by the manufacturer. As primers the following oligonucleotides were used:

Table 7. Sequence of the primers used for amplification of DNA fragments for plasmid cloning. The blue small letters indicate Not1 restriction sites.

Description	Nucleic acid sequence	Tm (ºC)
upstream primer	AAACAgcggccgcCATTATGGACGCTTACTCC	56
downstream primer	AAACAgcggccgcTAGAGCAGAACTTCGCTAA	54

3.2.10.3 Northern blot

RNA was separated in a 1.5 % agarose gel with 1 % formaldehyde in RNA buffer 1x (0.2 M MOPS, 50 mM sodium acetate pH 7.0, with 5 mM sodium EDTA,) with ethidium bromide, using RNA buffer 1x as electrophoresis buffer. The loading mix was prepared by mixing enough RNA for an amount of 25 µg, 5 µL RNA buffer, 7 µL formaldehyde, 20 µL formamide and 3 µL loading buffer (50 % (v/v) glycerol, 1 mM EDTA, 0.4 % (v/v) bromophenol blue, 0.4 % (v/v) xylene cyanol).

Samples were mixed, heated to 55 ºC for 15 min and loaded in the gel lanes. A differential potential of 37 V was applied overnight and the gel was visualized under UV light (λ= 254 nm) for loading confirmation.

The gel was washed three times in distilled water and once in H_2O with 0.1 % (v/v) DEPC. The gel was equilibrated in a 3 M NaCl, 0.3 M trisodium citrate buffer (SSC) for 45 min and the transference system was mounted. Using a bridge of 3MM paper in order to flow the SSC to the transfer system, the membrane was laid over the gel (putting some 3 MM paper at both ends) and tissue paper was overlaid with a height enough in order not to be saturated with buffer during the 16 h of transfer. A 1 kg weight was put on the top of the system. The system was left for 16 h in order to let the SSC flow to transfer the RNA from the agarose gel to the nitrocellulose membrane. RNAs were fixed in the membrane by heating it to 80 ºC for 2 h.

Membranes were washed twice in washing buffer (1 % (w/v) SDS, 20 mM Na_2HPO_4 pH 7.2 with 1 mM EDTA) at 65 ºC, pre-hybridized for 1 h at 65 ºC in 20 % (w/v) SDS, 0.5 % blocking reagent (Boehringer), 250 mM Na_2HPO_4 pH 7.2 with 1 mM EDTA and hybridized overnight in the same conditions with a labelled probe (internal to the *FAS1* open reading frame) at 2 ng/mL. Labelling had been performed by random priming PCR with digoxigenin-dUTP labelling mixture (Boehringer). Membranes were washed twice at 65 ºC with washing buffer, and immunodetection steps were carried out as described by the manufacturer (Boehringer) using CDP* (Tropix) as chemiluminiscent substrate. Signals were detected and quantified with a Lumi-Imager equipment (Boehringer).

3.2.11 Yeast transformation and plasmid construction

DNA extraction, purification, quantification and integrity check and polymerase chain reaction amplification were performed by standard methods [181].

3.2.11.1 Yeast transformation

Yeast cells were transformed using the lithium acetate procedure [182]. Cells were grown in YPD medium and around 10^8 cells were harvested by centrifugation. The pellet was washed and ressuspended in 50 µL lithium acetate/tris-EDTA buffer (10 mM Tris-HCl, pH 7.5 with 1 mM EDTA) and added to the transformation mix containing approximately 1 µg DNA sequence to insert, 1 µg single stranded DNA in lithium acetate/tris-EDTA buffer and PEG in lithium acetate/tris-EDTA to a final concentration of 30% (v/v). The mix was incubated for 30 min at 30 ºC and subjected to a thermal shock at 42 ºC for 15 min after which it was diluted in 10 mL of YPD and incubated for 37 ºC for 4 h. Finally the cells were harvested by centrifugation, concentrated in a small volume of YPD, and plated in YPD medium containing the adequate selective antibiotic (geneticin).

For yeast transformation with the non-integrative plasmid a shortened method was used where the 4 h growth step was eliminated and the transformants were immediately plated after thermal shock in ura^- plates (since the used yeasts are autotrophic for uracil but the used plasmid contains the *URA3* sequence; more details further).

3.2.11.2 Escherichia coli transformation

Bacterial transformation was performed by the standard calcium chloride method [181]. Competent DH5α cells were mixed with excess plasmid and incubated on ice for 10 min, followed by a thermal shock at 42 ºC for 2 min and an 1 min incubation on ice. LB medium was added to the mix and cells were incubated for 1 h at 37ºC. Cells were then plated in LB/ampicillin plates and incubated at 37 ºC until colonies were visible.

3.2.11.3 Plasmid construction

Two strategies were used in order to obtain cells with *FAS1* under the control of a doxycycline regulatable promoter. The first one involved the direct substitution of the native promoter in the yeast genome by integrative transformation **(a)** [183] and the second one the transformation with a non-integrative, high copy, self-replicative plasmid containing the *FAS1* open reading frame under control of the regulatable promoter **(b)** [184].

(a) The regulatable promoter was amplified by PCR from pre-existing plasmids [183]. In order to obtain recombination of the amplified fragments with the yeast genome the PCR

primers were constructed in order to add homologous regions to the promoter region of the *FAS1* ORF to the final amplification product.

Table 8. Sequence of the primers used for amplification of the cloning DNA fragments for promoter substitution. Small letters represent non homologous tail inserted for recombination.

Description	Nucleic acid sequence	Tm (ºC)
1st upstream primer	GGCCTTTTCATACTTGTTATCACTTACATTACAG	56
	AAGAACAAACAcagctgaagcttcgtaacgc	
2nd upstream primer	AAGAAACTACAAGAACATCATCCGGAAAATCAG	58
	ATTATAGACTAGGcagctgaagcttcgtacgc	
Downstream primer	AACCGTGAGATAGGGTTAATGGTCTTGTGGAGT	58
	AAGCGTCCATAATGgcataggccactagtggat	

(b) The *FAS1* Open Reading Frame was inserted in a plasmid (pCM189), harbouring the doxycycline regulatable promoter with 7 *tetO* boxes [184]. This was achieved by amplification of *FAS1* from the yeast genome using primers containing a tail sequence with restriction *loci* that, after digestion with the appropriate restriction enzymes, would form compatible ends with the ones formed in the pCM189 plasmid after similar digestion. The used primers were the same as those in Table 7.

After amplification and purification of the PCR amplification products, digestion with Not1 was performed both in the amplification fragments and in the vector plasmid. Digestion of the plasmid and PCR products was confirmed by visualization in an agarose gel. After treatment of the vector with alkaline phosphatase, in order to avoid plasmid re-ligation, ligation was performed and the resulting plasmids transformed in *E.coli* for amplification. Correct direction of the insert was confirmed by digestion with Pst1 (knowing that the vector plasmid has 8370 bp and the *FAS1* insert 6450 bp and that Pst1 restriction site is at nucleotide 151 of the insert and nucleotide 2559 of the vector). The correctly constructed plasmids were finally inserted in the *fas1*Δ strain and regulation of *FAS1* was confirmed by northern blot (see Results).

3.2.12 Cell wall integrity

Possible differences in cell wall structure in yeast cells were tested by SDS [185] and yeast lytic enzyme [186] sensitivity. For SDS sensitivity tests cells were cultured until mid-exponential fase, harvested by centrifugation at 5000 **g** for 5 min and washed with 0.1 M potassium phosphate buffer, pH 7.4. Serial dilutions (between 10^{-1} and 10^{-5}) were plated in YPD plates containing SDS [0-0.02 % m/v)]. Plates were incubated at 30 ºC for 48 h before visualization.

For yeast lytic enzyme sensitivity test cells were harvested when in mid-exponential phase, washed with 50 mM tris-HCl, pH 9.4 and ressuspended in the same buffer. Samples of 1 mL were transferred to 1 mL cuvettes and 0.2 units of yeast lytic enzyme were added (One lytic unit is defined as the quantity of enzyme catalyzing a 10% decrease in optical density at 600 nm (OD600) at 30℃ for 30 min). Cuvettes were kept 30 ºC and cell wall digestion was followed by measuring the absorbance at 600 nm of cell suspensions with 10-min intervals, during 90 min.

3.2.13 Plasma membrane composition studies

3.2.13.1 Plasma membrane isolation

Plasma membrane isolation and purification was made according to [187] with some minor modifications. Cells were cultured in 1 L of YPD medium until the mid-exponential phase. Cells were adapted using a steady state 150 µM of H_2O_2 for 90 min before harvesting. All centrifugation steps were performed at 4 ºC and the tubes and solutions were maintained in ice along all the isolation procedure. Cells were harvested by centrifugation at 5000 **g** for 5 min and washed with a 0.4 M sucrose solution in 25 mM imidazole-HCl pH 7.0. Cells were centrifuged at 5000 **g** for 5 min and the pellet was ressuspended in 1.5 mL of the same solution where a mixture of protease inhibitors (100 mM PMSF, 1 mg/mL leupeptine, 0.15 mg/mL benzamidine and 0.1 mg/mL pepstatine,) and 2 mL of glass beads were added. Cell lysis was achieved by *vortexing* cells in a bench *vortex* for 2 min. This mixing was performed for 3 times with 2 minutes interval on ice. Glass beads and cell debris were pelleted by centrifugation at 530 **g** for 20 min. The supernatant containing impure plasma membranes was transferred to a new tube and centrifuged at 22000 **g** for 30 min. The obtained pellet was ressuspended in 2 mL of 25 mM imidazole-HCl buffer pH 7.0 containing the protease inhibitor mix and applied in the top of a discontinuous gradient composed by three layers of 2.25 M (11.5 mL), 1.65 M (11.5 mL) and 1.1 M (10.5) of sucrose in 25 mM imidazole-HCl pH

7.0. The gradient was centrifuged at 80000 **g** for 18 h in a SW18 swinging bucket rotor (Beckman Coulter Inc.). The purified plasma membranes were recovered from the interface between the 2.25 M and 1.65 M sucrose layer of the gradient and diluted in 25 mM imidazole-HCl pH 7.0 buffer and centrifuged at 30000 **g** for 40 min. The purified plasma membrane pellet obtained was ressuspended in 1 mL of 25 mM imidazole-HCl pH 7.0.

3.2.13.2 Lipid extraction

Lipid extraction was performed from plasma membrane extracts using the Folch method [188]. Lipids were extracted with 20 volumes of a mix of chloroform/methanol (2:1, v/v), added to the plasma membrane extract (a small aliquot was taken before this addition in order to perform protein quantification). A solution of 0.88 % (m/v) KCl was added and the phases were left to separate at -20 ºC. The organic layer containing the lipid fraction was transferred to a new vessel and dried under nitrogen and ressuspended in the adequate solvent in the desired concentration.

3.2.13.3 2D thin-layer chromatography separation of phospholipids

The dried lipid extract was ressuspended in 100 µL of chloroform/methanol (1:1, v/v). A 10 µL aliquot was taken for total phospholipid quantification and the remaining was applied with a glass capillary tube in a 20x20 cm thin-layer chromatography silica gel G60 plate. The sample was applied in the lower left corner of the plate in a small spot and the plate was developed in the first dimension with chloroform/methanol/ammonia (65:35:5, v/v/v). The plate was then well dried, turned 90º clockwise and developed in the second dimension with chloroform/acetone/methanol/acetic acid/water (50:20:10:10:5, v/v/v/v/v) [189]. The phospholipid spots were visualised by iodine staining and marked with a pencil since the staining is reversible.

3.2.13.4 Phospholipid quantification

Phospholipid spots were scraped and transferred to clean glass tubes (it is very important to use tubes that have never been used for another technique and to never use detergents when washing them since detergent phosphates adsorbed to the tube walls will react). Silica from 3 different areas of the plate where no spots were seen with the iodine staining was also scraped out in order to be used as blanks. Inorganic phosphorous was obtained by acid

hydrolysis with 0.3 mL of 70 % (v/v) perchloric acid and heating at 170ºC for 45 minutes. Care was taken so that tubes were covered in order to avoid sample evaporation but not tightly closed in order not to accumulate gases and explode due to high pressures. Samples were cooled to room temperature and 1 µL of distilled water, 400 µL of 1.24 % (w/v) ammonium molybdate and 400 µL of 5 % (w/v) ascorbic acid were added and the tubes were incubated at 100 ºC for 5 min. In order to eliminate silica in suspension the samples were centrifuged for 20 minutes at 5000 **g**. The supernatant was recovered and absorbance at 797 nm was measured spectrophotometrically. A standard curve with of 0.05 to 0.3 mM NaH_2PO_4 was also made.

3.2.13.5 Fatty acid methylation and quantification by GS-MS

The dry lipid extracts were dissolved in 3 mL of a mix of methanol/HCl (5:1, v/v) and incubated for 24 h at 50 ºC in closed glass tubes [190]. This mix was then cooled to room temperature and 5 mL of a NaCl solution 5 % (w/v) were added. Fatty acids were extracted 2 times with 5 mL of n-hexane and the extract washed with 4 mL of 2 % (m/v) potassium bicarbonate. The resulting organic phase was dried under nitrogen. A solution of 1 mL of 14 % (m/v) borum trifluoride in methanol was added and the tubes were incubated in a sand bath at 100 ºC for 15 min in order to completely methylate all the fatty acids [191]. The tubes were cooled to room temperature and the methylated fatty acids extracted with 1 volume of water and 2 volumes of n-heptane. The mixture was mixed in a vortex and left until phase separation. The organic layer was collected to a new tube and dried under nitrogen atmosphere. The dried extract was finally dissolved in 200 µL of n-hexane for posterior analysis by GC-MS where 2 µL aliquots were used in splitless mode. GC-MS oven temperature was programmed to 100 ℃ for 1 min foll owed by a temperature ramp from 150 ℃ to 300℃ at a rate of 10 ℃/min and finally 10 m in at 300 ºC. The qualitative identification of the fatty acids was made by comparison with commercial standards or comparison with mass spectra in commercial libraries. The quantitative analysis was made with comparison with response factors to the correspondent commercial fatty acid methyl esters. Heptadecanoic acid (C17:0) was used as internal standard since it is not present in yeast.

3.2.14 Biophysical studies with fluorescent probes in intact cells

For the biophysical studies yeast cultures were grown to mid-exponential phase of growth, harvested by centrifugation at 5000 **g** for 5 min, washed twice with sterile water and then suspended in 100 mM sodium phosphate, 100 mM sodium chloride, 1 mM EDTA, pH 7.4

(fluorescence buffer) to a density of 0.6 OD_{600}/mL. The probe, dissolved in ethanol, was added to the cells to a final concentration of 2 μM (for both DPH and t-Pna), and incubated during 20 min for DPH and 5 min for t-Pna at room temperature or at controlled temperature, when necessary. The ethanol added was kept in a range which does not affect membrane properties. The same ethanol volume used to dissolve the probe was added to the cells as a control. After incubation, cells were immediately washed twice with and suspended in the same volume of buffer.

For the studies with Jurkat T cells an optimization of the cell concentration and fluorescent probe concentration was made and it was determined that the best conditions for the experiments would be cells at a cell density of 1 million cells/mL and 2 μM t-PnA. Cells were harvested, washed once with PBS, and ressuspended in fluorescence buffer in the same density. Intact cells were afterwards incubated with 2 μM t-PnA for 2 min at room temperature. In all cases groups of control and H_2O_2-treated cells for comparison were used in each experiment in order to guarantee similar experimental conditions for compared samples (especially regarding temperature). Fluorescence measurements were made on a Horiba Jobin Yvon FL-1057 spectrofluorometer equipped with double monochromators in excitation and emission at a 90º angle, Glan-Thompson polarizors. As radiation source an arch 450 W Xe lamp and a reference photodiode were used.

3.2.14.1 Steady-state fluorescence spectroscopy

For DPH studies in yeast excitation was made at 358 nm and emission measured at 430 nm, using 1 cm x 1 cm quartz *cuvettes* and 4 nm emission and excitation slits. The probe was incorporated for 20 min with a concentration of 2 mM [95]. For t-PnA studies both in yeast and Jurkat T cells, excitation was made at 320 nm (although the excitation maximum of the probe is 303nm, this was the wavelength used in order to avoid the excitation of aromatic amino acids present in proteins) and the emission was measured at 404 nm. A 1 cm x 0.4 cm quartz cuvette and 4 nm slits were used [192].

3.2.14.2 Emission and excitation spectra

For both *S. cerevisiae* and Jurkat T cells the emission and excitation spectra were obtained using a 2 nm emission and excitation slits in the absence of polarizers. The spectra were corrected with correction files provided by the manufacturer.

3.2.14.3 Steady-state anisotropy

The steady state anisotropy <*r*> was determined according to the equation [193]:

$$\langle r \rangle = \frac{I_{VV} - G \times I_{VH}}{I_{VV} - 2G \times I_{VH}}$$

(Equation 3)

where G is the polarizer instrumental correction factor given by the ration I_{HV}/I_{HH} [193] and V and H represent respectively the vertical and horizontal orientation of the polarizers. The first letter will correspond to the excitation polarizer and the second to the emission polarizer. For the anisotropy determination the value obtained with the blank sample was subtracted for each component individually before the calculation. In order to maintain a constant temperature the measurements were made using a recirculation water system with stirring.

3.2.14.4 Time-resolved fluorescence decay

Time-resolved fluorescence measurements were made in a Horiba Jobin Yvon FL3-22 spectrofluorimeter using the time-correlated single-photon counting (TSCPC) technique as described in [193]. This technique is based on the principle that the probability distribution of the emission of a photon in a determined time t is given by the temporal distribution in the form of a histogram of every photon emitted by the sample. The fluorescence lifetime (τ) can be defined as the characteristic time that a fluorophore resides in the excited state before returning to the ground state and is given by the formula,

$$I(t) = \sum_i \alpha_i \exp(-t / \tau_i)$$

(Equation 4)

where I is the fluorescence intensity and α_i the normalized pre-exponential to the unity and τ_i the lifetime of the component i [193].

Depending on its nature and photophysical properties, each fluorophore has a typical fluorescence lifetime, which can be affected by the local environment where it is inserted. When *trans*-parinaric acid is located in more ordered environments, a lifetime component appears in its fluorescence intensity decay with values ranging from ~20 ns up to ~50 ns depending on the type of lipid domain (raft-like or solid-like) [194].

The cell samples incubated with t-PnA were excited at 315 nm with a nanoLED-320 from Horiba Jobin Yvon. The emission was received at 404 nm and the time scale used was 111.0 ps/channel. A 1 cm x 0.4 cm cuvette and 4 nm slits were used [192].

3.2.15 Microscopy studies

3.2.15.1 Filipin staining

Living cells were harvested by centrifugation in the mid-exponential phase (0.5 OD_{600}/mL), washed once in SC medium, and concentrated 10 times in the SC growth media (phosphate buffers were tested and it was observed that filipin fluorescence is quenched in these media). Incubation with filipin was made directly on microscope slides, immediately before observation (0.5 µL of a 5 mg/mL filipin stock solution in ethanol was added to 10 µL of cell suspension). Fluorescent images were acquired using a PCO Sensicam-QE camera (Labocontrole, Lisbon, Portugal) attached to an Olympus IX-50 microscope using an Olympus X100 UplanApo (N.A.=1.40) objective. The exposure time was controlled through Image Pro-Plus 5.0 software (Media Cybernetics, Leiden, The Netherlands) and set constant throughout the experiments. Fluorescence excitation and emission were accomplished through a wide-band U-MWU2 filter block and, to reduce filipin bleaching, a 50k neutral density filter was used, together with the excitation filter. Image processing and data extraction, including the heterogeneity profile of cell membranes, were performed with Image Pro-Plus.

3.2.15.2 GFP constructs

Wild type and *fas1*Δ cells were transformed with the integrative plasmid Ylp211-*CAN1*-GFP (URA3, ampR), a kind gift from Dr. Widmar Tanner [126]. Yeast cells were transformed as previously described (3.2.11.1).

Optical sections with 2 µm course were acquired with a confocal microscope Leica SP-E CSLM using <20% of laser intensity, operation mode 512x512, 400 Hz (1/4 s per frame) with a x63 Plan Apo objective (NA=1.4). In order to allow quantification, gain and compensations were maintained constant. Image processing and data extraction, including the heterogeneity profile of cell membranes, were performed with Image Pro-Plus.

3.2.15.3 Immunofluorescence

Yeast cultures (5 mL) were grown in YPD to mid-exponential phase (0.5 OD_{600}/mL) and 500 µL of 37% formaldehyde was added directly to the culture (for a final concentration of 3.7 %) and incubated for 2 h at 30 ºC, 160 rpm. 1 mL of cells was harvested by centrifugation, washed with 0.1 M potassium phosphate buffer pH 7.4, ressuspended in the same buffer containing 5 mg/mL yeast lytic enzyme 50T and 1.42 M β-mercaptoethanol and incubated 1-1.5 hour at 37ºC. Spheroplasting was checked by mic roscopy, since cells with no cell wall lose the normal "shiny" appearance. Coverslip slides were covered with 1 mg/ml polylysine for 15 min and let dry. Around 20 µL of fixed and permeabilized cells were pipetted in the slides and left for about 5 min, after which the remaining liquid was aspirated. Coverslips were washed 3 times with PBS and left to dry. For blocking unspecific sites, 20 µl of PBS + 1 mg/mL BSA were pipetted to the coverslip and incubated for 30 min in a humid chamber, taking care in order to not let them dry from this point on. The blocking solution was aspirated and the coverslips washed 3 times with PBS. The coverslip was covered with 20 µL of diluted primary antibody (anti-Pma1p (Sc-48357; 1:50)) and incubated overnight at 4ºC in a humid chamber. The next day the primary antibody was aspirated, the slide washed 3 times with PBS and the secondary antibody added. Incubation was performed in the dark for 1 h at room temperature. After incubation the secondary antibody solution was aspirated off and washed 3 times with PBS. One drop of mounting solution was pipetted to the top of the coverslip and put on a microscope slide. Excess of mounting solution was blotted with a kimwipe and the coverslip sealed with nail polish and stored at -20ºC in the dark until visualized. Confocal microscopy conditions were the same as used for GFP visualization.

3.2.16 Microscopy with FTIC-conjugated cholera toxin

Cells were harvested, washed once with chilled PBS and fixed for 5 min on ice with 1% (v/v) paraformaldehyde. Cells were washed with PBS with BSA and then incubated with 6 µg/mL cholera toxin-FITC for 20 min. After washing with PBS-BSA, cells were immobilized in polylysine-coated microscope slides and mounted as described for yeast in section 3.2.15.

3.2.17 Flow Cytometry

GFP-transformed cells were grown to mid-exponential phase, harvested by centrifugation and ressuspended in PBS. Samples were analyzed on a FACScan flow cytometer (Becton Dickinson Immunocytometry Systems, BDIS) equipped with a 15 mW air-cooled 488 argon-

ion laser. Green GFP fluorescence was collected after a 530/30-nm bandpass (BP) filter. On each sample, a minimum of 10000 events was collected. Analysis of the multivariate data was performed with CELLQuesty software.

3.2.18 Digitonin sensitivity

Jurkat T cells were incubated with 1 mg/mL propidium iodide for 5 min, and 10 µg/mL of digitonin was added to the mixture. Incorporation of propidium iodide was followed along time by flow cytometry as described in [193].

4 Results I - Modulation of Fas expression by H_2O_2

A novel mechanism of adaptation to H_2O_2 – a decrease in plasma membrane permeability towards H_2O_2 thus making H_2O_2 diffusion into cells more difficult - was discovered recently in *S. cerevisiae* cells [57]. Since fatty acids play an important role as source of metabolic energy and as building blocks of membrane lipids, being able to influence membrane fluidity and also receptor or channel function, it seemed important to study their involvement in plasma membrane modulation by H_2O_2. Moreover, microarray analysis of *S. cerevisiae* gene expression in control and H_2O_2-adapted cells (work developed by former group member Nuno Pedroso for his PhD thesis [66, 107]) showed a down-regulation of about 1.5 fold of the expression of the *FAS1* gene, which codes for one of the fatty acid synthase (Fas) subunits after 15 min exposure to a steady-state concentration of 150 μM of H_2O_2. Here it is confirmed that the relation between adaptation to H_2O_2 and Fas down regulation.

In this study diploid strains were used since a *fas1*Δ mutant strain was required and *fas1*Δ strains derived from a haploid strain such as BY4741 are not viable unless the growth medium is supplemented with fatty acids [195]. This uptake of fatty acids supplemented in the media would provide an exogenous source of variability in plasma membrane fatty acid composition that is undesirable, considering the aim of this work.

4.1 Bolus addition versus steady-state H_2O_2 delivery

In a bolus addition, a single dose of H_2O_2 is added to the culture while in a steady-state addition glucose oxidase is added simultaneously in order to counteract H_2O_2 consumption by cells (see section 3.2.3 for more details on the method).

In order to understand how H_2O_2 concentration changes along the time of the experiment depending on the used technique, *S cerevisiae* wt cells were exposed either to 100 or 150 μM of H_2O_2 using the bolus and steady-state delivery methods and H_2O_2 concentration in the growth media was monitored along time (Figure 14).

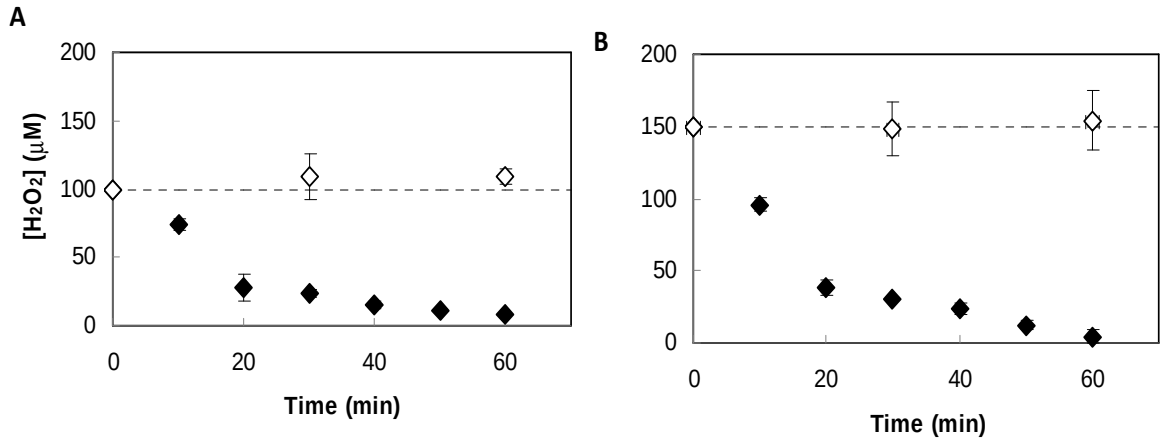

Figure 14. H_2O_2 concentration is near constant along time after steady-state cell exposure to H_2O_2 but is almost negligible 60 minutes after a bolus addition. H_2O_2 concentration in the growth media was measured every 10 min after a steady-state (open symbols) and a bolus (closed symbols) addition of H_2O_2 to wt cells at a cell density of 0.6 OD/mL. A - initial concentration of 100 μM H_2O_2; B- initial concentration of 150 μM H_2O_2.,Results are the mean ± SD; (n = 3).

In the bolus addition approach, an initial dose of H_2O_2 was given, which was rapidly consumed by the cellular antioxidant systems. In the present case, more than 50 % of the H_2O_2 added was consumed by *S. cerevisiae* cells during the first 20 min of incubation, and after 60 min the H_2O_2 concentration was negligible. Contrarily, when the steady-state approach was used, the concentration was maintained near constant along time, guaranteeing a constant delivery of H_2O_2 to the cells along time and the reproducibility of the experimental conditions.

S. cerevisiae haploid cells pre-exposed to steady-state 150 μM H_2O_2 for 15 min up to 90 min adapt, presenting a higher ability to survive to a subsequent exposure to a lethal dose of this oxidizing agent [57, 95]. In order to test if adaptation also occurs when diploid cells and if is dependent of the H_2O_2 delivery method, cell survival to a lethal dose of H_2O_2 (750 μM) was measured after a steady-state or bolus addition of an adaptive dose of H_2O_2 (150 μM) (Figure 15).

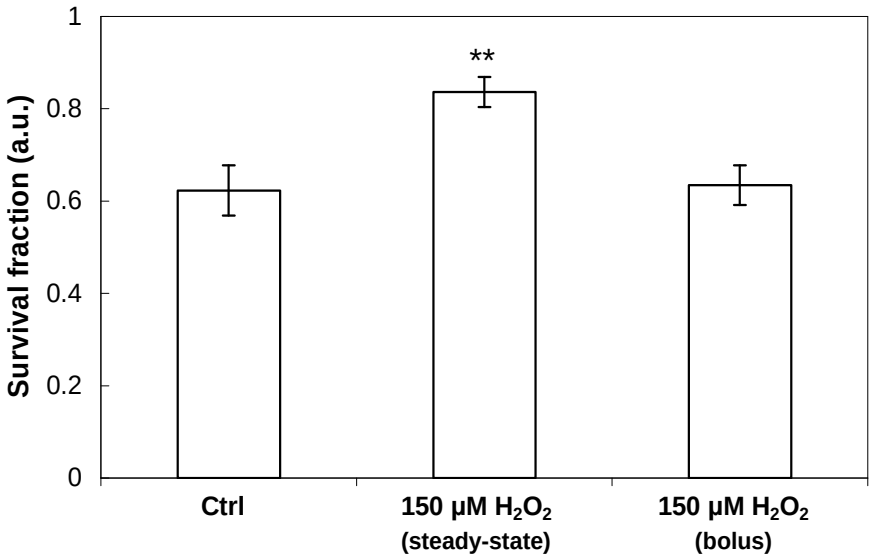

Figure 15. Cell survival to lethal doses of H_2O_2 increases in cells exposed to steady-state but not to bolus addition of H_2O_2. Survival fractions were determined in wt control cells and in H_2O_2-exposed cells (150 µM of H_2O_2 for 90 min) at a cell density of 0.6 OD/mL using the steady-state or bolus delivery method. Results are the mean ± SD; (n = 3). * P < 0.01, vs control.

In Figure 15 it can be seen that when the pre-exposure to 150 µM H_2O_2 is made using a bolus addition, adaptation does not occur, as cells pre-exposed to H_2O_2 present the same survival fraction as control cells. This result is not surprising, since studies in yeast adaptation to H_2O_2 using a bolus addition are usually performed using much higher concentrations of H_2O_2. Initial works in *S. cerevisiae* adaptation to H_2O_2 indicated that a challenge of 400 µM H_2O_2 (bolus addition) for 45 min was the most effective treatment to observe adaptation to H_2O_2 in *S. cerevisiae* cells [59]. Others exposed cells to doses as high as 700 µM H_2O_2 for 1 h in order to see the protective effect to a subsequent challenge with higher concentrations of these oxidants [17]. In more recent studies in Yap1 activation during adaptation cells were exposed to 300 µM H_2O_2 (bolus addition) for 1 h in order to see an adaptive response [61]. Once again it is important to reinforce that, since bolus additions were used, only the initial concentration of H_2O_2 is known, since cell consumption will lead to a decrease in H_2O_2 concentration along time. This is the main reason why such high concentrations are needed in order to observe adaptation. However, in our laboratory, haploid wt (BY4741) cells exposed to 300 µM H_2O_2 (bolus addition) for 1 h showed a decrease of about 30 % in the survival fraction ([196]) showing that this high dose is already lethal to the cell. In the steady-state delivery, although a lower concentration of H_2O_2 is initially added to the growth medium, the concentration is constant along time. Therefore

cells are exposed to a higher load of H_2O_2 in the whole experiment, which explains why adaptation is observed with such low concentrations of H_2O_2.

4.2 Fatty acid synthase down-regulation in adaptation to H_2O_2

As referred before, microarray studies in haploid H_2O_2 adapted cells showed a decrease in the expression of the *FAS1* gene, which codifies for the β sub unit of Fas [66]. This decrease was confirmed by Northern blot. *FAS1* mRNA levels decreased to about 90 % and 80 % of control levels after exposure to 150 μM H_2O_2 for 15 and 30 min respectively, returning to control levels after exposure to H_2O_2 for 60 min (Figure 16).

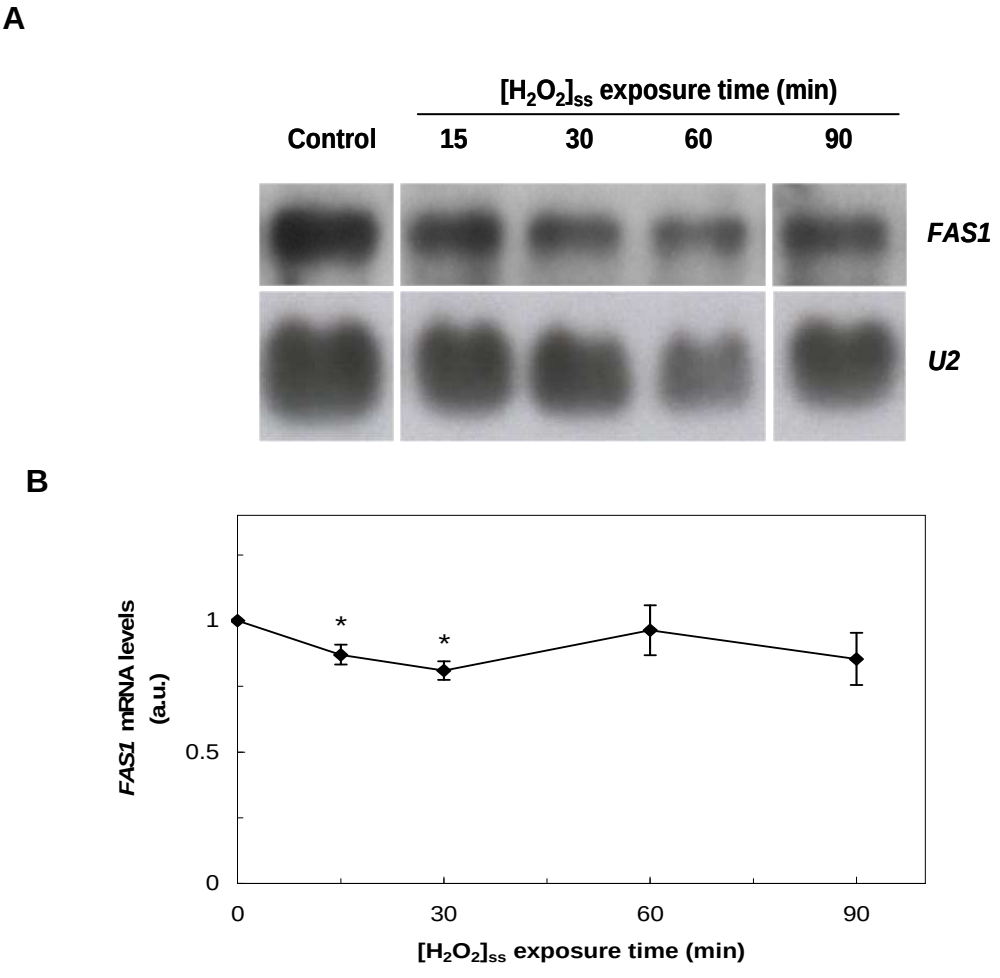

Figure 16. Adaptation to H_2O_2 causes a repression of *FAS1* expression in haploid wt cells. Samples of total mRNAs (30 μg) from haploid wt (BY4741) control cells or haploid wt cells treated with a 150 μM steady-state H_2O_2 concentration ($[H_2O_2]_{ss}$) were prepared and analyzed by Northern blot. A - transcripts in a representative experiment; B - quantitative representation of transcript. Results are the mean ± SD; (n = 3). U2 transcripts were used as an internal control. * $p < 0.05$ vs control.

Since differences in gene expression and regulation between haploid and diploid cells subjected to ethanol stress have been already described [197], it was necessary to confirm the existence of the same regulatory effect of H_2O_2 in Fas. Down-regulation of *FAS1* in adaptation by exposure to a steady-state adaptive concentration of H_2O_2 in the diploid strain was confirmed by northern blot (Figure 17).

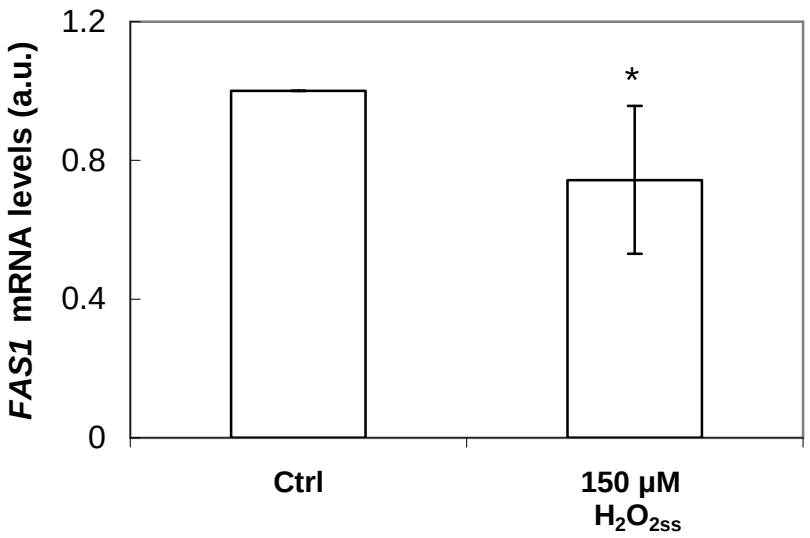

Figure 17. *FAS1* gene expression decreases adaptation to H_2O_2 in the diploid strain. Samples of total mRNAs (30 µg) from wt (BY4743) control cells and wt cells, treated with 150 µM H_2O_2 in steady-state (H_2O_2ss) for 60 min, at a cell density of 0.6 OD/mL were prepared and analyzed by Northern blot. Results are the mean normalized to control ± SD; (n = 3). U1 transcripts were used as an internal control. * $p < 0.1$ vs control.

Although *FAS1* expression was altered in H_2O_2-exposed cells, it was important to determine if Fas activity was also affected, since Fas activity is directly regulated by the levels of the *FAS1* product [162]. Fas activity decreased about 10 % after 60 min and to about 60 % of that in control cells after 90 min of exposure to 150 µM of H_2O_2, (Figure 18). In order to assure that the measured decrease in activity was not due to oxidation of the active center SH group, activity in H_2O_2-adapted cells was measured in the presence or absence of added cysteine (10 mM) or DTT (10 mM). In each condition there was no measurable change in Fas activity, guaranteeing that no enzyme inactivation was due to oxidation of SH groups involved in catalysis during exposure to steady-state H_2O_2 (Table 9).

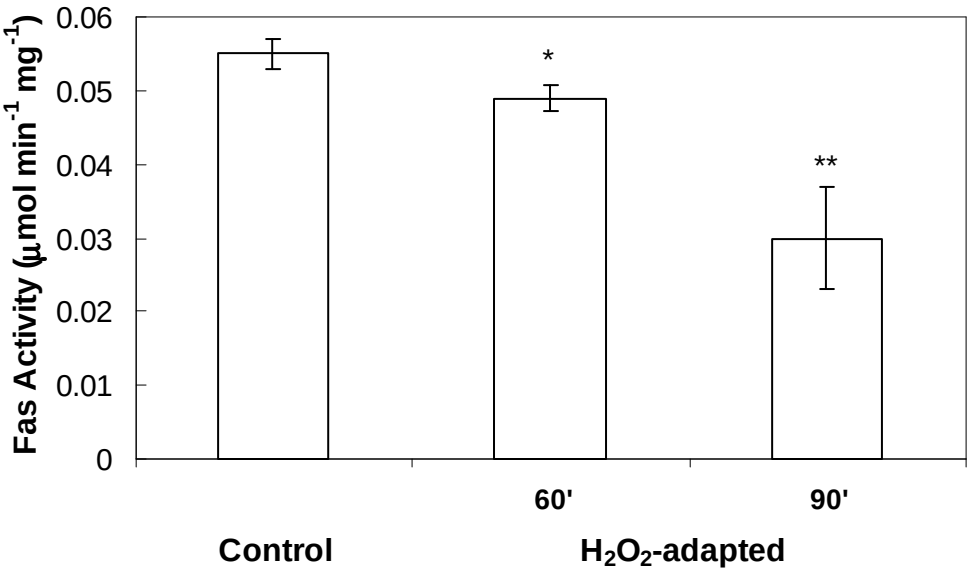

Figure 18. Fas activity decreases during adaptation to hydrogen peroxide. Fas activity was determined in wt cells (BY4743) subjected to a 150 µM steady-state H_2O_2 concentration ($[H_2O_2]ss$). mean ± SD; (n = 3). * p < 0.05 vs control, P<0.01 vs control.

Table 9. The decrease of Fas activity during adaptation to H_2O_2 is not due to oxidation of SH groups involved in catalysis. Fas activity in wt (BY4743) H_2O_2- adapted cells (150 µM steady-state H_2O_2 for 90 min) was measured in the absence of DTT and cysteine, in the presence of DTT and in the presence of cysteine. Results are the median ± SD; (n = 3).

Cysteine (mM)	DTT (mM)	Fas activity (µmol min^{-1} mg^{-1})
0	0	0.036 ± 0.04
10	0	0.036 ± 0.01
0	10	0.030 ± 0.07

4.2.1 Biphasic regulation of Fas by H_2O_2

In 2009 Kelley *et al* published a work [60] where yeast cells exposed to 100 and 150 µM H_2O_2 for 1 h presented an increase of *FAS1* expression (being not significant for the higher dose) instead of a down-regulation. The major difference between the two works was the mode by which yeast cells were exposed to H_2O_2. Kelley used a *bolus* addition of H_2O_2, while in this work a *steady-state* approach was used [57, 198]. Therefore, it was mandatory to

study whether H_2O_2 was delivered to cells influenced the results obtained for Fas regulation by H_2O_2.

FAS1 mRNA levels were measured in control cells and in cells exposed to different steady-state and bolus concentrations of H_2O_2 (Figure 19).

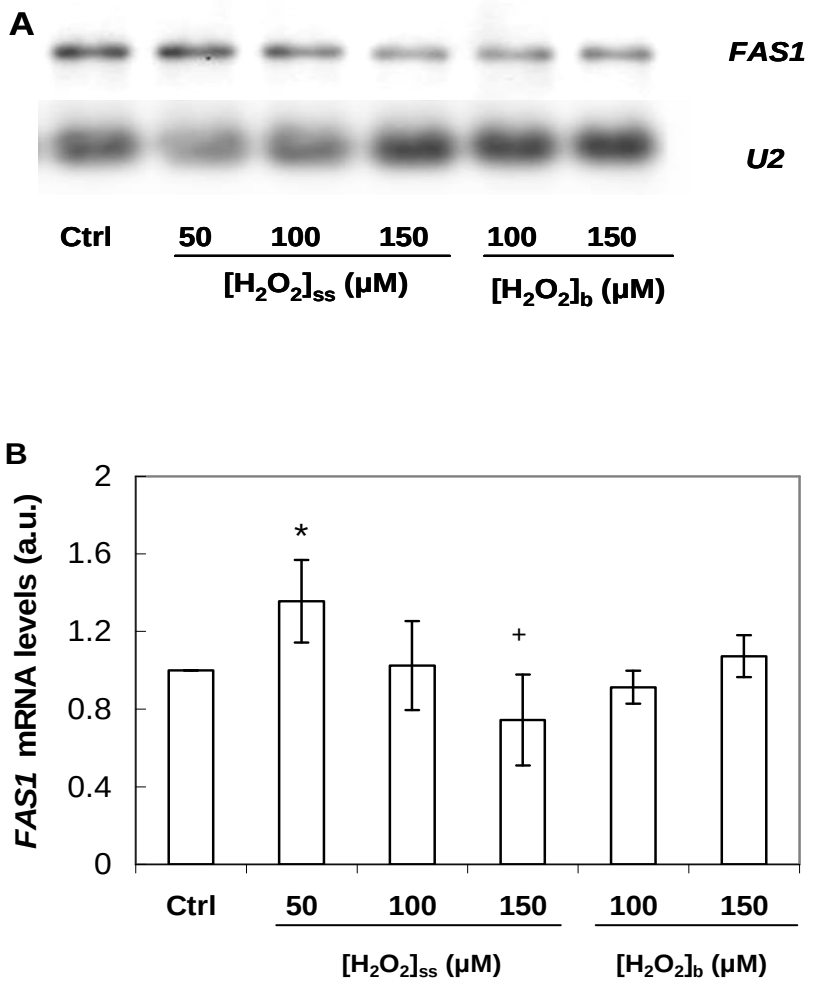

Figure 19. *FAS1* gene expression modulation by H_2O_2 is concentration- and delivery method dependent (steady-state or bolus). Samples of total mRNAs (30 μg) from *wt* (BY4743) control cells and *wt* cells, treated with different steady-state ([H_2O_2]ss) or bolus ([H_2O_2]]b) concentrations of H_2O_2 for 60 min, at a cell density of 0.6 OD/mL were prepared and analyzed by Northern blot. A - transcripts in a representative experiment; B - quantitative representation of transcript levels from three independent experiments. Results are the mean normalized to control ± SD; (n = 3). U1 transcripts were used as an internal control. * $p < 0.05$ vs control, + $p < 0.1$ vs control.

The most interesting feature in Figure 19 is the biphasic effect exerted by H_2O_2 on the *FAS1* mRNA levels. Cells exposed to a steady-state 50 μM H_2O_2 showed a 35 % increase in *FAS1* gene expression, while for steady-state 150 μM H_2O_2 there was a 26 % decrease in *FAS1*

mRNA levels. It was not possible to reproduce the stimulatory effect obtained by Kelley *et al.* [60] when delivering H_2O_2 as a bolus addition, although a small non-significant increase in *FAS1* mRNA levels was observed for a 150 µM H_2O_2 bolus addition. The apparent contradictory results are reconciled and were most probably due to the different doses of H_2O_2 that cells were exposed to. Low levels of H_2O_2, such as 50 µM in a steady-state, or the 100 µM bolus addition under the experimental conditions of Kelley *et al.* [60] lead to an increase in *FAS1* mRNA levels, while higher H_2O_2 concentrations (150 µM in a steady-state) decrease *FAS1* mRNA levels.

Next, it was important to investigate how the changes in *FAS1* mRNA levels induced by H_2O_2 are reflected in Fas activity (Figure 20).

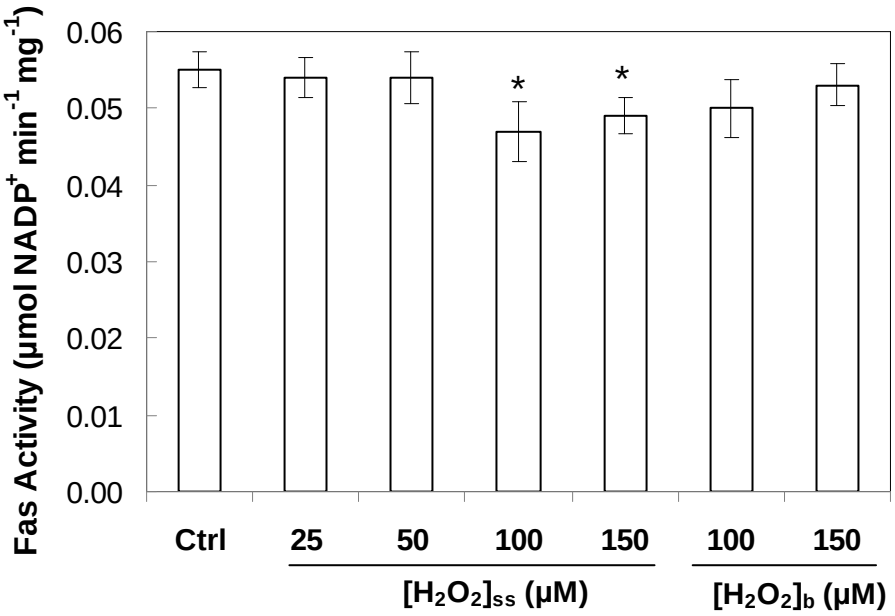

Figure 20. Fas activity decrease is dependent on H_2O_2 concentration but also on the use of a steady-state or bolus exposure to H_2O_2. Fas activity was determined in wt control cells and in wt cells after 60 min of addition of different concentrations of H_2O_2 to the growth media using a steady-state delivery ($[H_2O_2]$ss) or a bolus addition ($[H_2O_2]$b). Cell density was 0.6 OD/mL. Results are the mean ± SD; (n = 3). * $p < 0.05$ vs control.

Fas activity decreased 15 % and 11 % when cells were exposed to steady-state 100 µM and 150 µM H_2O_2, respectively. On the contrary, Fas activity did not change when cells were exposed to lower H_2O_2 concentrations during the experiment (either steady-state H_2O_2 (25 µM and 50 µM), or H_2O_2 bolus additions up to 150 µM). This lack of correlation between *FAS1* mRNA levels and Fas activity indicated that H_2O_2 is exerting regulatory roles also at

the protein level, involving processes other than transcription, like translation or protein turnover, a common observation in regulation of enzyme activity [176, 185, 199]. This complex behaviour is not unexpected when using an oxidative stimulus and it has been studied in detail in *S. cerevisiae* cells using menadione as the oxidant agent [199]. The precise molecular mechanisms underlying the observed behaviour are outside the scope of this thesis, but either post-transcriptional modification, mRNA stability and ribosomal transit, translation inhibition or increased protein turnover can explain the observed results. Previous results in stationary-phase *S. cerevisiae* cells exposed to menadione also showed that the increases found in Mn-superoxide dismutase, Cu,Zn-superoxide dismutase, and glutathione reductase mRNA levels were not paralleled by increased protein levels and enzymatic activities due to regulation not only at the transcription level but also at the post-transcriptional, translational, and post-translational levels [199]. Studies in translational responses of *S. cerevisiae* cells to H_2O_2 showed that many of the mRNAs translationally up-regulated in response to H_2O_2 did not show concomitant increases in transcript levels but an increase of ribosomes associated to certain mRNAs [200]. This phenomenon allows cells to keep a source of ribosome-associated mRNAs that can be rapidly translated when needed, showing that the response to oxidative stress requires both translational and transcriptional reprogramming. This accumulation of ribosome-associated mRNAs can also explain the increase of *FAS1* expression without increase in Fas activity observed for an exposure to steady-state 50 µM H_2O_2.

In conclusion, the results presented in this chapter confirm the existence of a regulation of Fas by exposure to adaptive doses of H_2O_2, reinforcing its role of in *S cerevisiae* adaptation to H_2O_2. Moreover, it is shown this regulation is highly dose dependent, being that it was observed a biphasic modulation of Fas by H_2O_2. Therefore, the importance of using highly controlled techniques of H_2O_2 delivery (as the example of the steady-state delivery method) is here strengthened. It is also noticeable that down-regulation of Fas by an adaptive dose of H_2O_2 is not due to an enzyme oxidative inactivation but by a decrease in *FAS1* expression.

5 Results II - The effect of down- and upregulation of *FAS1* expression in yeast resistance to H_2O_2 and in plasma membrane permeability to H_2O_2

5.1 Studies in cells with downregulated Fas expression (*fas1*Δ)

In order to confirm the role of Fas in cell adaptation to H_2O_2 a *fas1*Δ strain was used. This strain, which is derived from the wt BY4743 diploid strain, has a deletion of one of the *FAS1* alleles (as described earlier the haploid strain with deletion of the *FAS1* gene is not viable unless the media is supplemented with fatty acids, which would influence the plasma membrane composition).

5.1.1 Fas activity and cell resistance to lethal doses of H_2O_2

Fas activity was measured in control and H_2O_2-adapted (exposed to 150 μM of H_2O_2 for 90 min) wt and *fas1*Δ cells (Figure 21).

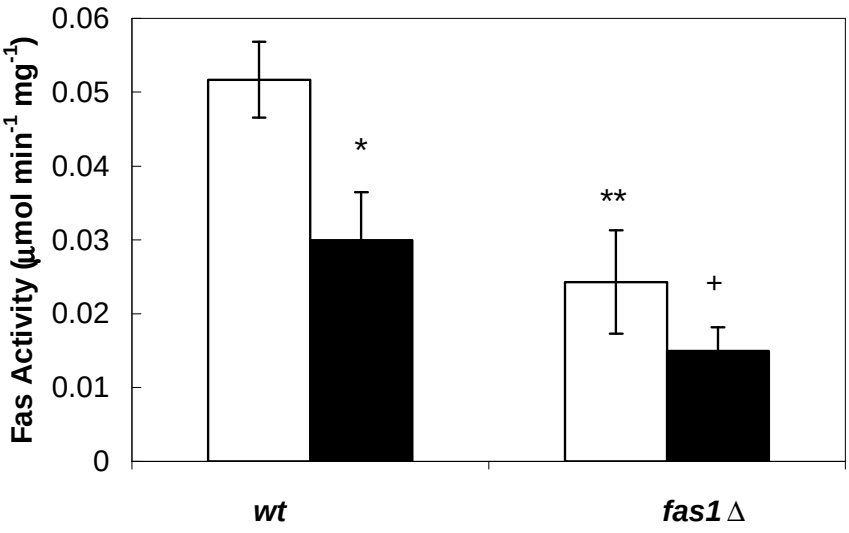

Figure 21. Fas activity in *fas1*Δ cells is lower than in wt cells and decreases during adaptation to H_2O_2. Fas activity was determined in wt and *fas1*Δ control (open bars) and H_2O_2-adapted cells (closed bars). Cells were adapted using steady-state 150 μM H_2O_2 for 90 min. Values are the mean ± SD; (n = 3). * $p < 0.05$, ** $p < 0.01$ vs wt control cells, + $p < 0.05$ *vs fas1*Δ control cells.

Once again it was confirmed that exposure to an adaptive dose of H_2O_2 leads to a decrease in Fas activity in wt cells. Measurements of Fas activity also confirmed that the deletion of the *FAS1* allele decreased Fas activity to about 50 % of that found in wt cells and that in *fas1*Δ cells adaptation to H_2O_2 also decreased Fas activity.

To test whether lower Fas levels correlated with higher resistance to H_2O_2 the cell survival fraction in the presence of low lethal doses of H_2O_2 was measured. As shown in Figure 22, *fas1*Δ cells were more resistant to the lethal doses of 0.75 and 1.5 mM H_2O_2 than the wt strain. This increased resistance was also observed after both strains were adapted to H_2O_2 by pre exposure to adaptive doses of this agent. Interestingly, the survival fraction of the *fas1*Δ control cells was similar to that H_2O_2-adapted wt cells. The increased resistance conferred by deletion of *FAS1* did not occur at 3 mM H_2O_2, while for 6 mM H_2O_2, the increased resistance conferred by both *FAS1* deletion and adaptation to H_2O_2 was lost (Figure 22).

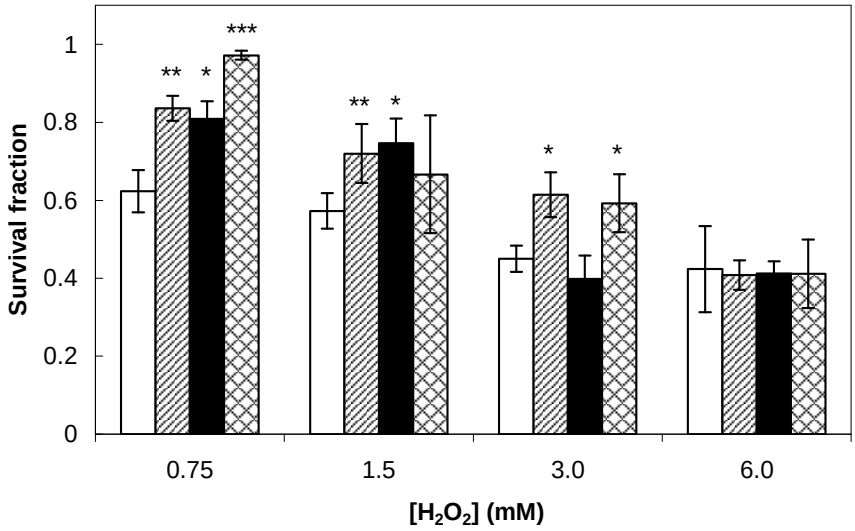

Figure 22. Resistance to low but not to high H_2O_2 lethal doses is dependent on Fas activity. The survival fraction was determined for control wt cells (□), H_2O_2-adapted wt cells (▨), control *fas1*Δ cells (■) and H_2O_2-adapted *fas1*Δ cells (⊠) after exposure to lethal bolus doses of H_2O_2 for 60 minutes, at 30ºC. Cells were adapted using steady-state 150 µM H_2O_2 for 90 min. Results are the mean ± SD; (n ≥ 3). * $p < 0.05$, ** $p < 0.01$, *** $p < 0.001$ *vs* control wt cells.

Supporting the importance of Fas for the cellular response to H_2O_2 is the inverse correlation between Fas activity and cell resistance to H_2O_2 observed for a low lethal dose (0.75 mM) of H_2O_2 (Figure 23). As expected, this correlation was lost for higher lethal H_2O_2 doses, where probably induction of antioxidant H_2O_2-removing enzymes plays an important role.

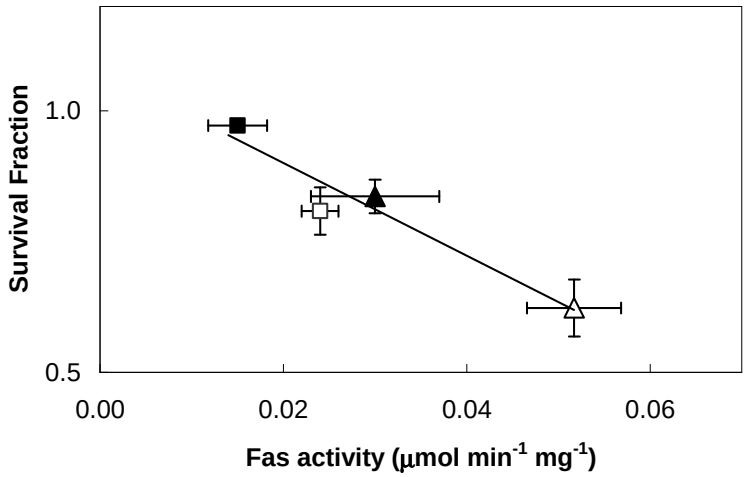

Figure 23. Fas activity and the survival fraction to low H_2O_2 lethal doses correlate inversely. The survival fraction determined after exposure to a lethal dose of 0.75 mM of H_2O_2 (represented in Figure 24 was plotted against the correspondent Fas activity (represented in figure 7) in control wt cells (△), H_2O_2-adapted wt cells (▲), control *fas1*Δ cells (□) and H_2O_2-adapted *fas1*Δ cells (■). Cells were adapted using steady-state 150 μM H_2O_2 for 90 min.

5.1.2 Increased resistance of fas1Δ is neither due to cell wall nor H_2O_2-removing-enzymes

Having shown that down-regulation of Fas constitutes an important cellular response to H_2O_2, next the mechanism by which Fas repression could confer such resistance to H_2O_2 was examined. Taking into account the importance of H_2O_2-removal enzymes [36], a hypothetical cross-talk mechanism between repression of Fas expression and induction of these antioxidant enzymes was examined. As shown in Figure 24, catalase activity was similar in both *fas1*Δ and wt cells, while cytocrome *c* peroxidase activity was lower in *fas1*Δ cells than in wt cells. These results show that the higher resistance of the *fas1*Δ cells to H_2O_2 is not due to higher activities of the main H_2O_2-removing enzymes.

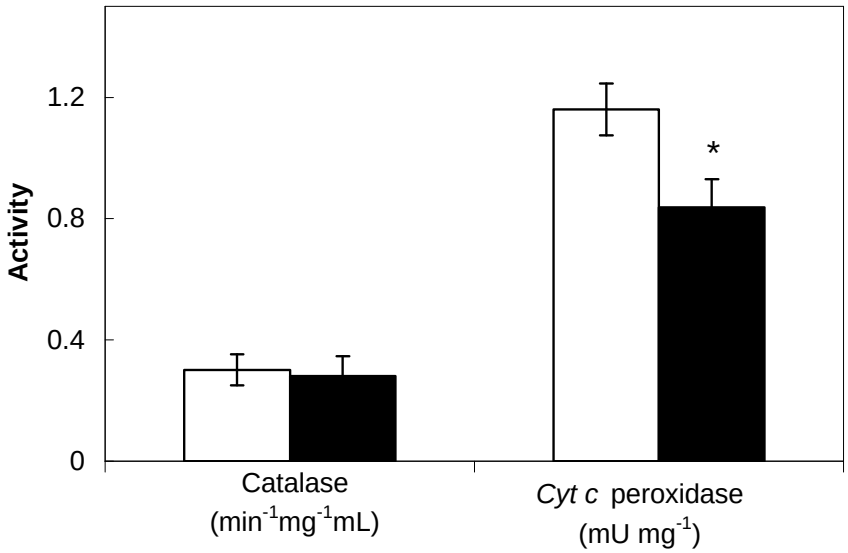

Figure 24. *fas1*Δ cells have lower cytochrome *c* peroxidase and the same catalase activity than wt cells. Catalase and cytochrome *c* peroxidase activities were measured in wt (open bars) and *fas1*Δ (closed bars). Results are the mean ± SD; (n ≥ 3). * p<0.01 *vs* wt.

Since the cell wall and plasma membrane are the two barriers that, by limiting the diffusion of H_2O_2 into the cell, can protect cells from the lethal action of external H_2O_2 [135] and taking in account that fatty acids are also components of the cell wall [201], next it was tested if there were cell wall changes in the *fas1*Δ strain that could explain its higher resistance to H_2O_2. Differences in cell wall β-glucan layer or changes in the external mannoprotein layer can be qualitatively assessed by changes in cell sensitivity to yeast lytic enzyme [202, 203], which is a mixture of enzymes with β-1,3-glucanase and protease activities. However, as can be seen in Figure 25 A there were no differences in cell wall sensitivity to yeast lytic enzyme between wt and *fas1*Δ cells, showing that no major differences in the cell wall exist between the two strains. Cell sensitivity to SDS may also be used to screen for alterations in cell wall integrity [185]. Again, no major differences between *wt* and *fas1*Δ cells were found by using a spot assay at two different concentrations of SDS (Figure 25 B).

According to these results, there were not any observable changes in the cell wall properties in *fas1*Δ cells compared with wt cells, suggesting that the plasma membrane plays an important role in the increased resistance of *fas1*Δ cells to H_2O_2.

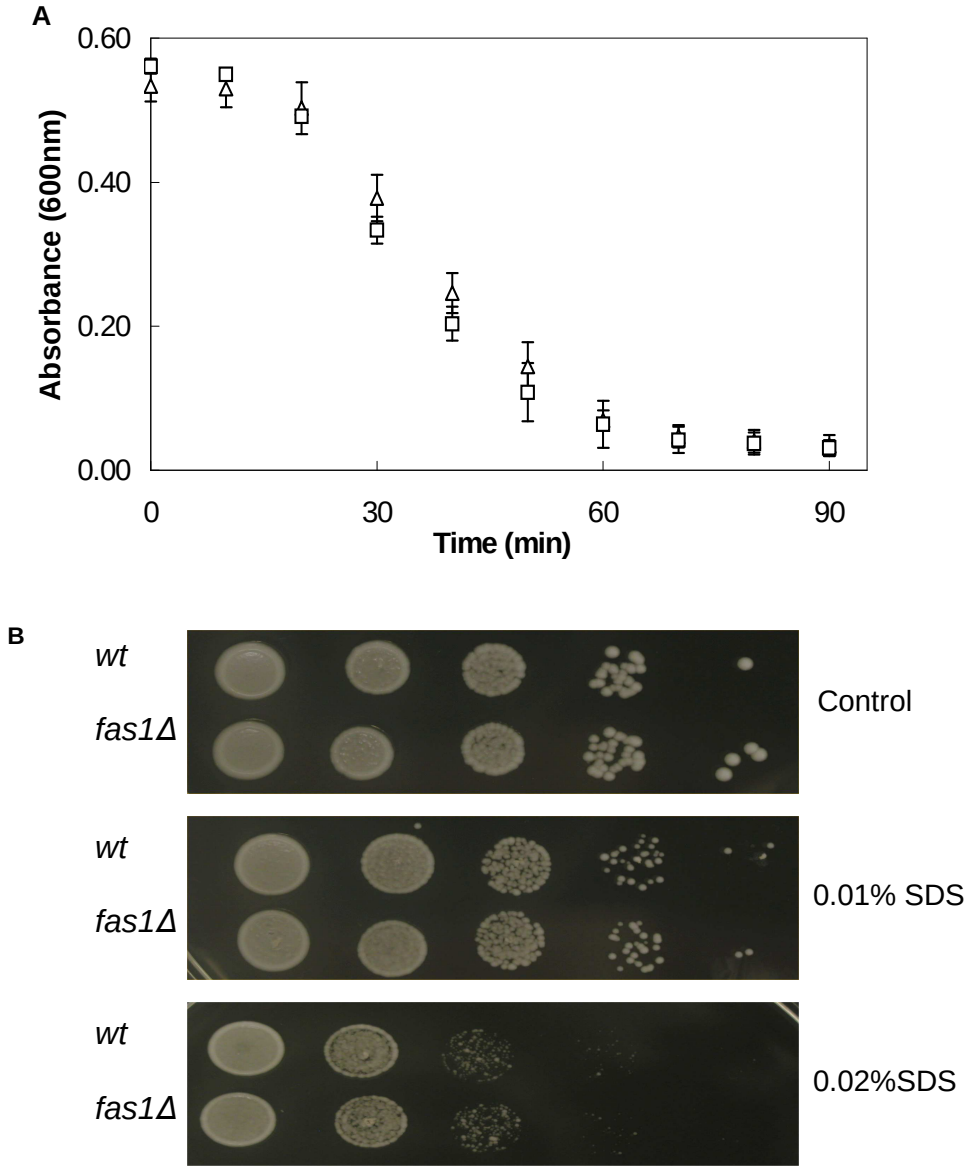

Figure 25. The cell wall in wt and *fas1*Δ cells has similar resistance to yeast lytic enzyme digestion and to SDS. A – Digestion of cell wall by yeast lytic enzyme cell was followed by monitoring the absorbance at 600 nm. wt cells (△); *fas1*Δ cells (☐). Results are the mean ± SD; (n=3); B - Serial dilutions of a culture were performed and spotted in YPD plates containing different concentrations of SDS (% (v/v)). Photographs were taken after 48 h of growth at 30 ºC. Representative experiment is shown; (n=3).

5.1.3 Changes in H_2O_2 plasma membrane permeability are probably localized and site-specific.

The permeability rate constant for H_2O_2 diffusion through the plasma membrane can be determined based on the rates of H_2O_2 consumption in intact and in permeabilized cells [48, 57]. Both in intact and permeabilized cells H_2O_2 consumption rates were similar for both wt and *fas1*Δ strains (Table 10) and, under the experimental conditions used, were mostly due

to catalase since the *ctt1*Δ strain showed a much lower H_2O_2 consumption. For intact cells, H_2O_2 consumption rates were much lower than in permeabilized cells for both the wt and the *fas1*Δ strains, because the plasma membrane is rate-limiting H_2O_2 diffusion into the cell. In the absence of catalase, the endogenous H_2O_2-consuming activities are not fast enough and so the plasma membrane does not rate-limit H_2O_2 diffusion into the cell, as indicated by the similar H_2O_2 consumption rates in intact and permeabilized *ctt1*Δ cells. Thus, k_{perm} could not be calculated by this method in *ctt1*Δ cells.

Table 10. The H_2O_2 gradient and H_2O_2 plasma membrane permeability are similar in wt and *fas1*Δ cells. H_2O_2 consumption was measured in wt and *fas1*Δ intact and digitonin-permeabilized cells and the respective consumption ($k_{intact\ cells}$ and $k_{catabolism}$) and permeability rate constants (k_{perm}) were calculated. Results are the mean ± SD; (n=4); * P < 0.01 *vs* wt and *fas1*Δ cells.

Strain	$k_{intact\ cells}$ (min^{-1}/OD_{600})	$k_{catabolism}$ (min^{-1}/OD_{600})	k_{perm} (min^{-1}/OD_{600})
wt	0.013 ± 0.002	0.041 ± 0.012	0.020 ± 0.001
*fas1*Δ	0.013 ± 0.002	0.033 ± 0.002	0.023 ± 0.004
*ctt1*Δ	0.004 ± 0.002*	0.004 ± 0.004*	-

The wt and *fas1*Δ cells showed no differences in the H_2O_2 membrane permeability rate constant as a result of the similar rates of consumption in both intact and permeabilized cells. This result suggests that, if membrane permeability alterations do occur with the *FAS1* allelle deletion, they must be site-specific, since no differences in the overall H_2O_2 plasma membrane permeability were measurable.

5.2 Studies in cells with upregulated Fas expression

5.2.1 Construction of a Saccharomyces cerevisiae strain with regulatable fatty acid synthase activity

In order to study the behaviour of a strain with different *FAS1* expression levels, two strategies were used to obtain a strain with the *FAS1* gene under the control of regulatable promoter: 1) substitution of the *FAS1* promoter for a doxycycline regulatable promoter in the wt strain [204]; 2) construction of a plasmid with the *FAS1* ORF under control of a

doxycycline regulatable promoter and transformation of the *fas1*Δ strain with the obtained plasmid [183].

5.2.1.1 Substitution of the *FAS1* promoter by a doxycycline regulatable promoter

The *FAS1* promoter was substituted by transformation of wt cells with an integrative plasmid containing a doxycycline regulatable promoter. Two different promoters with 2 and 7 tet boxes (being the obtained transformant strains denominated as tetO2*FAS1* and tetO7*FAS1*, respectively) were used to obtain strains with different levels of expression of *FAS1* [183, 204].

To confirm the regulation of Fas in these strains, Fas activity was measured in the transformant strain without doxycycline and 4 h after the addition of 2 µg/mL doxycycline to the growth media (Figure 27).

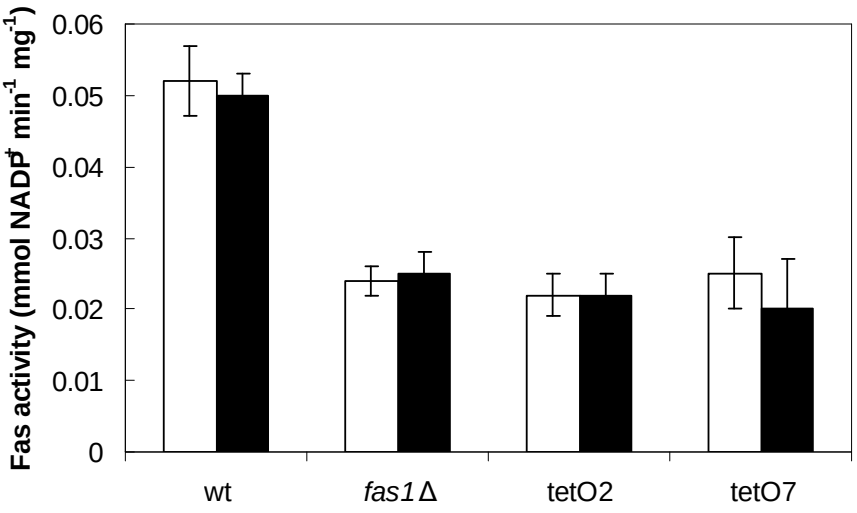

Figure 26. Fas activity of the tetO2 and tetO7 transformant strains is similar to the one in *fas1*Δ strain. Fas activity was determined in wt, *fas1*Δ, tetO2 and tetO7 cells without doxycycline (open bars) and 4 h after addition of 2 µg/mL doxycycline to the growth media (closed bars). Results are the mean ± SD; (n = 3).

Since a tetracycline-repressible direct system was used, tetO-driven expression should occur in the absence of the effector (tetracycline or other molecules of the same antibiotic family), while addition of the latter inhibits the tTA activator and switches off gene expression [204].

Therefore, knowing that Fas activity is directly dependent of *FAS1* gene expression [198], it was expected that an increase of Fas activity would occur in the transformant strains grown in the absence of doxycycline in the growth media and a decrease of Fas activity to the wt levels would occur after exposure to the antibiotic. However, these results were not observed, indicating that some problem may have occurred in the construction of the strains. In fact the transformant strains had a level of Fas activity similar to the one of the *fas1*Δ strain (Figure 27), suggesting that one of the alleles of the *FAS1* gene was disrupted irreversibly during the transformation and integration process, which could explain also the absence of viable transformants when the integration was tried in the haploid wt strain (results not shown). When a diploid strain is transformed integration occurs in only one of the two homologous chromosomes at a time [205], explaining the maintenance of one functional allele. Since the substitution of the *FAS1* gene promoter was unsuccessful, another approach was used in order to obtain a strain with regulatable gene expression.

5.2.1.2 Transformation of *fas1*Δ cells with a non-integrative autonomously replicating plasmid with *FAS1* under control of a doxycycline-regulatable promoter

*fas1*Δ cells were transformed with a multicopy plasmid, containing the *FAS1* open reading frame under control of a tetracycline-regulatable promoter containing 7 tetO boxes (pCM189) [183]. The resulting strain (*fas1*Δ-p*FAS1*) presented higher levels of *FAS1* mRNA, as confirmed by Northern blot (Figure 27) and, in the presence of doxycycline in the growth medium, the mRNA levels decreased to those of the *fas1*Δ strain. Moreover, the expression levels of the gene in the original strain *fas1*Δ were not affected by the presence of doxycycline in the growth media.

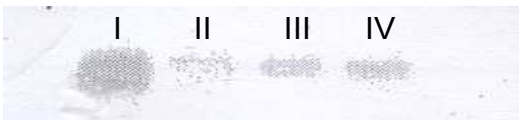

Figure 27. The *fas1*Δ-pFAS1 transformant strain has higher expression levels of the *FAS1* gene which are decreased in the presence of doxycycline. *FAS1* mRNA levels were analysed by Northern blot in: I – *fas1*Δ-p*FAS1* cells without doxycycline; II - *fas1*Δ-p*FAS1* cells exposed to 2 µg/mL doxycycline for 6 h; III – *fas1*Δ cells without doxycycline; IV - *fas1*Δ cells exposed to 2 µg/mL doxycycline for 6 h.

To confirm the regulation of Fas activity in the transformant strain, Fas activity was measured in *fas1*Δ-pFAS1 cells without doxycycline and in the presence of different concentrations of the antibiotic in the growth media for 2 hours (determined as the optimal time for complete gene repression) (Figure 28).

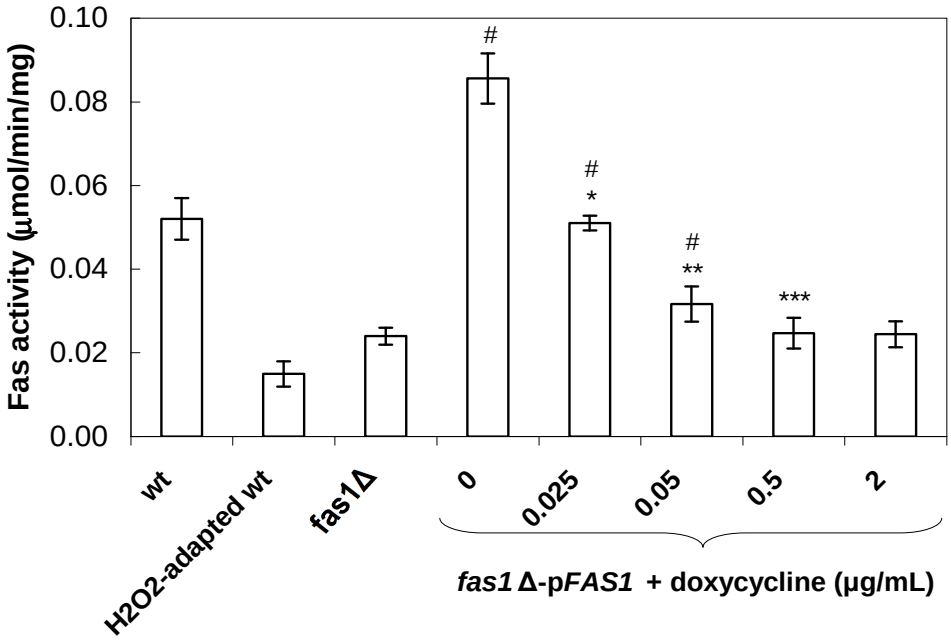

Figure 28. Fas activity is higher in the *fas1*Δ-p*FAS1* strain and decreases gradually in the presence of increasing concentrations of doxycycline. Fas activity was measured in *fas1*Δ-p*FAS1* cells in the absence of doxycycline and in the presence of 0.025, 0.05, 0.5 and 2 µg/mL doxycycline in the growth media. Data for wt cells, H_2O_2-adapted wt cells and *fas1*Δ cells were taken from Figure 21. Cells were adapted using steady-state 150 µM H_2O_2 for 90 min. Results are the mean ± SD; (n = 3). * P<0.05 vs *fas1*Δ-p*FAS1* + 0 µg/ml doxycycline; ** P < 0.01 vs *fas1*Δ-p*FAS1* + 0 µg/mL doxycycline; *** P < 0.001 vs *fas1*Δ-dox + 0 µg/mL doxycycline; # P < 0.001 *vs fas1*Δ.

The transformed *fas1*Δ-p*FAS1* strain presents a 4-fold increase of Fas activity relatively to the *fas1*Δ strain. Fas activity decreases in the presence of doxycycline in a concentration-dependent manner. In the presence 0.5 µg/mL or higher concentrations of doxycycline the Fas activity of the transformant cells decreases to the values measured for the *fas1*Δ strain. These changes in Fas activity occur because, as referred previously, *FAS1* and *FAS2* are co-regulated in order to maintain proportional levels of the Fas α- and β subunits. Therefore, *FAS2* gene expression and, consequently, Fas activity are dependent of *FAS1* mRNA levels [162, 198]. As a control for the influence of transformation with a non-integrative plasmid and the presence of doxycycline in the growth media in Fas activity, Fas activity was also measured in *fas1*Δ cells transformed with the empty plasmid (*fas1*Δ–pCM189) and in *fas1*Δ

cells grown for 2 h in the presence of 2 µg/mL doxycycline. In both cases no significant alterations in Fas activity were measured (0.025 ± 0.006 for *fas1*Δ–pCM189; 0.024 ± 0.003 for *fas1*Δ + 2 µg/mL doxycycline *vs* 0.024 ± 0.002 for *fas1*Δ).

5.2.2 *Plasma membrane permeability to H_2O_2 and cell survival to lethal doses of H_2O_2 correlate with FAS1 expression levels in the Fas overexpressing strain.*

Since fatty acids are the major constituents of the plasma membrane it was expected that changes in their biosynthesis pathway would change plasma membrane properties. It was previously determined that *S cerevisiae* cells adapted to H_2O_2 and, consequently, with decreased levels of Fas activity, have lower plasma membrane permeability to H_2O_2 [57]. As described in 5.1.3, no differences were found between overall plasma membrane permeability to H_2O_2 between wt and *fas1*Δ cells, probably because these changes are localized and not detected by our measurements of the bulk plasma membrane permeability [198]. Also, the levels of catalase (which are the ones measured by our technique) were not altered in the *fas1*Δ cells when compared to *wt* cells. Plasma membrane permeability was determined for *fas1*Δ-p*FAS1* cells in the absence and presence of 0.5 and 2 µg/ml of doxycycline (Table 11). Once again as a control for the effects by transformation and doxycycline, the constants for *fas1*Δ–pCM189 and *fas1*Δ + 2 µg/mL doxycycline were determined.

Table 11. The plasma membrane permeability to H_2O_2 increases with the increment of Fas activity in *fas1*Δ-pFAS1 transformant cells and decreases with the repression of *FAS1* by the addition of doxycycline. H_2O_2 consumption in intact and permeabilized cells was measured in transformant cells without or with 0.5 and 2 µg/mL doxycycline. The respective H_2O_2 consumption ($k_{\text{intact cells}}$ and $k_{\text{catabolism}}$) and the H_2O_2 permeability rate constants (k_{perm}) were calculated from the experimental data. Results are the mean ±SD (3 ≥ n ≥ 4) . * P < 0.05; ** P < 0.01; *** P < 0.001 *vs* *fas1*Δ cells.

Strain	$k_{\text{intact cells}}$ ($\text{min}^{-1}/\text{OD}_{600}$)	$k_{\text{catabolism}}$ ($\text{min}^{-1}/\text{OD}_{600}$)	k_{perm} ($\text{min}^{-1}/\text{OD}_{600}$)
***fas1*Δ**	0.013 ± 0.002	0.033 ± 0.002	0.023 ± 0.004
+ 2 µg/mL doxycycline	0.014 ± 0.002	0.032 ± 0.005	0.021 ± 0.004
fas1*Δ-p*FAS1	0.022 ± 0.001***	0.056 ± 0.006**	0.041 ± 0.006***
+ 0.5 µg/mL doxycycline	0.020 ± 0.001*	0.048 ± 0.010*	0.034 ± 0.003**
+ 2 µg/mL doxycycline	0.015 ± 0.002	0.035 ± 0.009	0.020 ± 0.007
fas1*Δ–p*CM189	0.014 ± 0.000	0.030 ± 0.001	0.025 ± 0.002

FAS1 overexpression led to an increase of H_2O_2 consumption both in intact and permeabilized cells, indicating that there was an increase in catalase activity in these conditions, since under our experimental conditions only H_2O_2 consumption by cytosolic catalase is measured (see Table 10). The addition of 0.5 µg/mL of doxycycline to the growth medium led to a decrease in H_2O_2-consumption rates in both intact and permeabilized *fas1*Δ-pFAS1 cells but, only in the presence of 2 µg/mL of doxycycline the values decreased to the same of the original transformed cells, *fas1*Δ. In a recent study it was found that *Saccharomyces cerevisiae* cells depleted of the yeast acyl-CoA-binding protein have an increased expression in several fatty-acid-metabolism-associated genes (including *FAS1*) together with an increase in *CTT1* expression (the gene associated with cytosolic catalase T), establishing a relation between catalase and fatty acid metabolism [206].

Next, cell survival to lethal doses of H_2O_2 was studied in the *fas1*Δ-pFAS1 cells when expressing different levels of Fas. The lethal dose used was lowered than that used in the studies with Fas downregulation (Figure 22), since the exposure to 750 µM of H_2O_2 decreased the survival fraction of the controls (*fas1*Δ–pCM189 and *fas1*Δ + 2 µg/mL doxycycline) when compared to *fas1*Δ cells (not shown). .When cells were exposed to 400 µM H_2O_2 for 60 min (Figure 29) although *fas1*Δ–pCM189 cells containing the empty plasmid showed the same survival fraction as *fas1*Δ cells, a lower survival was still seen for *fas1*Δ cells in the presence of doxycycline. This indicated that the presence of doxycycline exacerbated the lethal effect of H_2O_2. Nevertheless, it was decided to pursue the study with 400 µM H_2O_2 since lower doses of H_2O_2 would not induce the desired lethal effect.

When exposed to 400 µM H_2O_2 *fas1*Δ cells were more resistant than wt cells (Figure 29). The transformation of *fas1*Δ cells with the plasmid overexpressing *FAS1*, with a consequent increase in Fas activity, led to a 60 % decrease of cell survival when compared with the respective control *fas1*Δ–pCM189 cells. Moreover, decreasing Fas activity by adding doxycycline to *fas1*Δ-p*FAS1* cells, led to more than 2-fold increase in cell survival. Thus the results in Figure 29 together with those in Figure 23 suggest a strong inverse correlation between Fas activity and cell survival to lethal H_2O_2 doses.

Although plasma membrane permeability to H_2O_2 is about 2 fold higher in *fas1*Δ-p*FAS1* cells than in *fas1*Δ-pCM189 cells, the former are more than two folder less sensitive to lethal doses of H_2O_2.The effect of an increased plasma membrane permeability is therefore amplified when observed in terms of cell survival to H_2O_2, reinforcing the role of the plasma membrane in cell resistance to H_2O_2.

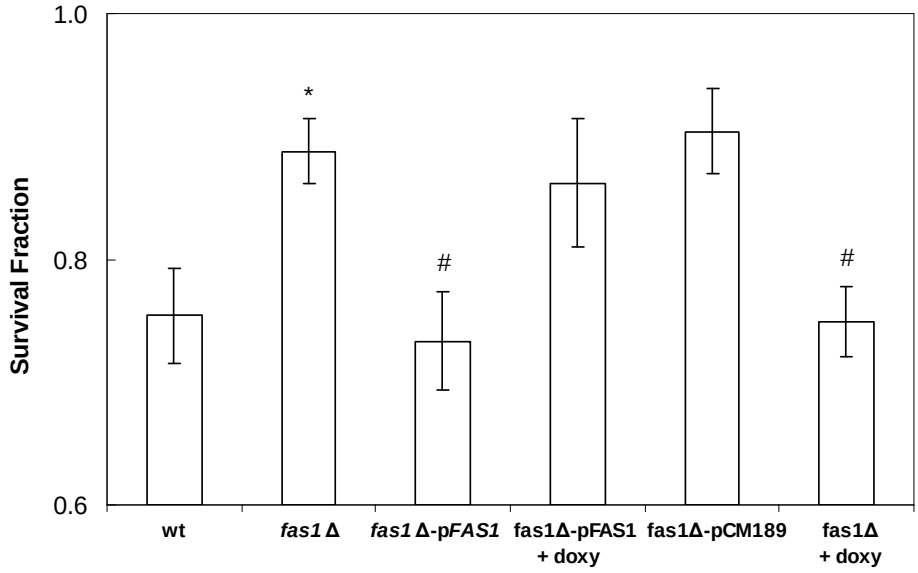

Figure 29. Cell survival to lethal doses of H_2O_2 decreases with overexpression of *FAS1*. Survival fractions were determined for wt, *fas1*Δ and *fas1*Δ-p*FAS1* cells without doxycycline and in the presence of 2 µg/mL doxycycline, after exposure to a lethal dose of 400 µM of H_2O_2 for 60 min. Survival fraction in the same conditions was also determined for the controls *fas1*Δ-pCM189 cells and *fas1*Δ cells with 2 µg/mL doxycycline. Results are the mean ± SD (n = 3). * $P < 0.05$ *vs* wt, # $P < 0.05$ *vs fas1*Δ.

Finally, it is also important to mention that care should be taken when using doxycycline-regulated promoters in studies involving H_2O_2, because doxycycline decreased by approximately 50 % the survival of *fas1*Δ cells to 400 µM H_2O_2 (Figure 29). When measuring cytochrome *c* peroxidase activities, a small decrease in this antioxidant enzyme was measured (Table 12). Although statistically non-significant, the fact that doxycycline, by itself, is exerting some effects in the cell antioxidant defences can not be ignored. It is widely accepted that doxycycline is innocuous to yeast and global expression studies showed that doxycycline has no significant effect on gene transcription levels in *S. cerevisiae* [207]. However, in S*. cerevisiae,* resistance to certain tetracycline antibiotics has a mode of action dependent on oxidative damage, since studies in mutants in antioxidant and redox-balance systems, showed that cells lacking superoxide dismutase are more sensitive to tetracycline antibiotics [208]. One property that could account for oxidative stress generated by tetracyclines is the high metal-binding affinities of these antibiotics, forming complexes that can act as centers for redox cycling activity and/or free radical generation [208]. It is also known that doxycycline, like all the tetracycline antibiotics, when present at the low concentrations required for anti-bacterial treatment (1-2 µg/mL), is an inhibitor of mitochondrial protein synthesis [209].

Table 12. Exposure to doxycycline leads to a small decrease in cytochrome *c* peroxidase activity. Cytochrome *c* peroxidase activity was measured in wt, *fas1*Δ, *fas1*Δ –pFAS1, *fas1*Δ –pFAS1 + 2 µg/mL doxycycline, *fas1*Δ + 2 µg/mL doxycyclin and *fas1*-pCM189. Results are the mean ± SD; (n ≥ 3). * p<0.01 *vs* wt.

Strain	Cytochrome *c* peroxidase activity (mU/mg)
wt	1.16 ± 0.05
*fas1*Δ	0.84 ± 0.06*
*fas1*Δ-p*FAS1*	0.83 ± 0.07
*fas1*Δ-p*FAS1* + doxycycline (2 µg/mL)	0.79 ± 0.06
*fas1*Δ + doxycycline (2 µg/mL)	0.78 ± 0.05
*fas1*Δ –pCM189	0.83 ± 0.05

In conclusion, the results presented in this chapter confirm the role of Fas in the acquired resistance to H_2O_2 that occurs in adaptation, by establishing a strong inverse correlation between Fas activity and cell resistance to H_2O_2. Moreover, increasing FAS activity leads to a higher membrane permeability and higher susceptibility of lethal H_2O_2 doses. On the other hand, the increased resistance to H_2O_2 observed in *fas1*Δ cells is not associated with lower membrane permeability, indicating possibly that localized changes in the plasma membrane are important for resistance to H_2O_2.

6 Results III – Do different levels of Fas activity affect plasma membrane lipid composition and organization?

The occurrence of changes in the plasma membrane composition and organization in *S. cerevisiae* haploid wt cells adapted to H_2O_2 has already been described [66] and in diploid wt cells the activity of Fas decreases during adaptation to H_2O_2 (Figure 18). In this chapter the composition, biophysical properties and microdomain distribution of the plasma membrane in strains expressing different levels of Fas were analysed in order to understand how Fas modulation leads to higher resistance to H_2O_2.

6.1 Plasma membrane phospholipids and fatty acids composition is altered in cells with lower Fas activity

6.1.1 The plasma membrane of H_2O_2-adapted cells has higher PC/PE and lower PI/PS while differences in fas1Δ are less accentuated

Phospholipids are regarded as a primary structural element of the biological membranes consist of a glycerol backbone esterified with fatty acids in the *sn*-1 and *sn*-2 positions, and a phosphate group in the *sn*-3 position [210]. Moreover, membrane composition in phospholipids can affect its curvature, thickness and fluidity [73], properties that can change the membrane permeability to H_2O_2.

The plasma membrane from wt-, H_2O_2–adapted wt cells and *fas1*Δ cells was isolated and phospholipid composition analysed by 2D-TLC (Figure 30).

There were no differences between total phospholipid content between the studied strains (wt, 302 ± 10 nmol Pi/mg protein; *fas1*Δ, 320 ± 14 nmol Pi/mg protein; H_2O_2-adapted wt, 316 ± 9 nmol Pi/mg protein). As described previously by other authors [211], phosphatidylcoline (PC) is the most abundant phospholipid in the plasma membrane of both strains. Adaptation to H_2O_2 led to an increase of around 12 % in PC content while deletion of one of the *FAS1* alleles led to a non-significant increase of around 8 % in PC. Since PC is the most abundant phospholipid in the plasma membrane, changes in its amount can lead to changes in the biophysical properties of the plasma membrane (e.g. fluidity and intrinsic curvature) [73]. In opposition, PE levels decreased in about 14 % with adaptation to H_2O_2. Once again this decrease was non-significant for *fas1*Δ cells when compared to wt cells. The PC/PE ratio in the plasma membrane increases both from wt to *fas1*Δ and wt H_2O_2-adapted cells, being the

only significant difference in adaptation (Table 13). PC and PE are present in different shapes and it is known that the ratio between these two phospholipid levels can affect plasma membrane physical properties like curvature and rigidity [73, 212]. Since a simple solubility-diffusion mechanism is proposed for glucose or other small uncharged particles membrane transport [213] it is plausible that the alteration of PC/PE ration could be responsible for the observed decrease of plasma membrane permeability to H_2O_2 observed in adaptation. The increase in PC/PE ration in *fas1*Δ cells plasma membrane is not significant, which is coherent with the absence of measurable differences of bulk plasma membrane permeability to H_2O_2.

It was also observed an increase in phosphatidylinositol (PI) and a decrease in phosphatidylserine (PS) in the plasma membrane of H_2O_2-adapted cells and in *fas1*Δ cells comparatively to the wt cells. Once again, for the *fas1*Δ strain, differences in the levels of PI and PS were not as pronounced as in H_2O_2-adapted wt cells. Alterations in the amount of these phospholipids in membranes have not been described as affecting their permeability properties, so they may be associated with regulation mechanisms.

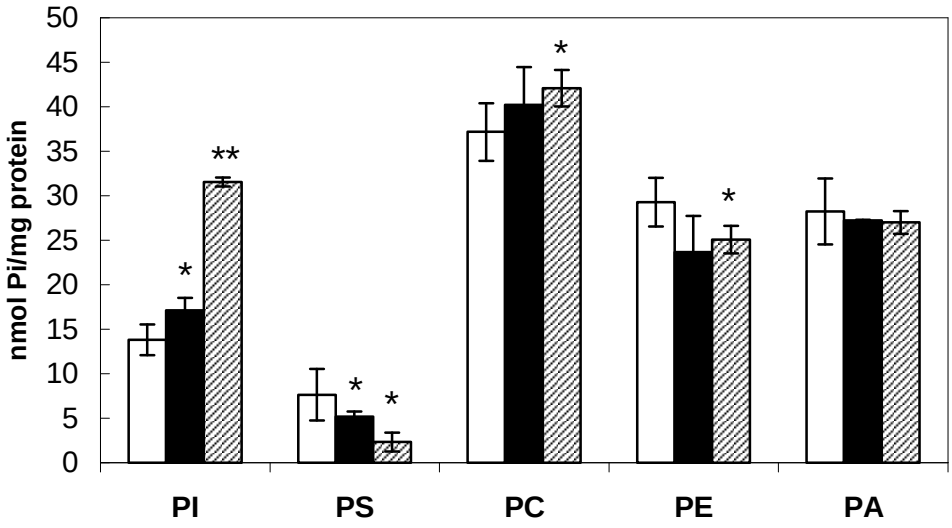

Figure 30. The plasma membrane of cells with lower Fas activity has a higher content of PI and PC and a lower content of PS and PE. Plasma membrane content of phosphatidylinositol (PI), phosphatidylserine (PS), phosphatidylcholine (PC), phosphatidylethanolamine (PE) and phosphatidic acid (PA) was determined by quantitative 2D-TLC in wt- (□), *fas1*Δ- (■) and H_2O_2-adapted wt cells (▨). Values are the mean ± SD ($3 \geq n \geq 4$). * $P < 0,05$; ** $P < 0.001$ *vs* wt.

Table 13. Adaptation leads to an increase in PC/PE ratio. PC/PE ratio was determined from the values presented in Figure 30. (3 ≥ n ≥ 4). * P < 0.05 *vs* wt

Strain	PC/PE
wt	1.27 ± 0.18
*fas1*Δ	1.70 ± 0.28
wt H_2O_2-adapted	1.68 ± 0.11*

6.1.2 The plasma membrane of fas1*Δ cells has higher amounts of very-long-chain fatty acids*

Alterations in plasma membrane fatty acid composition can lead to alterations in membrane fluidity and permeability. Although no bulk differences in plasma membrane permeability were found between wt and *fas1*Δ cells it was determined whether a decreased Fas level lead to changes in the plasma membrane fatty acid profile (Table 14) in order to understand if localized alterations of the plasma membrane could be involved in the higher resistance to H_2O_2.

The plasma membrane total fatty acid content and the unsaturated/saturated fatty acids ratio were similar for both strains. The majority of plasma membrane saturated and monounsaturated fatty acids were 16 and 18 carbons long, as previously described for *S.cerevisiae* cells [55, 66, 214], and similar levels were detected in both strains. However, there were large changes in membrane VLCFA (very-long-chain fatty acids) ranging from 20 to 26 carbons long. The *fas1*Δ strain plasma membrane presented higher levels of lignoceric acid (C24:0) and cerotic acid (C26:0) (respectively a 40 and 50 % increase) when compared with the wt strain. This large increase in the VLFCA content was not reflected in the plasma membrane permeability to H_2O_2, because this permeability was similar in both wt and *fas1*Δ strains (Section 5.1.3) but the interaction of Fas with elongation enzymes [151] can probably explain the large increase observed in the levels of C24:0 and C26:0 on deletion of *FAS1*. Being minor membrane components, VLFCA could probably induce localized alterations in the membrane that were not detected by the measurement of the bulk plasma membrane permeability. VLCFA are able to cross the plasma membrane midplane (a phenomenon known as “interdigitation”) leading to increases in overall plasma membrane rigidity [215] and thus decrease plasma membrane permeability to H_2O_2. Another hypothesis is that alterations in plasma membrane during adaptation to H_2O_2 entail the formation of lipid rafts, which are

membrane microdomains rich in sphingolipids. This phenomenon was already observed in haploid H_2O_2-adapted cells (were, together with the decrease of C18:1 and C20:0, the levels of VLCFA in the plasma membrane were increased to about 30 %) [66] and will be approached later on this thesis (3.2.15). This way, it seemed logical that the next step should be to isolate and analyse plasma membrane microdomains in order to detect possible differences in lipid composition.

Table 14. The plasma membrane content of the very-long-chain fatty acids lignoceric acid (24:0) and cerotic acid (C26:0) is higher in *fas1*Δ cells than in wt cells. The plasma membrane of wt and *fas1*Δ cells was isolated and fatty acid composition was determined by GC-MS. Values are the mean ± SD (3 ≥ n ≥ 5). * P < 0.05; ** P < 0.001 *vs* wt.

	Strain	
Fatty acid (µmol/mg protein)	***wt***	***fas1*Δ**
C14:0	0.016 ± 0.006	0.015 ± 0.005
C16:1	0.292 ± 0.091	0.228 ± 0.058
C16:0	0.183 ± 0.044	0.181 ± 0.039
C18:1	0.291 ± 0.066	0.292 ± 0.016
C18:0	0.084 ± 0.010	0.091 ± 0.010
C20:0	0.003 ± 0.000	0.004 ± 0.001
C22:0	0.008 ± 0.001	0.011 ± 0.002
C24:0	0.006 ± 0.001	0.010 ± 0.002*
C26:0	0.020 ± 0.002	0.039 ± 0.005**
Total fatty acids	0.846 ± 0.136	0.754 ± 0.109
unsaturated/saturated	1.821 ± 0.193	1.642 ± 0.237

6.2 Characterization of plasma membrane microdomains

6.2.1 Isolation of detergent insoluble domains lead to disruption of the microdomains

One of the characteristics used for rigid microdomain isolation is their insolubility in low concentrations of cold non-ionic detergents. Due to this characteristic, microdomains are frequently defined as detergent-resistant membranes (DRM) [216]. Pma1p is an H^+-ATPase and one of the most abundant proteins in the yeast plasma membrane [217]. This protein is usually used as a marker of lipid rafts in yeast, being detected by western blot in the fractions containing DRM after extraction [111].

The most common method for the extraction of membrane microdomains is the incubation with 1% Triton X-100 at 4 ºC and recovery of the upper half of a 5-30 % sucrose [216] or iodixanol [111] gradient. However, detergents can isolate not only domains from the plasma membrane but also from intracellular membranes [218] so the used strategy was to isolate the plasma membranes by sucrose gradients (as described in 3.2.13.1) and extract rafts by centrifugation after incubation with cold Triton X100. The presence of Pma1p in the soluble and insoluble fractions was detected by Western blot (Figure 31).

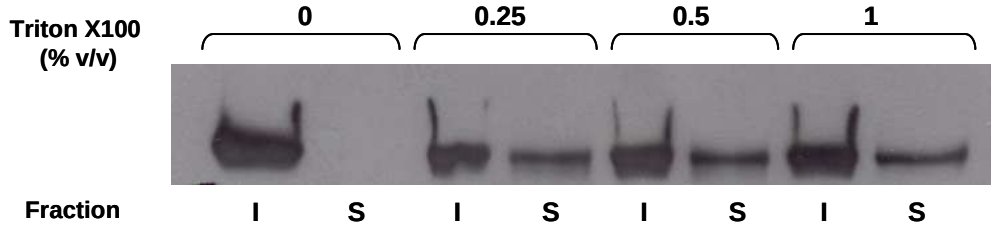

Figure 31. Pma1p is present not only in Triton X100 insoluble fraction of the plasma membrane but also in the soluble fraction. Plasma membranes from wt cells were isolated and incubated with different concentrations of Triton X100 at 4ºC and Pma1p presence was detected by Western blot. Representative experiment. S- soluble fraction; I- insoluble fraction.

As it is visible in Figure 31, samples incubated with different concentrations of cold Triton X100, contained Pma1p not only in the detergent insoluble fraction (that theoretically should be constituted by the rigid microdomains usually described as lipid rafts) but also in the soluble fraction (that was expected to contain the more fluid domains of the membrane

where no Pma1p is present). Only in the control sample, where no detergent was added, Pma1p remained just in the insoluble fraction. What can probably explain this result is that, during plasma membrane extraction and sample manipulations, many microdomains are disassembled, leading to delipidation of Pma1p and loss of its detergent insolubility. Since a lot of controversy has been associated with methos of lipid raft extraction and viability of the obtained results, *in vivo* analysis was carried out to continue this investigation [219].

6.2.2 Biophysical studies in intact cells

Since isolation of microdomains showed to be inefficient since it did not allow studying these structures in a state similar to the one found in intact membranes, biophysical studies with fluorescent probes were performed. These studies allow the understanding of the global or localized fluidity of the plasma membrane.

DPH (1,6-Diphenyl-1,3,5-hexatriene) is a fluorescent probe that incorporates into the lipid bilayer, presenting fluorescence polarization characteristics that directly correlate with the microviscosity of the labelled region [193]. Previous work showed an increase in DPH anisotropy (indicating lower membrane fluidity) with adaptation to H_2O_2 in haploid wt cells [95]. Fluorescent anisotropy at different temperatures was measured in intact cells labelled with DPH (Figure 32).

As expected there was a correlation between anisotropy and temperature (Figure 33). At lower temperatures higher anisotropy values were measured, indicating the existence of more rigid membranes. This result was expected since it is known that at low temperatures, hydrated phospholipid bilayers exist as highly ordered gels with the C-C bonds of their fatty acyl chains in the rigid *trans* conformation. This formation allows only slight torsional mobility and hence a tighter packing of the acyl chains is achieved. As the temperature is raised the molecular mobility of the fatty acyl chains gradually increases until, at a characteristic temperature, an abrupt thermal-phase transition occurs concomitantly with an increase in heat absorption and mobility of the fatty acyl chains. The bilayer then exists in a highly disordered, liquid-crystalline state and the C-C bonds have a partially gauche conformation with an increase in torsional mobility, being the bilayers in a ‘fluid’ state [220]. However, there were no visible differences in anisotropy between wt, *fas1*Δ and *fas1*Δ–p*FAS1* cells, suggesting that the lipid regions where DPH is inserted have similar fluidity in both cells. DPH partitions equally well into solid or fluid lipid domains of the membrane and, in a heterogeneous system like a biological membrane it can be considered as evenly distributed in the lipid bilayer. The measured anisotropies are therefore a weight average of all lipid

domains [221]. The results for fatty acid composition obtained in section 6.1 suggest that differences in plasma membrane are localized, so the inadequacy of DPH to measure these differences must be considered.

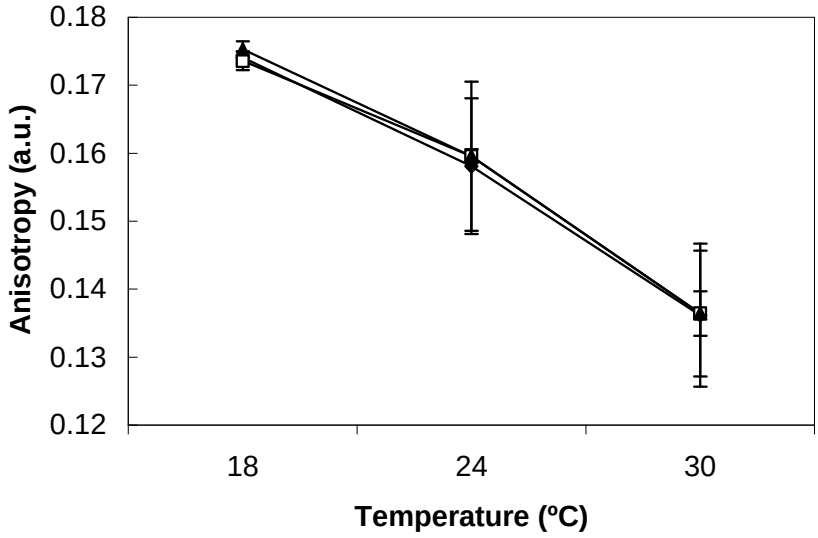

Figure 32. Fluorescence anisotropy with DPH is similar for cells with different Fas activity. Fluorescence anisotropy was determined in wt (closed losangles), *fas1*Δ (open squares) and *fas1*Δ–p*FAS1* (closed triangles) intact cells at 18ºC, 24ºC and 30ºC after incorporation with the fluorescent probe DPH. Results are the mean ± SD (n = 3).

In order to detect differences in localized microdomains of the membrane, *trans*-parinaric acid (tPnA), a fluorescent probe which preferentially partitions into lipid ordered phases was used. tPnA was incorporated in intact cells and the respective emission spectra (Figure 33) and time-resolved lifetime decay were determined (Table 15).

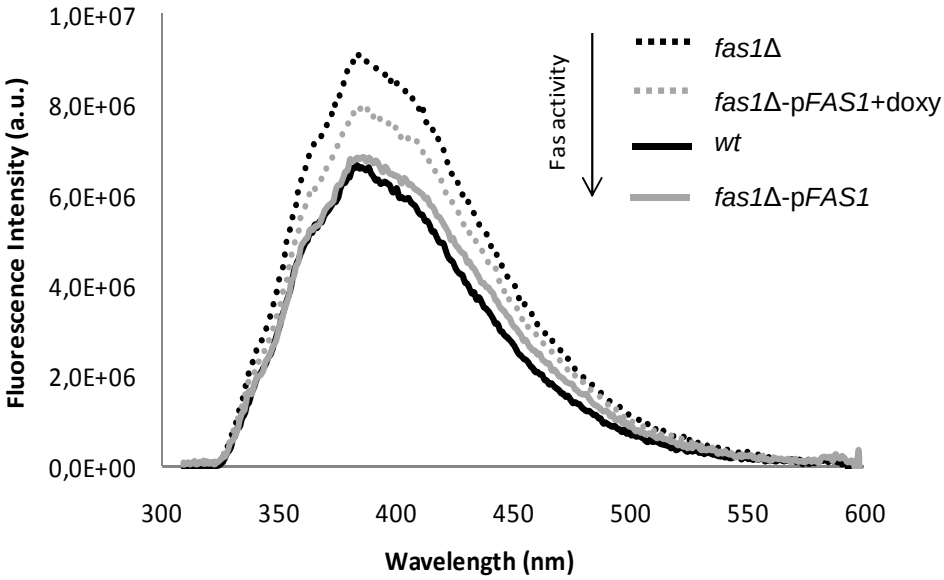

Figure 33. The fluorescence intensity of *trans*-parinaric acid in cells correlates with Fas activity. Emission spectra of the fluorescent probe *trans*-parinaric acid for wt cells (black line), *fas1*Δ cells (black dots), *fas1*Δ-p*FAS1* cells (grey line) and *fas1*Δ-p*FAS1* + 2 µg/ml doxycycline (grey dots) cells. Results are a representative experiment from a total of 4 independent experiments.

Although the same number of cells and probe concentration were used in all experiments, there were measurable differences in the maximum fluorescence intensities in the emission spectra obtained for wt, *fas1*Δ and *fas1*Δ-p*FAS1* in the presence or absence of doxycycline in the growth media (Figure 33) (it is also important to notice that the fluorescence intensity levels at 320 nm were equal for all strains). The cells with lower Fas activity (*fas1*Δ) presented the higher maximum fluorescence intensity and the strain over-expressing *FAS1* (*fas1*Δ-p*FAS1*) and, consequently, with higher Fas activity presented a decrease in maximum fluorescence. When doxycycline is added to *fas*1Δ–p*FAS1* cells Fas activity decreases to the levels found in *fas*1Δ cells, but the fluorescence intensities did not increase to the levels found for *fas*1Δ cells. This may show that changes that occur in plasma membrane by Fas overexpression are not completely reversible. The incomplete reversibility can also be associated to artefacts due to the cell transformation by itself.

Since *trans*-parinaric acid partitions preferentially into membrane ordered domains, and presents higher fluorescence intensities in raft-like domains rich in sphingolipids than in non-raft domains due to an increased quantum yield in the gel phase [222], it can be concluded that lower Fas activities increased the number of more rigid domains in the plasma

membrane. These results are in agreement with the observation that the *fas1*Δ strain plasma membrane has higher levels of the very-long-chain fatty acids lignoceric (C24:0) and cerotic (C26:0) acid, mainly present in the backbone of sphingolipids (section 6.1.2).

In order to confirm these results, the lifetime decay of intact cells incorporated with tPnA was determined (Table 15). Fluorescence lifetime (τ) can be defined as the characteristic time that a fluorophore resides in the excited state before returning to the ground state. Depending on its nature and photophysical properties, each fluorophore has a typical fluorescence lifetime, which can be affected by the local environment where it is inserted. When tPnA is located in more ordered environments, a lifetime component appears in its fluorescence intensity decay with values ranging from ~20 ns up to ~50 ns depending on the type of lipid domain (gel ordered if clearly above 30 ns and liquid ordered if below 30 ns) [194].

Table 15. The decrease of Fas activity leads to an increased rigidity of the more rigid domains of the plasma membrane. tPnA lifetime decay was measured and the correspondent lifetime components (A) and pre-exponential factors (**B**) were determined in wt, *fas1*Δ, *fas1*Δ-p*FAS1* and *fas1*Δ-p*FAS1* + 2μg/mL doxycycline intact cells after incorporation with the fluorescent probe tPnA. Results are the median ± SD (n = 3). + P < 0.05 vs wt cells; * P < 0.05; ** P < 0.01; *** P < 0.001 *vs* *fas1*Δ cells.

	wt	***fas1*Δ**	***fas1*Δ-p*FAS1***	***fas1*Δ-p*FAS1+dox***	***fas1*Δ- pCM189**	***fas1*Δ+dox**
τ1 (ns)	1.443 ± 0.140	1.408 ± 0.226	1.140 ± 0.037**	1.410 ± 0.108	1.563 ± 0.250	1.485 ± 0.241
T2 (ns)	6.223 ± 0.217	6.238 ± 0.420	5.653 ± 0.098**	6.171 ± 0.220	6.442 ± 0.559	6.338 ± 0.431
T3 (ns)	36.824 ± 0.219	38.614 ± 0.751^{+}	35.159 ± 0.972***	36.490 ± 0.655	37.114 ± 0.647	38.963 ± 0.749
P1	0.290 ± 0.018	0.295 ± 0.018	0.337 ± 0.006***	0.297 ± 0.014	0.285 ± 0.020	0.288 ± 0.022
P2	0.099 ± 0.006	0.105 ± 0.011	0.116 ± 0.001	0.103 ± 0.006	0.094 ± 0.014	0.102 ± 0.012
P3	0.016 ± 0.001	0.017 ± 0.001	0.016 ± 0.050	0.016 ± 0.001	0.016 ± 0.002	0.017 ± 0.001

The emission was fitted to a decay function with 5 lifetime components. The shortest one is negligible, since it represents light dispersion while the longest one is negligible since it has a contribution of less than 1% of the other lifetime components, and was considered as being artefactual [223]. As expected for tPnA inserted in biological membranes, three major

components of the lifetime decay of *trans*-parinaric acid in *Saccharomyces cerevisiae* intact cells were determined (Table 15). The longer lifetime component can be associated with the fraction of probe localized in the gel phase, while the short components can be associated with the probe fraction localized in the fluid phase. Analysing the weight of each lifetime component, which is given by the parameter P, it is possible to see that the longer component was the one with the minor contribution, indicating that the majority of the plasma membrane is in a fluid state, while a small fraction is ordered as raft domains. This component is higher than 30 ns in all strains studied, in agreement with recent results with tPnA in living cells of *S. cerevisiae* [118] showing the presence of gel-like domains. wt and *fas1*Δ cells present similar lifetime decay parameters except for the longer component (τ3), which is higher for *fas1*Δ cells indicating that these domains are more rigid in the *fas1*Δ strain. *fas1*Δ-p*FAS1* cells present not only a decrease in all lifetime components in relation to *fas1*Δ cells (showing a decrease of rigidity in all the domains of the plasma membrane) but also an increase in the pre-exponential factor associated to the shorter lifetimes (P1) (indication an increase in abundance of this type of domains). The addition of 2 µg/mL of doxycycline to *fas1*Δ-p*FAS1* cells with the consequent repression of *FAS1* expression leads to a decrease of the τ and P components to the values observed for wt cells. Although a small decrease τ3 found in *fas1*Δ-pCM189 cells, this is non-significant, (as it is in cells transformed with the plasmid over expressing *FAS1*), showing that the alterations in τ3 are not due only to the transformation process but mainly to *FAS1* overexpression. The control *fas1*Δ + dox present no differences in relation to the *fas1*Δ, showing that doxycycline does not lead to changes in plasma membrane fluidity and therefore the used system is suited for fluorescence studies of membrane microdomains.

In conclusion, the results presented show that studies in intact cells should be preferred rather than isolation of plasma membrane microdomains with detergent. The manipulations along the isolation protocol can disrupt the microdomains, and the final product will be different from the one present in intact cells. On the other hand, studies by incorporation of probes in intact cells allow studying microdomains as they occur in membranes. tPnA fluorescence studies showed that a decrease in Fas activity leads to an increase not only in abundance but in rigidity of gel-like domains of the plasma membrane.

6.2.3 Microscopy studies with fluorescent probes

In *Saccharomyces cerevisiae* large membrane microdomains can be visualized in living cells [125]. The proteins of the plasma membrane of *S.cerevisiae* distribute in at least three different modes: (1) they are concentrated in discrete patches; (2) occupy a mesh shaped

compartment, which spreads between the patches; or, (3) are homogenously dispersed throughout these two areas [125, 126, 224]. In the next section results from the studies of the distribution and abundance of these membrane compartments *in vivo* are presented.

Filipin is a fluorescent polyene antibiotic that interacts with 3'-β-hydroxy sterols and allows the *in vivo* staining of plasma membrane domains rich in sterols [225]. The effect of filipin in the phospholipid membrane is regulated by the concentrations of filipin in the aqueous solution and by the sterol concentration in the bilayer. More precisely, the filipin-phospholipid interaction is regulated by the filipin aggregation state in the aqueous medium and the sterol domain formation in the membranes [226]. This way, filipin has been widely used for sterol localization and, more specifically, for ergosterol localization in fungi [128, 197, 227, 228].

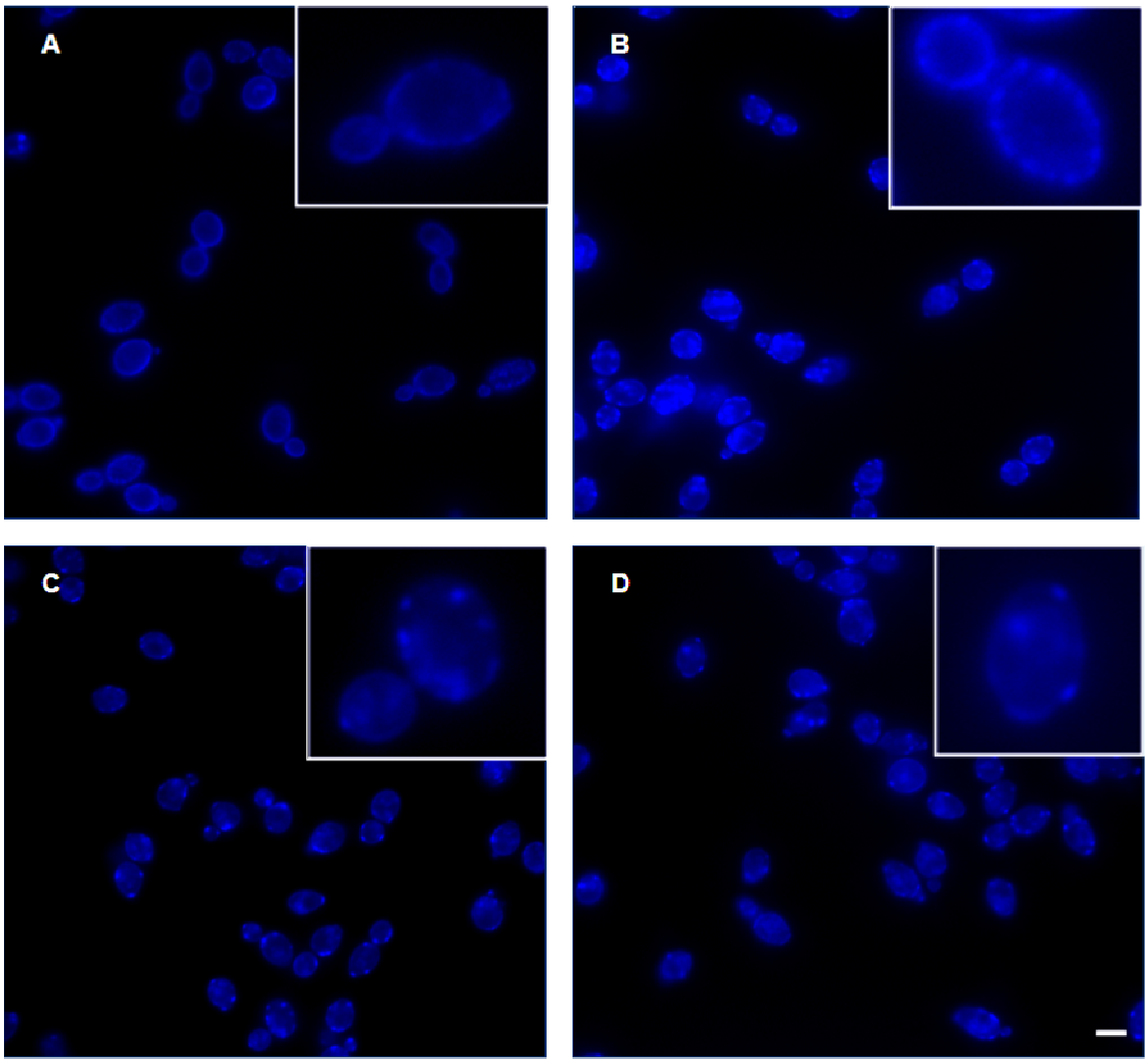

Figure 34. Changes in *FAS1* gene expression levels lead to a reorganization of plasma membrane sterol-rich domains. Microscopy images of intact cells after incubation with filipin. A- wt cells; B- *fas1*Δ cells; C- *fas1*Δ-p*FAS1* cells; D- *fas1*Δ-p*FAS1* cells +2 μg/mL doxycycline. Representative images of four independent experiments. Scale bar = 5 μM.

Irradiation of filipin with UV light leads to a very rapid photobleaching, turning the visualization very hard and leading to the impossibility to compare fluorescence intensity between samples. However, it is possible to measure the heterogeneity of filipin distribution, and, therefore, to measure differences in plasma membrane ergosterol distribution between strains. The heterogeneity profile was measured with help of an image analysis program (Image Pro-plus, Media Cybernetics, Inc.) by drawing a line along the plasma membrane of each individual cell and measuring of the distribution of fluorescence intensity along this line. Figure 35 represents the typical profile obtained for filipin fluorescence distribution along the plasma membrane of wt- and *fas1*Δ cells.

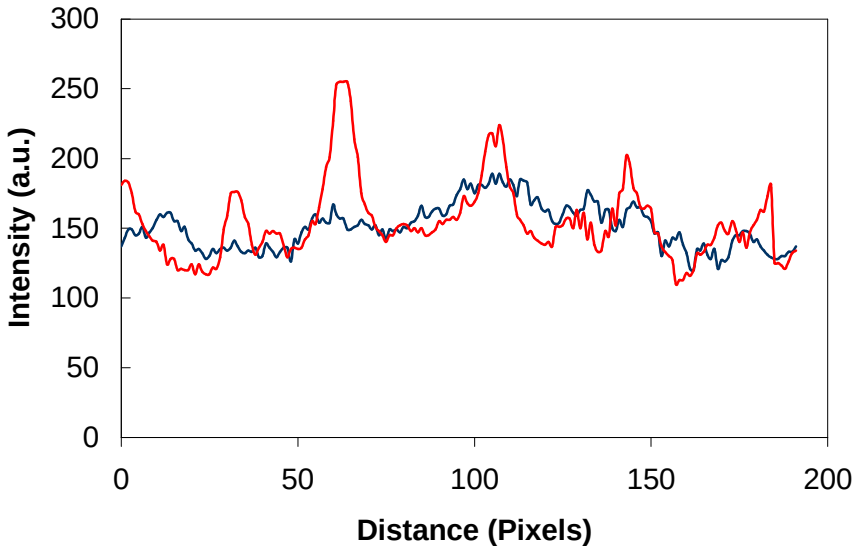

Figure 35. Line profile of the plasma membrane filipin fluorescence distribution in wt and *fas1*Δ cells. wt (blue line) and *fas1*Δ (red line) cells were stained with filipin, images acquired with a fluorescence microscope and heterogeneity of fluorescence distribution obtained by image analysis. The profile was determined.

Values for heterogeneity of fluorescence distribution can be obtained from the standard deviation of the fluorescence intensity along the plasma membrane by image analysis (Table 16).

Table 16. *fas1*Δ cells have a higher heterogeneity of the plasma membrane ergosterol distribution than wt cells. Heterogeneity profiles were determined from confocal microcopy images from cells stained with filipin. Results are the mean ± SD. Values obtained from 40 cells selected from pictures acquired in four independent experiments. * P<0.001 *vs* wt cells

Cells	Heterogeneity of ergosterol distribution (a.u.)
wt	1.79 ± 0.709
*fas1*Δ	2.36 ± 0.629*
*fas1*Δ-p*FAS1*	1.82 ± 0.537
*fas1*Δ-p*FAS1* + 2 µM doxycycline	1.88 ± 0.627
*fas1*Δ-pCM189	2.44 ± 0.505
*fas1*Δ + 2 µM doxycycline	2.52 ± 0.545

*fas1*Δ cells had a 24 % higher heterogeneity of the plasma membrane ergosterol distribution than the wt cells (Table 16). In Figure 35B it can be clearly seen that in the plasma membrane of *fas1*Δ cells there was an increased patched profile in comparison with the wt cells (Figure 35A). Therefore, a decrease in Fas activity leads to an increased heterogeneity of the ergosterol distribution in the plasma membrane. This result is consistent with what was previously observed in H_2O_2-adapted cells where there is an increased heterogeneity of the ergosterol distribution in the plasma membrane while *FAS1* expression is downregulated [66]. The strain overexpressing *FAS1* presented values of heterogeneity in the plasma membrane ergosterol distribution similar to the ones of the wt strain and the addition of doxycycline to the growth medium did not lead to an increase of these values, suggesting that changes observed in ergosterol domains distribution with changes in Fas activity are not reversible with the reestablishment of Fas activity to the original levels. The control strains (pictures not shown) present no differences in the heterogeneity of the plasma membrane ergosterol distribution when compared to the *fas1*Δ cells, showing that ergosterol distribution in the plasma membrane is not affected by the transformation process or by the presence of doxycyclin.

In order to confirm the results obtained with filipin staining, strains expressing the fusion protein Can1p-GFP were constructed and analysed by confocal microscopy. The plasma

membrane of *S. cerevisiae* contains patchy compartments denominated as MCC (membrane compartment occupied by Can1), occupied, among others, by the arginine/H^+-symporter Can1p [125] and enriched in ergosterol [126].

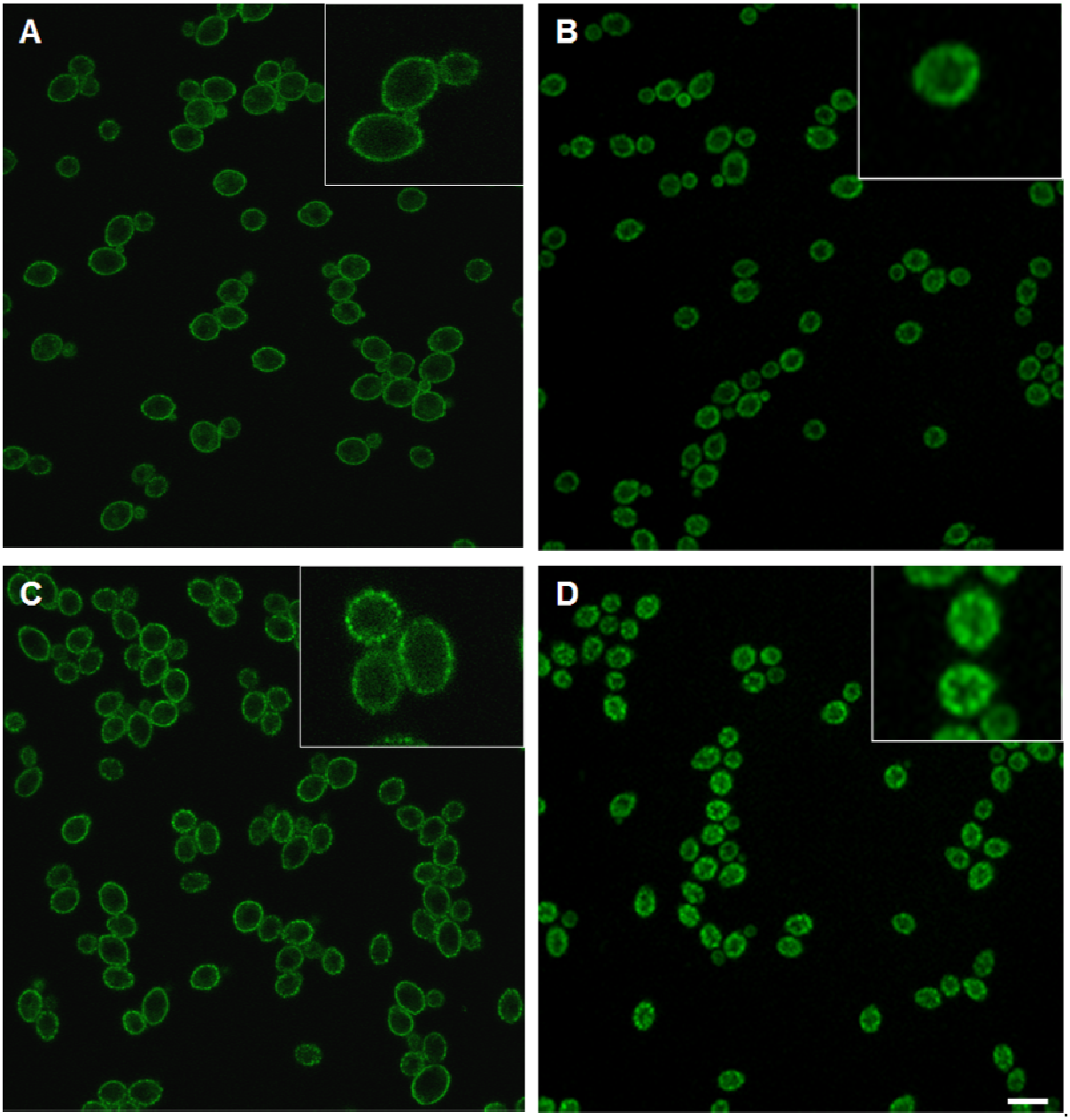

Figure 36. A decrease in Fas activity leads to a reorganization of Can1p-GFP in the plasma membrane. Confocal microscopy images from cells expressing the fusion protein Can1p-GFP. A- wt cells, equatorial confocal section; B- wt cells, surface confocal section; C - *fas1*Δ cells, equatorial confocal section; D - *fas1*Δ cells, surface confocal section. Representative images of three independent experiments. Scale bar = 10 μM.

Once again the distribution of fluorescence in the plasma membrane was translated to numbers by determination of the GFP heterogeneity profile, as described earlier for filipin.

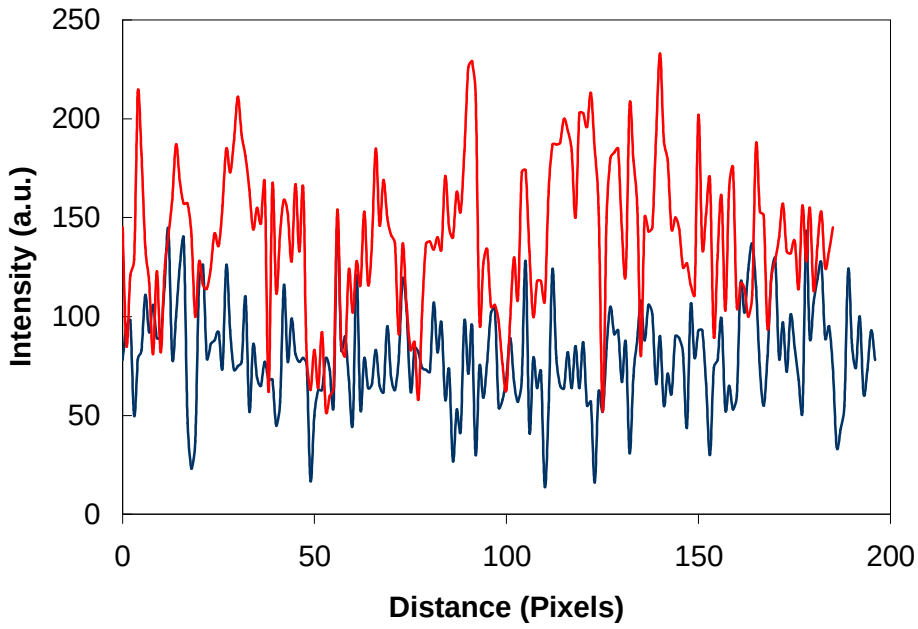

Figure 37. Line profile of plasma membrane Can1p-GFP fluorescence distribution in wt- and *fas1*Δ cells. Wt- (blue line) and *fas1*Δ (red line) cells expressing the Can1p-GFP fusion protein were constructed, images acquired with a confocal microscope and the profile of fluorescence distribution obtained by image analysis. Line profiles were obtained from images of the equatorial confocal section. Representative experiment of 3 independent experiments.

Table 17. Can1p-GFP distribution in the plasma membrane has a higher heterogeneity in *fas1*Δ cells. Heterogeneity profiles were determined from confocal microscopy images of cells expressing the fusion protein Can1p-GFP. Heterogeneity distribution was detrmined from images of the equatorial confocal section Results are the mean ± SD of 70 cells selected from pictures acquired in three independent experiments. * P < 0.001 *vs* wt cells

Strain	**Heterogeneity in Can1p-GFP distribution (a.u.)**
wt	26.90 ± 3.70
*fas1*Δ	34.82 ± 4.66 *

As can be seen in Figure 37 there are differences in Can1p-GFP plasma membrane staining pattern between wt and *fas1*Δ cells. The patchy pattern is more visible in *fas1*Δ cells, suggesting that the downregulation of Fas leads to a reorganization of MCC compartments. The measured heterogeneity in Can1p-GFP distribution confirmed this result, since in the plasma membrane of *fas1*Δ cells there was an increase of about 23 % in the heterogeneity of Can1p-GFP distribution (Table 17). It is important to notice that the percentage of increase in the heterogeneity profile was similar to the one observed for the cells stained with filipin (which presented an increase of 24% in heterogeneity for *fas1*Δ cells), giving more evidence that the MCC compartments are enriched in ergosterol [126] (and co-localize with the microdomains stained by filipin). These results are also consistent with the ones obtained in the studies of adaptation to H_2O_2 in the haploid BY4741 strain [196], where an increase in Can1p-GFP heterogeneity in the plasma membrane was observed with adaptation to H_2O_2 (where downregulation of Fas occurs). In order to find whether this change in the heterogeneity was due to differences in the plasma membrane levels of Can1p-GFP Can1p-GFP levels were determined in the different strains by flow cytometry (Figure 38).

As can be seen in Figure 38 Can1p levels in *fas1*Δ cells were higher than in wt cells. Adaptation to H_2O_2, which decreases Fas activity, also led to an increase in the levels of plasma membrane Can1p levels in wt cells. These results suggest that a decrease in Fas activity not only leads to the reorganization of ergosterol-enriched microdomains (occupied, among others, by Can1p), but also to an increase in the number of these compartments in the plasma membrane. This is not surprising, knowing that ergosterol plays an essential role in bulk membrane function, affecting membrane rigidity, fluidity, and permeability [229]. Also a cross-talk between fatty acid metabolism and ergosterol biosynthesis in order to maintain the homeostasis in plasma membrane composition has been previously observed [230].

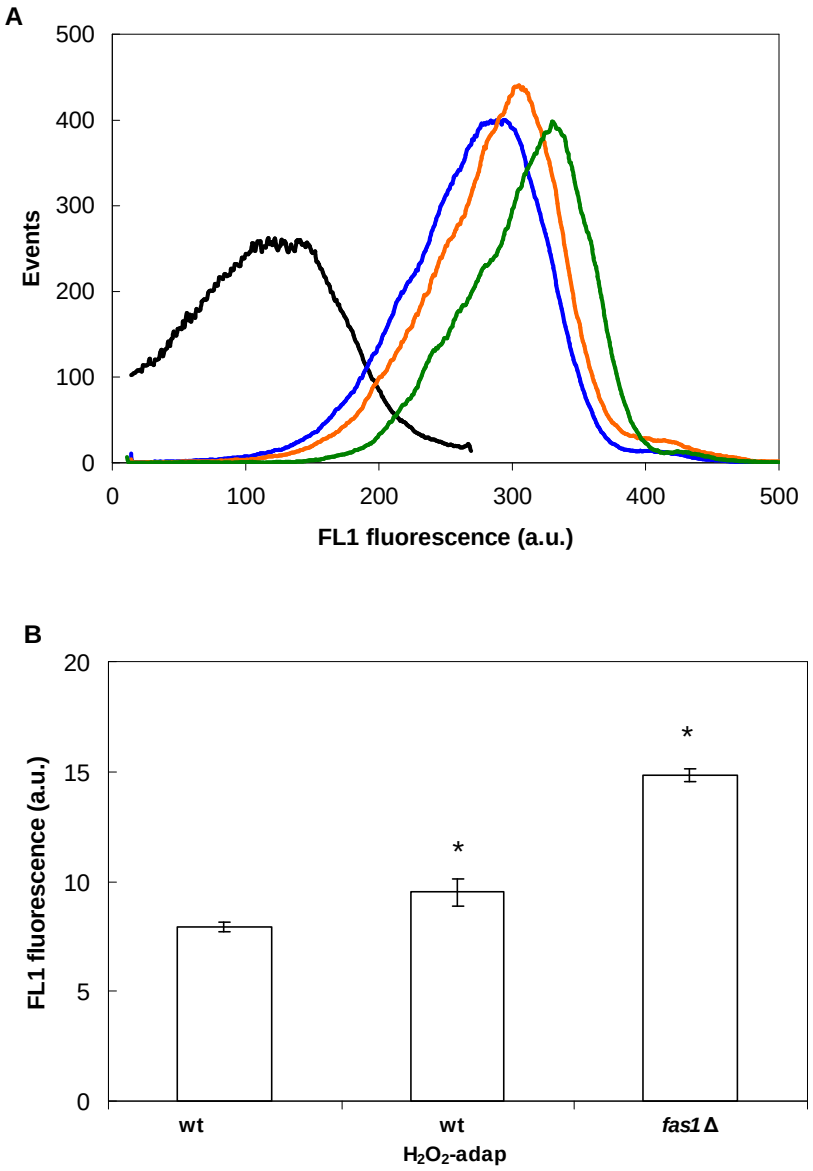

Figure 38. Can1p-GFP levels increase when Fas activity decreases. A quantitative analysis of Can1p-GFP was performed by flow cytometry fluorescence measurements in wt- and *fas1*Δ cells expressing the fusion protein Can1-GFP. Cells were adapted using steady-state 150 µM H_2O_2 for 90 min. A – Plot of FL1 fluorescence signal of one representative experiment of 3 independent experiments. Control- black line; wt – blue line; wt H_2O_2-adapted - orange line; *fas1*Δ – green line; B – quantitative representation of maximum of fluorescence intensity in the FL1 channel. The presented values of fluorescence are only due to GFP since control fluorescence was subtracted to each value. Results are the mean ± SD (n=3). * $P < 0.01$ *vs* wt cells.

Another type of microdomain has been described in the plasma membrane of *S. cerevisiae*. This domain is designated as MCP (membrane compartment occupied by Pma1p) [125], contains the plasma membrane protein H^+-ATPase Pma1p and resides in the mesh area

between the MCC patches [127]. It has been observed that C26-containing lipids are essential for the formation of functional lipid-protein complexes containing Pma1p, suggesting that these compartments are enriched in sphingolipids [231]. In order to study the distribution of these domains in the plasma membrane with variation of Fas activity, cells were probed with the antibody against Pma1p and with a fluorescent secondary antibody and images were acquired by confocal microscopy (Figure 39).

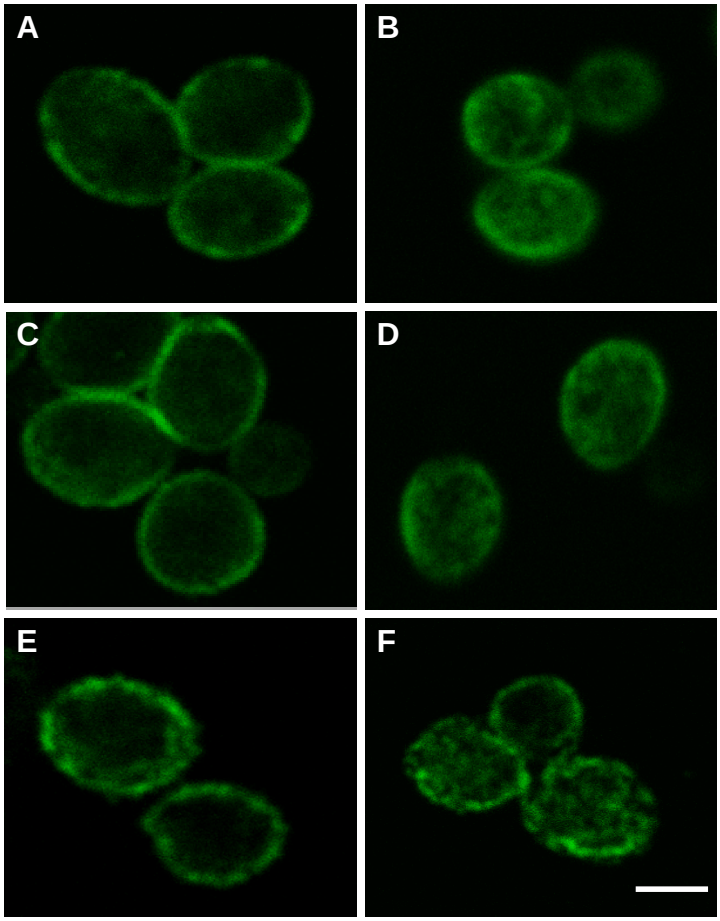

Figure 39. The patchy distribution of Pma1p in the plasma membrane does not change with downregulated Fas activity and increases with adaptation to H_2O_2. Confocal microcospy images from cells after immunostaining of Pma1p. A – wt cells, equatorial confocal section; B - wt cells, surface confocal section; C - *fas1*Δ cells; equatorial confocal section; D - *fas1*Δ cells; surface confocal section; E – H_2O_2-adapted wt cells, equatorial confocal section; F - H_2O_2-adapted wt cells, surface confocal section. Representative images of 3 independent experiments. Scale bar = 5 µM.

Table 18. The heterogeneity of plasma membrane Pma1p distribution does not change with Fas downregulation. Heterogeneity is the standard deviation of line profiles of the plasma membrane from confocal microscopy images of cells after immunostaining against Pma1p. Values are the mean ± SD of 70 cells selected from pictures acquired in 3 independent experiments. * P<0.001 *vs* wt cells

Cells	Heterogeneity of Pma1p distribution (a.u.)
wt	26.65±3.56
*fas1*Δ	26.93±3.63
H_2O_2-adapted *wt*	34.80±4.84*

The heterogeneity of Pma1p distribution in the plasma membrane was the same in wt and *fas1*Δ cells, but it increased in H_2O_2-adapted wt cells, suggesting that adaptation to H_2O_2 leads to a reorganization of MCP compartments in the plasma membrane. In order to perform a quantitative analysis, Pma1p levels in the plasma membrane were determined by Western blot (Figure 40). Western blot studies confirmed a higher (about 42 %) amount of Pma1p in the plasma membrane of H_2O_2-adapted wt cells relatively to wt control cells. A small increase of about 20 % in Pma1p relative amount in *fas1*Δ relatively to the wt cells was also detected (the difference would probably be significant with a higher number of experiments since the tendency is always the same in each independent experiment). As referred earlier, previous studies by Gaigg *et al*. [231] showed that sphingolipids are dispensable for raft association and Pma1p delivery to the cell surface but the C26:0 fatty acid is crucial in this process. This way it was expected that the *fas1*Δ strain would have an increased amount of Pma1p in the plasma membrane since it presents an increase of almost 50 % of C26:0 in the plasma membrane (Table 14). Also, previous studies of plasma membrane composition during adaptation to H_2O_2 in haploid cells showed that in H_2O_2-adapted cells, C26:0 became the major very-long-chain fatty acid owing to an 80% decrease in 2-hydroxy-C26:0 levels and a 50 % decrease in C20:0 levels, probably related to the down-regulation of fatty acid elongation and ceramide synthase genes [66].

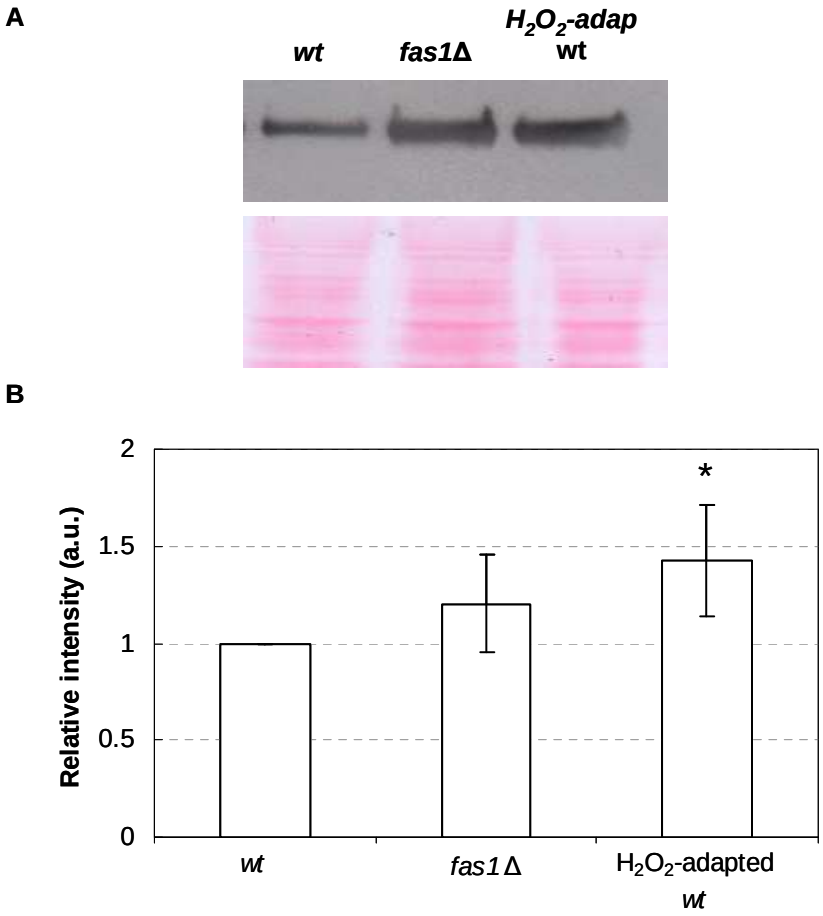

Figure 40. Adaptation to H_2O_2 but not Fas downregulation leads to an increase in plasma membrane Pma1p levels. Plasma membrane isolates of wt-, H_2O_2-adapted wt- and *fas1*Δ cells were analysed by Western blot with an anti-Pma1p antibody. Adaptation was performed using steady-state 150 µM H_2O_2 for 90 min. A- Representative image from 3 independent experiments of a Western blot with anti-Pma1 antibody and Ponceau staining used as loading control; B- quantitative analysis of Western blot results. Results are the mean ± SD (n = 3). * P < 0.05 *vs* wt cells

In conclusion, the results presented in this chapter show that major changes occur in the plasma membrane by alterations in Fas activity. There is an alteration in the phospholipid profile, an increase in VLCFA levels, an increased rigidity in gel-like domains and a visible reorganization of lipid domains in the plasma membrane.

7 Results IV - Preliminary studies in plasma membrane modification in Jurkat T-cells subjected to non-lethal doses of H_2O_2

In the previous chapters it was shown that the exposure of *S.cerevisiae* cells to low, non-lethal doses of H_2O_2 leads to changes in plasma membrane fluidity and organization, in order to form a protective barrier to the entrance of H_2O_2 to the cell. These changes occur to some extent by modulation of fatty acid synthase activity. In the present chapter preliminary studies in human lymphoma cells (Jurkat T cell line) were performed in order to understand if a similar phenomenon is observed in human cells.

7.1.1 Jurkat T cells pre-exposed to a non-lethal dose of H_2O_2 have increased plasma membrane permeability to H_2O_2 and are more sensitive to digitonin permeabilization

In order to conduct these experiments it was first necessary to select the H_2O_2 concentration that should be used. Previous work in Jurkat T cells showed that exposure to a steady-state concentration of 5 μM H_2O_2 for 30-120 min did not induce significant apoptosis [58]. Later work confirmed that a steady-state exposure to 5 μM of H_2O_2 for up to 4 h did not lead to cell death as observed by higher doses (Pedro Pereira, data not published). It was also confirmed that Jurkat T cells do not adapt after the exposure to steady-state 5 μM H_2O_2 for 4 h, since they were not more resistant to subsequent lethal doses of H_2O_2 (Figure 41). However, since higher doses of H_2O_2 lead to cell apoptosis, the preliminary work was done using this concentration of H_2O_2. Future work should be developed in order to conduct studies using adaptive doses of H_2O_2.

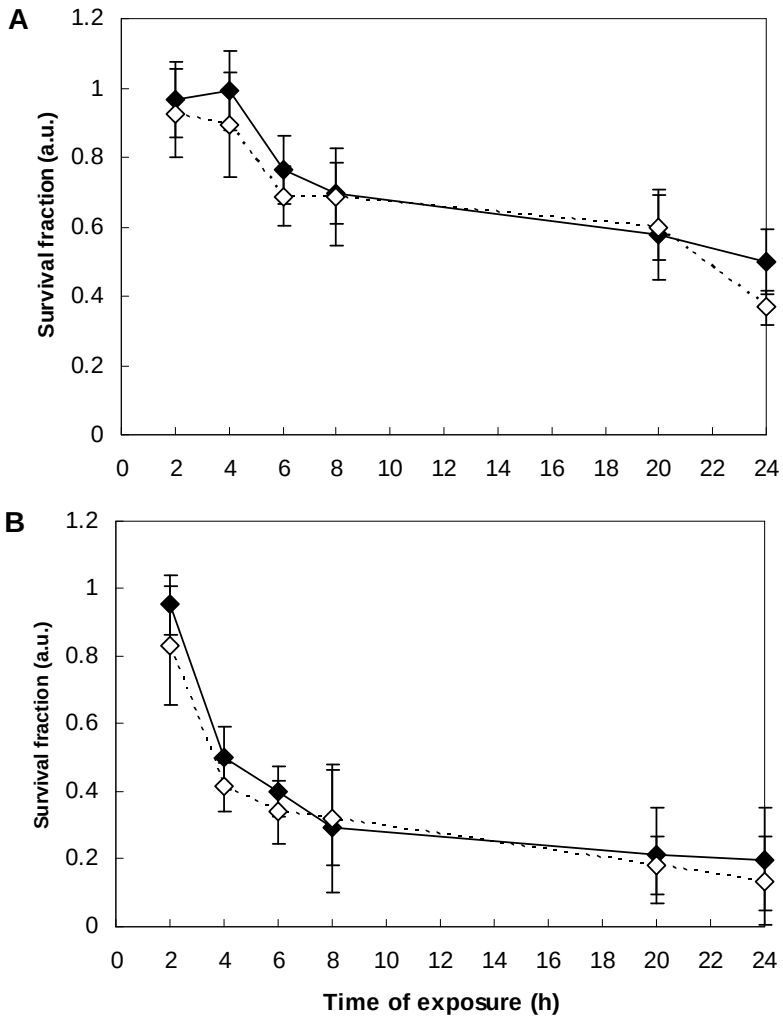

Figure 41. Pre-exposure to 5 µM H_2O_2 for 4 hours does not induce adaptation in Jurkat cells. Cells were exposed to 5 µM H_2O_2 in steady-state for 4 hours and survival fraction was measured 2, 4, 6, 8, 20 and 24 hours after adition of 50 µM (A) or 100 µM (B) of H_2O_2 in *bolus* (closed symbols). The survival fraction was also measured in control cells not pre-exposed to H_2O_2 (open symbols). Results are the mean ± SD (n=4).

Another indispensable control is whether lipid peroxidation is occurring in the chosen conditions of H_2O_2 exposure, since this phenomenon leads to alterations in plasma membrane fluidity and permeability. Fatty acid peroxidation makes the membranes more rigid, making them more porous and thus increasing their permeability [232]. In order to avoid misinterpretation of the obtained results, the absence of lipid peroxidation (which also leads to changes in plasma membrane properties) was confirmed by TBARS (ThioBarbituric Acid Reactive Substances) analysis.

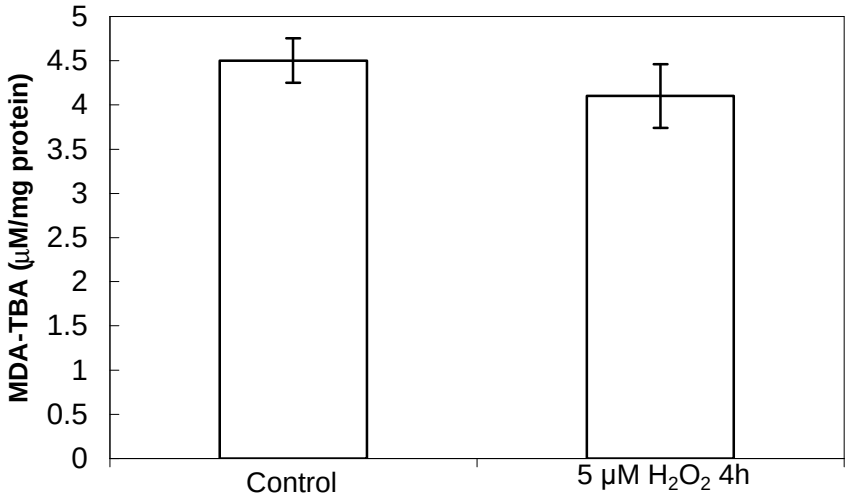

Figure 42. Exposure of Jurkat T cells to steady-state 5 μM H_2O_2 for 4 h does not induce lipid peroxidation. MDA-TBA complex fluorescence was measured in Jurkat T control cells and cells exposed to steady-state 5 μM H_2O_2 for 4 h. Results are the mean ± SD (n=3).

The results presented in Figure 42 confirm that no measurable lipid peroxidation occurs when cells are exposed to steady-state 5 μM of H_2O_2 for up to 4 h. This way, subsequent studies were made by exposing Jurkat T cells to steady-state 5 μM H_2O_2 for 1, 2 and 4 h. Time resolved biophysical studies were performed in Jurkat T cells incorporated with tPnA (Table 19), a lipid probe that partitions preferentially into ordered membrane domains.

Once again, as expected for tPnA inserted in biological membranes, three major components of the lifetime decay of *trans*-parinaric acid were obtained for intact Jurkat T cells (Table 19). The longer lifetime component (τ3) corresponds to the fraction of probe localized in the more rigid phase and is also the most abundant phase in the plasma membrane, as determined by the value P3. The short components (τ1 and τ2) are associated with the probe fraction localized in the fluid phase. As it can be observed in Table 19, pre-exposure of Jurkat T cells to 5 μM H_2O_2 for a period of time as short as 1 h leads to a significant decrease in the longest lifetime, indicating that there is an increase in the fluidity of these domains. Since these are the major components of the membrane, it could be predicted that there is an overall increase in plasma membrane permeability after exposure to H_2O_2. The observed fluidity increase was more accentuated for longer times of exposure.

Table 19. Plasma membrane rigid domains become more fluid after Jurkat T cell exposure to H_2O_2. Lifetime decay was measured and the correspondent lifetime components (τn) and pre-exponential factors (Pn) were determined in control cells and cells exposed to steady-state 5 μM H_2O_2 for 1,2 and 4 hours cells after incorporation with the fluorescent probe tPnA. Values are the mean ± SD, (n=3). * P < 0.05 *vs* control.

	Control	5 μM H_2O_2 (1h)	5 μM H_2O_2 (2h)	5 μM H_2O_2 (4h)
τ1 (ns)	0.942±0.289	0.824±0.058	0.786±0.026	0.780±0.025
T2 (ns)	4.779±0.467	4.277±0.304	4.287±0.119	4.314±0.130
T3 (ns)	19.377±1.316	16.851±0.973*	16.365±1.245*	16.184±1.263*
P1	0.013±0.005	0.014±0.009	0.014±0.005	0.015±0.014
P2	0.130±0.016	0.146±0.031	0.155±0.012	0.156±0.027
P3	0.580±0.142	0.636±0.149	0.625±0.043	0.621±0.104

In order to understand if the plasma membrane sterol composition is altered after pre-exposure to H_2O_2, a digitonin sensitivity study was performed. Digitonin is a steroid glycoside that interacts specifically with 3β-hydroxysterols [233] and permeabilizes membranes by complexing with the membrane cholesterol [234].

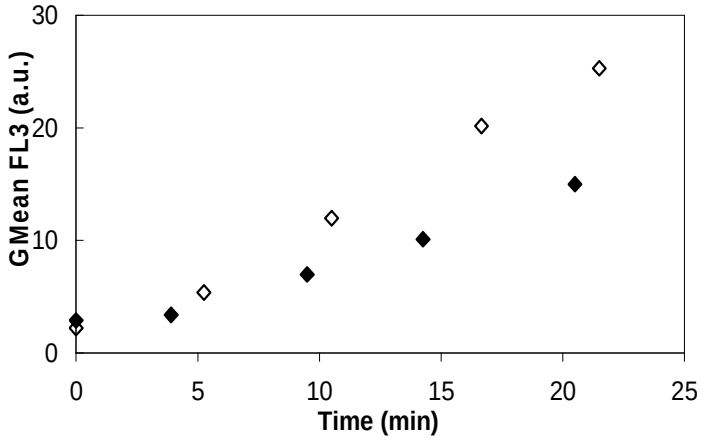

Figure 43. Cells exposed to H_2O_2 are more sensitive to digitonin permeabilization than control cells. Control and H_2O_2-exposed cells (5 μM for 4 hours) were incubated with digitonin and propidium iodide (which enters and stains permeabilized cells, but not intact cells) and the fluorescence intensity was measured along time by flow cytometry. Closed symbols: control; open symbols: H_2O_2-exposed cells (steady-state 5 μM H_2O_2, 4 h). Representative experiment of 3 independent experiments.

It is also known that digitonin permeabilization is dependent on membrane sterol content, since it is widely used for selective fractionation. The treatment of cells with a low concentration of digitonin selectively permeabilizes the plasma membrane due to its relatively high cholesterol content, and the nuclear envelope, poor in sterols remains intact. The cytoskeleton is largely undisturbed [235]. In Figure 43 it is visible a considerable difference in propidium iodide incorporation between control and H_2O_2-treated cells. Cells pre-exposed to steady-state 5 μM H_2O_2 presented a higher rate of propidium iodide incorporation. This occurs due to their higher sensitivity to digitonin, being their plasma membrane more rapidly permeabilized. This result suggests that the plasma membrane of H_2O_2-exposed cells is richer in cholesterol than the non-exposed cells. Cholesterol is an *amphipatic* molecule that contains a hydrophilic and hydrophobic portion and is essential to maintain the rigidity of the plasma membrane by immobilization of the outer surface of the membrane (by the interaction of the sterol ring with the fatty acid chain of the phospholipids). At the high concentrations it is found in eukaryotic cellular plasma membranes (close to 50 percent) cholesterol helps to separate the phospholipids so that the fatty acid chains do not interact and crystallize, turning the membrane too rigid [236]. This way, an increase in the cholesterol content of H_2O_2 pre-exposed cells is consistent with the observation of the increase of plasma membrane fluidity.

7.1.2 Plasma membrane cholera toxin microdomains increase after exposure to H_2O_2

The plasma membrane of Jurkat T cells is also organized in microdomains, containing the T cell receptor complex, integrins, GPI-linked molecules, acylated molecules, cholesterol and ganglioside GM1 [237]. In order to understand how these plasma membrane microdomains are affected by exposure to H_2O_2, Jurkat T cells were labelled with a FTIC-conjugated B subunit of the cholera toxin, which is known to bind specifically to the GM1 receptor [238] and has been widely used as a marker for membrane detergent resistant domains in the plasma membrane.

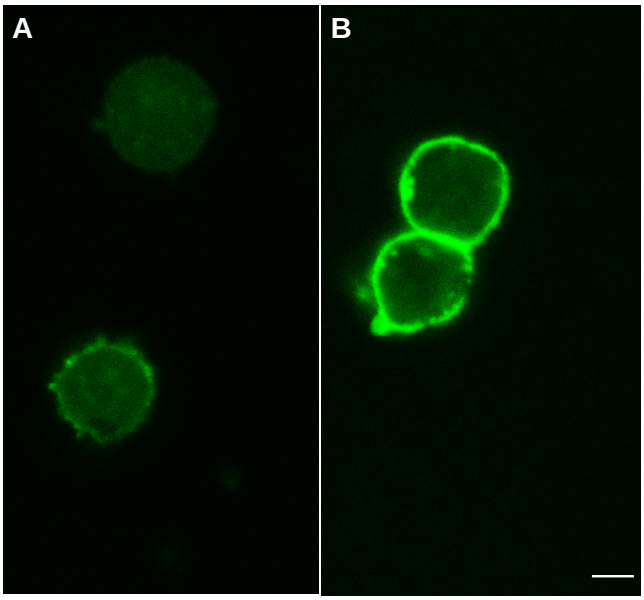

Figure 44. Exposure to non-lethal doses of H_2O_2 increases the amount of GM1 in the plasma membrane of Jurkat T cells. Jurkat T Cells were labelled with FTIC conjugated cholera toxin B subunit and visualized by fluorescence microscopy. A- control cells; B – Cells exposed to steady-state 5 μM H_2O_2 for 4 h. Representative experiment of two independent experiments. Scale bar = 10 μm

The fluorescence microscopy images obtained from cells labelled with the FTIC-conjugated B subunit of the cholera toxin (Figure 44) showed that the fluorescence intensity of the plasma membrane was higher in cells pre-exposed to 5 μM of H_2O_2 for 4 h. The observed result indicated that there was an increase of GM1 abundance in the plasma membrane after exposure to the low H_2O_2 concentration used. It is known that the GM1 ganglioside localizes in cholesterol-enriched domains [239], and so the observed increase is consistent with the increase cholesterol levels predicted from the higher sensitivity to digitonin. Gangliosides showed to play an important role in cell protection against ethanol, since exogenously administered monosialoganglioside GM1 enhances recovery from, or protection against cellular injury, including that caused by ethanol [240]. Also, Laser Raman spectroscopy and fluorescence polarization suggested that GM1 induces membrane phase separation and that the order of hydrocarbon chains increases and membrane fluidity decreases with increase in GM1 content [241], being consistent with the observed decrease of fluidity in H_2O_2-exposed cells in t-PnA fluorescence studies (Table 19).

7.1.3 Plasma membrane modifications in Jurkat T cells are not due to modulation of Fas

In the previous sections of this thesis it has been shown that fatty acid synthase plays an important role in *Saccharomyces cerevisiae* plasma membrane alterations induced by exposure to adaptive doses of H_2O_2. Since alterations in the plasma membrane of Jurkat cells exposed to steady-state low doses of H_2O_2 for short periods of time are also observed, it was important to understand if fatty acid synthase was also involved in the observed changes. Fas is minimally expressed in most normal human tissues except the liver and adipose tissue, where it is expressed at high levels [168]. It is also selectively expressed in some types of cancer cells (breast, prostate, colon, ovary, and endometrium), being considered a putative tumor marker [242]. In Jurkat T cells Fas expression is very low, being hard to measure experimentally differences in gene expression or in Fas activity. This way, Fas protein levels were determined by Western blot (Figure 45A).

Results show that there are no measurable differences in Fas protein amount between control and cells exposed to 5 μM of H_2O_2 for 4 hours. Since short times of H_2O_2 exposure were used, there is a possibility that there was not enough time to allow proper protein regulation and turnover and, therefore, not enough time to have observable changes in Fas levels. This way another experience was performed, where protein extraction was only performed 24 h after the exposure to H_2O_2 for 4 h (Figure 45B), however no differences between Fas levels were observed.

In conclusion, the results presented in this chapter show that Jurkat cells exposed to non-lethal doses of H_2O_2 for short periods of time show alterations in plasma membrane fluidity, digitonin sensitivity and also GM1 microdomains. These alterations are not due to lipid peroxidation and Fas seems not to be involved in plasma membrane changes. All in all, the presented preliminary results are guidance to further investigation in H_2O_2 adaptation processes in Jurkat cells.

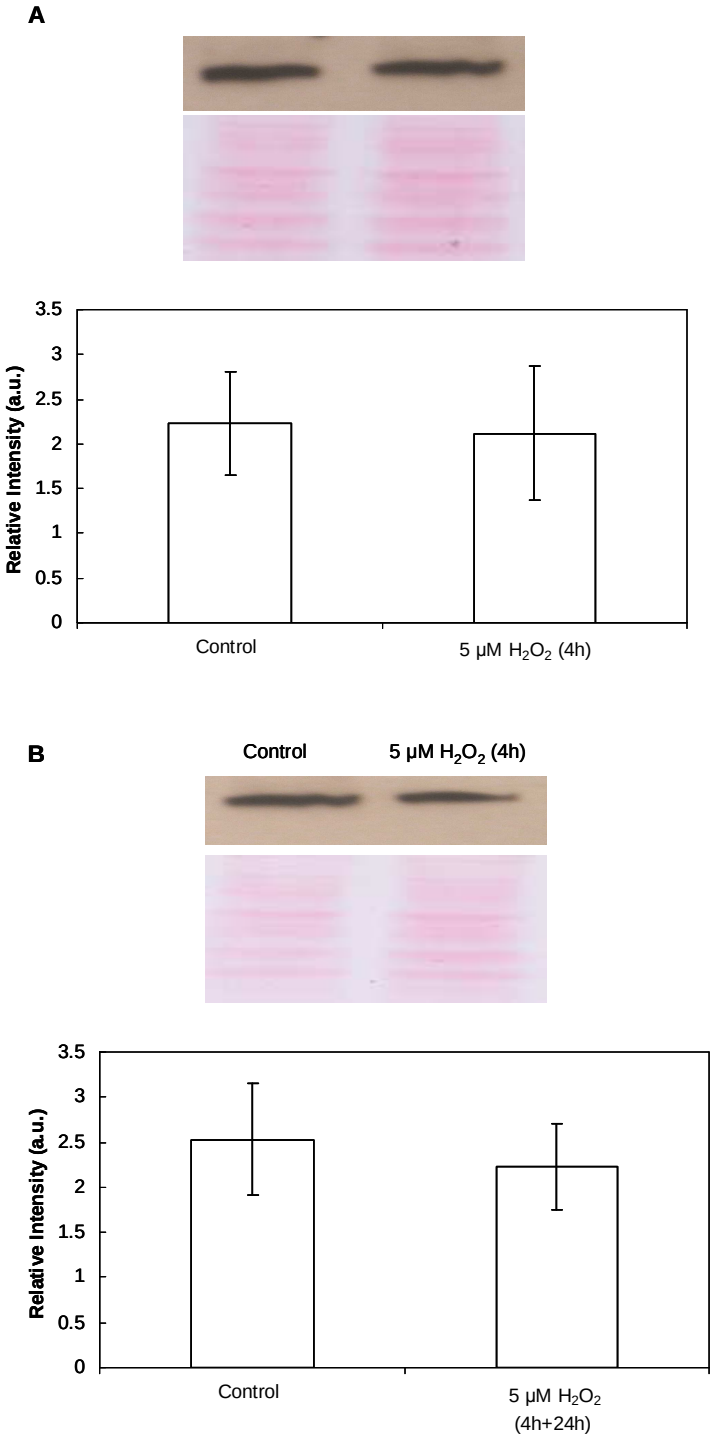

Figure 45. Fas levels in Jurkat T cells are not altered by exposure to H_2O_2. Whole cell lysates of control and H_2O_2-exposed cells (steady-state 5 µM H_2O_2, 4 h) were analysed by Western blot with an anti-Fas antibody. The figure shows a representative image from 3 independent experiments; of Western blot with anti-Fas antibody and Ponceau staining used as loading and the respective quantitative analysis of Western blot results. A- Protein levels after 4 hours of exposure to steady-state 5 µM H_2O_2; B – oProtein levels 24 h after exposure to steady-state 5 µM H_2O_2 for 4 h. Results are the mean ± SD (n = 3).

8 General Discussion and Conclusions

The present work elucidates several important aspects that are crucial for the understanding of cell adaptation to H_2O_2. The work focused on the observation that adaptive doses of H_2O_2 down-regulate Fas and links this regulation to the increased cell resistance to this oxidizing agent and to a reorganization of plasma membrane microdomains.

Adaptation to oxidative stress is a complex phenomenon and several pathways have been implicated in this cellular response, including induction of antioxidant enzymes [54], repair mechanisms, proteasomal and lysosomal activation [56], and induction of heat-shock proteins [54]. In recent years, the plasma membrane emerged as a novel cellular site involved in this response since its permeability to H_2O_2 is decreased during adaptation, acting as a cellular barrier to its entrance in the cell [57]. The mechanism by which this process occurs is not yet fully understood but, as the main constituents of the plasma membrane, lipids are good candidates to play a key role in the changes occurring in the plasma membrane during adaptation to H_2O_2.

mRNA microarray analysis of genes showed that several genes involved in lipid metabolism had altered expression in cells adapted to H_2O_2 [66]. One of the genes with altered expression was *FAS1*, which codifies for the β-subunit of fatty acid synthase, the protein responsible for the *de novo* synthesis of fatty acids in yeast [140, 141]. Reinforcing the role of Fas for H_2O_2 adaptation was the establishment of an inverse correlation between Fas activity and cell resistance to lethal doses of H_2O_2. The decrease of Fas activity by 50%, through deletion of *FAS*1 in one allele, was sufficient to increase resistance to low lethal doses of H_2O_2. Likewise, upregulation of Fas decreases survival to low lethal H_2O_2 doses. Since no increases in the main H_2O_2 removing-enzymes (catalase and cytochrome *c* peroxidase) were found (with *fas1*Δ cells presenting even a lower cytochrome *c* peroxidase activity than wt cells), this increased resistance could be related to an increase of available NADPH by lowered consumption of this co-factor in fatty acid synthesis by Fas. NADPH can be directed to the thioredoxin peroxidase and glutaredoxin pathways, essential for the maintenance of the redox state of the cell [16]. Fas modulation of the NADPH pool has already been proposed as a probable mechanism of protection of *S. cerevisiae* cells in response to α-synuclein [166]. Another hypothesis is that, since fatty acids play an important role as a source of metabolic energy, and as building blocks of membrane lipids, being able to influence membrane fluidity and also receptor or channel function, alterations in fatty acid synthesis could lead to changes in plasma membrane properties. Changes in plasma

membrane fluidity influence not only the free diffusion of molecules across the membrane bilayer but can also alter the activity of integral membrane proteins [243] that participate in transport across the plasma membrane and sensing of extracellular stimulus. The mechanism by which H_2O_2-adapted *S. cerevisiae* cells become more resistant to H_2O_2 has already been associated with changes in plasma membrane fluidity [95] and permeability to H_2O_2 [57]. However, while a decrease in plasma membrane permeability to H_2O_2 can be measured in H_2O_2-adapted cells [57], no changes in bulk plasma membrane permeability to H_2O_2 were detected in *fas1*Δ cells, suggesting that any hypothetical changes in plasma membrane by down-regulation of Fas are localized. Nevertheless, when Fas was overexpressed, plasma membrane permeability to H_2O_2 increased, returning to control levels upon elimination of the overexpression in the transformed strain. These observations underlie the complexity of the phenomena under study and establish Fas as an important modulator of plasma membrane permeability to H_2O_2, although in a range of Fas activity higher than that found in the diploid strain used here.

Coming back to *fas1*Δ cells where no overall changes of permeability were detected, several observations support the occurrence of more subtle membrane changes. In fact, several changes in phospholipid and fatty acid composition were detected. Regarding phospholipids, an increase in the phophatidylcholine/phosphatidylethanolamine (PC/PE) ratio and an increase in phosphatidylinositol (PI) accompanied by a decrease in phosphatidylserine (PS) levels were the main observed alterations in the plasma membrane of *fas1*Δ cells. The increase in the PC/PE ratio has already been observed in previous studies of adaptation in haploid wt cells [66]. Changes in PC/PE ratio can lead to major changes in plasma membrane intrinsic curvature and, consequently, in its permeability to H_2O_2 and other agents, since PC and PE present different shapes. PC presents a cylindrical shape, being preferentially disposed in bilayers, while PE is a conical shape and organizes preferentially in non-bilayer structures [73, 212]. The increase of the PC/PE ratio of plasma membrane lipid vesicles as already been described as decreasing the glucose permeability of these membranes [244, 245]. A lower level of the non-bilayer lipid PE would decrease the tension within the phospholipid layer with a consequent decreased permeability of the membrane [245]. On other hand, the coupled regulation of PI and PS has been described previously as a form of maintaining of the lipid net charge in the abnormal lipid metabolism of inositol-starved yeast [246]. Since there are no studies describing a relation between membrane permeability or fluidity and changes in the ratio of these phospholipids and, since PI plays an important role in signalling processes, the implication of these results in the increased resistance to H_2O_2 is probably due inositol action in signalling cascades rather than in changes of plasma membrane permeability to H_2O_2. Signalling pathways mediated by

inositol and inositol intermediates can also be suggested as being involved in plasma membrane modulation by Fas down-regulation by H_2O_2, since a inositol-sensitive upstream activating sequence (UAS_{INO1}) is common among genes associated with lipid metabolism (including the *FAS*1 gene), establishing a linkage between them [206]. Previous work established a relation between *FAS1* expression and the *INO1* gene, which expresses the protein Ino1p that catalysis a rate limiting step for PI synthesis from CDP-DAG and inositol, by showing that wt cells with increased transcription of the *FAS1* gene show decreased levels of *INO1* mRNA [206]. The increase of plasma membrane PI levels with down-regulation of Fas observed in this work may be an additional evidence of this relation.

An increase in VLCFA in the plasma membrane of *fas1*Δ cells was also observed. In yeast, VLCFA are predominantly present in the ceramide backbone of sphingolipids [247] which, together with ergosterol and specific proteins, organize as discrete domains in membranes [110]. The strong interactions between sphingolipids and/or sterols are just high enough to hold them together in small microdomains, (usually designated as lipid rafts) [110], and represent a phase separation in the fluid lipid bilayer. The structural characteristics of sphingolipids can influence the order of the lipid phase and the curvature and thickness of membranes [248] and the interest in membrane sphingolipid-enriched domains has raised in the last years. Membrane remodelling by sphingolipid microdomains has been already described in cell response to viral infection [249], interaction of protein toxins [250] and plasma membrane damage in wounded cells [251]. Biological membranes usually are constituted by liquid ordered (lo) phase and liquid disordered (ld) phase domains. In addition, in *S. cerevisiae*, the existence of highly ordered gel-like domains enriched in sphingolipids was recently described [118]. The existence of these domains in the strains used in this study was confirmed by fluorescence studies with t-PnA. Moreover, it was observed that a decrease in Fas activity leads to an increase of the rigidity of these domains. The increased rigidity may be associated with the higher levels of VLCFA in the membrane, constituents of sphingolipids, which associate in these specific gel-like domains. In this work, the two most abundant plasma membrane microdomains in yeast were studied: the MCC and the MCP domains. Although these have been considered as being distinct, stable domains, it would not be not surprising to observe some degree of dependence between them. Although formed by discrete domains, the plasma membrane is a dynamic system and alterations in organization or constitution in one type of domain would certainly induce alterations in other domains, in order to maintain the membrane equilibrium. Actually, recent work has described the occurence of exchange of some proteins between MCC and MCP [252].

The MCP domains occupy a mesh-shaped compartment which spreads between the MCC discrete domains [128] and contains the H^+-ATPase pump Pma1p. Sphingolipids showed to be essential to Pma1p insertion in the plasma membrane [129] and VLCFA have been described as essential for the formation of MCP domains [231], suggesting that the Pma1p compartments are probably enriched in these lipids. Microscopy studies showed no differences in Pma1p distribution in the plasma membrane of *fas1*Δ. The significant increase of VLCFA in the plasma membrane in these cells was accompanied by a small increase in Pma1p membrane levels (maker protein of MCP domains). This is consistent with the results obtained from biophysical studies with t-PnA, which suggested that a decrease in Fas activity lead to an increase not only in abundance but in rigidity of gel-like domains of the plasma membrane. Biophysical studies in *S. cerevisiae* by Aresta-Branco *et al.* [118] gave evidence that the gel-like domains detected by the probe t-PnA are probably related to the MCP domains, which comprise a large portion of the plasma membrane. The results obtained suggest that the down-regulation of Fas may regulate the segregation of sphingolipids into MCP domains (decreasing their fluidity) and entail the formation of new domains. The increase of VLCFA in MCP could be a stabilizing factor against the internalization of Pma1p, leading to the detected small increase in its levels. Pma1p is a very stable integral membrane protein but it can be rapidly internalized by endocytosis under certain circumstances (e.g. perturbations of plasma membrane lipid composition [253] and salt stress [106]) and stored inside the cell until recycled to the plasma membrane or degraded in the vacuole. Changes in Pma1p levels could contribute to internal pH deregulation and to a decrease of membrane potential [106], leading to a decreased ability to survive under H_2O_2 stress conditions. The maintenance of the proton gradient in the cell by Pma1p also contributes to a higher energy production, which can be used in protection mechanisms against H_2O_2.

The MCC domains consist in distinct patchy structures (estimated to have ~300 nm) that are enriched in ergosterol [126]. Filipin staining of intact cells showed that ergosterol forms patches in the plasma membrane, which reorganize with down-regulation of Fas. The obtained images also suggest an increase in the number of ergosterol-rich domains in the *fas1*Δ strain. These results are consistent with the previously observed increase in ergosterol heterogeneity of distribution on the plasma membrane of H_2O_2-adapted cells [66], since Fas is down-regulated during adaptation to H_2O_2. Microscopy and flow cytometry studies of Can1p-GFP transformant cells revealed not only a reorganization in the location of this protein in the plasma membrane, but also an increase of its amount in *fas1*Δ cells. Can1p has been widely accepted as a protein marker for the MCC domains, and it has been observed that membrane domains stained by filipin co-localize with MCC domains [126]. The

results obtained in this work show that down-regulation of Fas leads not only to a reorganization but also to an increased amount of Can1p (and probably of MCC domains) in the plasma membrane. The biological function of MCC is not yet understood and contradictory results have been presented. However, it has been associated with a protective function in protein turnover [128] and it is known to be associated with eisosomes. Eisosomes have been described as endocytic sites, however, the role of eisosomes in endocytosis regulation is a matter of debate [252]. One possible function of MCCs and eisosomes is to regulate protein and lipid abundance by sorting them into distinct, spatially separated pools where they are stabilized or from where they can be endocytosed selectively [131]. This way, it can be hypothesised that the regulation of MCC domains by down-regulation of Fas can be the mechanism by which the cell controls internalization of plasma membrane proteins somehow involved in acquired resistance to H_2O_2. Eisosomes also define sites of plasma membrane and MCC organization, since in *pil1*Δ cells (lacking the protein Pil1p, essential for eisosome assembly [133]), all MCC markers analyzed so far, including sterols, lose their characteristic punctuate pattern and spread along the plasma membrane [126, 128, 133]. The mechanism by which eisosomes organize the plasma membrane is yet unknown, however, it has been suggested that eisosome core components Pil1p and Lsp1p belong to the membrane-sculpting Bin/amphiphysin/Rvs (BAR) superfamily of proteins [254]. The BAR domain is a class of phospholipid binding domains, that bind membranes through electrostatic interactions between the negative charges of the membranes and the positive charges on the structural surface of homo-dimeric BAR domain superfamily [255]. Moreover, BAR domains sense and induce curvature in the membrane, facilitating the formation of invaginations or protrusions. The generation of curvature and the production of phosphoinositides involved in signal transduction appear to be correlated in events such as endocytosis and other morphological changes [255].

This way, sphingolipids and intermediates of sphingolipid metabolism may play an important role in the down-regulation of MCC domains by Fas. It is known that sphingolipids play an important role in signalling in a variety of cellular processes; e.g., the case of ceramides as potent inducers of apoptosis in response to stress induced by ionizing radiation [256] and long chain bases (LCBs) and their derivatives as participants in the heat shock response in yeast [85]. When sphingolipids are inserted in membranes, their complex glycan head group also acts as surface exposed membrane element that can be recognized by a variety of proteins [257]. Regulation of sphingolipid biosynthesis is highly dependent on the availability of substrates. The sphingolipid signalling heat shock response in *S. cerevisiae* results from changes in substrate availability rather than by direct enzyme activation. Specifically, endogenous fatty acid synthesis and uptake of extracellular serine were both shown to be

required for heat-induced sphingolipid synthesis [258]. In the present work, the putative increase of plasma membrane sphingolipids by down-regulation of Fas, is probably due to a shunting of newly synthesised fatty acid between competing pathways (since no exogenous source of fatty acids is present in the experimental conditions used, and it is known that import from the medium or endogenous synthesis by Fas are the only two possible sources of fatty acids in *S.cerevisiae* [259]). Also, an increase in serine uptake or synthesis might be present. This may explain the observed decrease in plasma membrane levels of PS, since intracellular serine may be deviated from the phospholipid synthesis to the sphingolipid synthesis pathway. The increase of LCB levels exerts an inhibitory effect in the phosphorylation of Pil1p by Pkh-kinases. If Pil1p is hypophosphorylated, more protein assembles into eisosomes, forming enlarged eisosomes that show altered organization [133]. Since eisosomes showed to be essential to the organization and size of MCC domains, the inhibition of Pil1p phosphorylation by LCB shows to be a consistent hypothesis for the reorganization of MCC domains in Fas down-regulation. Previous studies in plasma membrane modulation by H_2O_2 (where a down-regulation of Fas was observed) showed that the increased heterogeneity profile of plasma membrane ergosterol enriched domains is also associated with an increase of Pil1p associated with the plasma membrane [66].

Interestingly, in this work it was also observed for the first time that H_2O_2 induces a biphasic effect on the levels of *FAS1* mRNA. In a relative narrow range of H_2O_2 extracellular concentrations the stimulatory effect of H_2O_2 turns into an inhibitory effect. This type of dose-dependent response to H_2O_2 has been previously observed for other cellular processes. In TNF-α-dependent NF-κB activation in HeLa and MCF-7 cells, an inhibitory or stimulatory effect is observed depending on the H_2O_2 concentration added simultaneously with TNF.α [52, 260]. In Jurkat-T cells, intracellular concentrations below 0.7 μM showed to be regulatory, between 0.7 and 3 μM induced apoptosis, while higher than 3 μM induced necrosis [58]. In *Schizossacharomyces pombe* some signalling mechanisms are highly dose-dependent and some individual transcription factors were also found to be activated only within a limited range of H_2O_2 concentrations [261]. Therefore, the results shown here reinforce that, when working with extracellular delivery of H_2O_2 in vitro, controlling H_2O_2 dosage along time is crucial, since small differences in H_2O_2 concentration can lead to variable, even opposing, results, as observed for the expression of *FAS1*. The profile of H_2O_2 consumption by cells will depend on the particular conditions of the experiments and, consequently, reproducibility of the observations between different laboratories is problematic [260]. The steady-state delivery shows to be much more rigorous and controllable and, taking in account the existence of continuous source of H_2O_2 *in vivo*, it also simulates better the cellular environment as compared with the bolus addition approach [260].

The preliminary studies in Jurkat T-cells show that a non-lethal dose of H_2O_2 also leads to alterations in plasma membrane biophysical properties and microdomains. These changes were not due to lipid peroxidation.. Fas seemed not to be involved either, however more experiments are need. One important observation was the increase of GM1 levels in the plasma membrane of H_2O_2-exposed cells. Previous studies showed that GM1 is capable of inhibiting the oxidative stress induced by ethanol in primary cultures of rat hepatocytes , via an effect on the pool of low molecular weight iron [262]. It was also observed that both the hydrophilic sugar heads and the hydrophobic hydrocarbon chains of GM1 contribute to the regulation of membrane architecture [241]. This way, it can be hypothesised that this protein may play an important role in plasma membrane alterations caused by exposure to non-lethal doses of H_2O_2.

All together, the presented work clarifies the role of *S. cerevisiae* fatty acid synthase in the increased resistance to H_2O_2 and the associated modulation of plasma membrane microdomains. Moreover, it introduces Fas as a novel candidate in oxidative stress response. This may relation is even more interesting knowing that Fas activity and fatty acid *de novo* synthesis is crucial in tumor cell development. Adaptation in cancer cells has also gained much attention in the past years, since it can explain not only the development of cancer, but also the acquired resistance to chemotherapeutic agents observed in some types of cancer cells. Accumulation of ROS under various endogenous and exogenous stress stimuli may induce lethal damage in cells. In certain cancer cells, persistent ROS stress may induce adaptive stress responses including activation of redox-sensitive transcription factors, such as NF-κB and Nrf2, leading to an increase in the expression of ROS-scavenging enzymes, such as superoxide dismutase, elevation of survival factors, and inhibition of cell death factors, such as caspases. In yeast, exposure to adaptive doses of H_2O_2 leads to activation of Yap1, a bZIP DNA-binding protein of the AP-1 family that controls many proteins of the H_2O_2 stimulon [44]. ROS-mediated DNA mutations or deletions also promote genomic instability and thus provide an additional mechanism for stress adaptation [13]. All these events enable cancer cells to survive with the high level of ROS and maintain cellular viability. Furthermore, the increase in glutathione during adaptation can enhance the export of certain anticancer drugs and their inactivation, increasing cell survival but rendering cancer cells more resistant to chemotherapeutic agents [13].

However, much more is still to uncover, since lipid metabolism is an extremely complex system under tight regulation and several points of cross-talk between pathways.

8.1 Future perspectives

Although much has been unravelled about fatty acid synthase regulation by H_2O_2 and the consequent plasma membrane alteration, more work must be developed in order to completely understand the mechanism by which it occurs The observation and quantification of Pil1p associated with the plasma membrane of wt and fas1Δ cells would help to confirm if the observed alterations in plasma membrane organization of MCC domains is associated with a reorganization of eisosomes as suggested in this thesis. Also, in order to understand how plasma membrane protein turnover modulates the observed alterations in the plasma membrane, a proteomic study of plasma membrane proteins with down regulation of Fas should be made.

Since only preliminary studies were made in human cells, more work should be developed in order to establish a relation between Fas and the detected alterations in plasma membrane properties after exposure to sub-lethal doses of H_2O_2. A titration of time of exposure to 5 μM of H_2O_2 should be made in order to observe cell adaptation to H_2O_2. Also a genomic approach should be made in order to understand which genes are altered by the pre-exposure to H_2O_2. In order to simplify the genomic study and considering once again that lipids are the major constituents of the plasma membrane, being cucial for the biophysical properties of the membrane, a screening of genes involved in lipid metabolism should be made. The establishment of a relation between Fas and cell resistance to H_2O_2 could be made by the observation of cell resistance to different lethal doses of H_2O_2 after repression of Fas. This repression can be attained by cell incubation with a Fas inhibitor (e.g. cerelulin) or by the repression of gene expression with specific interference RNA. Also, other cell lines can be used, especially the ones where it is known that Fas activity is increased (e.g. MCF-7). All in all, the results obtained in the present study open a new door for the development of s new line of research in order to establish similarities in human cells with the phenomena observed in yeast.

9 References

[1] National Auronautics and Space Administration. Earth Fact Sheet. 21-4-0011. Available at http://www.nasa.org

[2] Schopf J.W., Hayes J.M., Walter M.R. Earth's Earliest Biosphere: Its Origin and Evolution. Princeton, NJ: Princeton University Press; 1983, p. 361-84.

[3] Morris J.G. O2 and the obligate anaerobe. *J Appl Bacteriol* ;**40**:229;1976

[4] Gerschman R., Gilbert D.L., Nye S.W., Dwyer P., Fenn W.O. Oxygen poisoning and x-irradiation - A mechanism in common. *Science* ;**119**:623-6;1954

[5] Halliwell B., Gutteridge J.M.C. Free Radicals in Biology and Medicine. New York: Oxford University Press; 2007.

[6] Sies H. Oxidative Stress II. Oxidants and antioxidants. London: Academic Press; 1991.

[7] Chance B., Sies H., Boveris A. Hydroperoxide metabolism in mammalian organs. *Physiol Rev* ;**59**:527-605;1979

[8] Heikal O.A. Mechanisms of cell Death. Molecular, cellular and tissue toxicity. 2009. Lecture 6.

[9] Boveris A., Oshino N., Chance B. Cellular production of hydrogen peroxide. *Biochem J* ;**128**:617-30;1972

[10] Boveris A., Cadenas E. Mitochondrial production of super-oxide anions and its relationship to antimycin insensitive respiration. *FEBS Lett* ;**54**:311-4;1975

[11] Loschen G., Azzi A., Flohe L. Superoxide radicals as precursors of mitochondrial hydrogen peroxide. *FEBS Lett* ;**42**:68-72;1974

[12] Gardner P.R., Fridovich I. Superoxide sensitivity of the *Escherichia coli* aconitase. *J Biol Chem* ;**266**:19328-33;1991

[13] Trachootham D., Alexandre J., Huang P. Targeting cancer cells by ROS-mediated mechanisms: a radical therapeutic approach? *Nature Reviews Drug Discovery* ;**8**:579-91;2009

[14] Hekimi S., Lapointe J., Wen Y. Taking a "good" look at free radicals in the ageing process. *Trends in Cell Biology* ;2011

[15] Arbiser J.L., Petros J., Klafter R., Govindajaran B., McLaughlin E.R., Brown L.F. et al. Reactive oxygen generated by Nox1 triggers the angiogenic switch. *Proc Natl Acad Sci U S A* ;**99**:715-20;2002

[16] Herrero E., Ros J., Bellí G., Cabiscol E. Redox control and oxidative stress in yeast cells. *Biochim Biophys Acta* ;**1780**:1217-35;2008

[17] Jamieson D.J. *Saccharomyces cerevisiae* has distinct adaptive responses to both hydrogen peroxide and menadione. *J Bacteriol* ;**174**:6678-81;1992

[18] Bienert G.P., Moller A.L., Kristiansen K.A., Schulz A., Moller I.M., Schjoerring J.K. et al. Specific Aquaporins Facilitate the Diffusion of Hydrogen Peroxide across Membranes. *J Biol Chem* ;**282**:1183-92;2007

[19] Giorgio M., Trinei M., Migliaccion E., Pelicci P.G. Hydrogen peroxide: a metabolic by-product or a common mediator of ageing signals? *Nat REv Mol Cell Biol* ;**8**:722-8;2007

[20] Antunes F., Salvador A., Marinho H.S., Alves R., Pinto R.E. Lipid peroxidation in mithocondrial inner membranes. I. An integrative kinetic model. *Free Radic Biol Med* ;**21**:917-43;1996

[21] Winterbourn C.C., Hampton M.B. Thiol chemistry and specificity in redox signaling. *Free Radic Biol Med* ;**45**:549-61;2008

[22] Wu R., Ma Z., Liu Z., Terada L.S. Nox4-derived H_2O_2 mediates endoplasmic reticulum signaling through local Ras activation. *Mol Cell Biol* ;**30**:3553-68;2010

[23] Geiszt M., Leto T.L. The Nox family of NAD(P)H oxidases:host defense and beyond. *J Biol Chem* ;**279**:51715-8;2004

[24] Veal E.A., Day A.M., Morgan B.A. Hydrogen peroxide sensing and signalling. *Mol Cell* ;**26**:1-14;2007

[25] Schrader M., Fahimi H.D. Peroxisomes and oxidative stress. *Biochim Biophys Acta* ;**1763**:1755-66;2006

[26] Li Y., Huang T.T., Carlson E.J., Melov S., Ursell P.C., Olson J.L. et al. Dilated cardiomyopathy and neonatal lethality in mutant mice lacking manganese superoxide dismutase. *Nat Genet* ;**11**:376-81;1995

[27] Elchuri S., Oberley T.D., Qi W., Eisenstein R.S., Jackson Roberts L., Van Remmen H. et al. CuZnSOD deficiency leads to persistent and widespread oxidative damage and hepatocarcinogenesis later in life. *Oncogene* ;**24**:367-80;2005

[28] Muller F.L., Song W., Liu Y., Chaudhuri A., Pieke-Dahl S., Strong R. et al. Absence of CuZn superoxide dismutase leads to elevated oxidative stress and acceleration of age-dependent skeletal muscle atrophy. *Free Radic Biol Med* ;**40**:1993-2004;2011

[29] Imlay J.A. Cellular defenses against superoxide and hydrogen peroxide. *Annu Rev Biochem* ;**77**:755-76;2008

[30] Cohen G., Fessl F., Traczyk A., Ruis H. Isolation of the catalase A gene of *Saccharomyces cerevisiae* by complementation of the *cta1* mutation. *Mol Gen Genet* :74-9;1985

[31] Spekav W., Fessl F., Rutka A., Traczyk A., Skoneczy M., Ruis H. Isolation of the catalase T structural gene of *Saccharomyces cerevisiae* by functional complementation. *Mol Cell Biol* ;**3**:1545-51;1983

[32] Petrova V.Y., Rasheva T.V., Kujumdzieva A.V. Catalase enzyme in mitochondria of *Saccharomyces cerevisiae*. *Elec J Biotech* ;**5**:29-41;2002

[33] Radi R., Turrens J.F., Chang L.Y., Bush K.M., Crapo J.D., Freeman B.A. Detection of Catalase in Rat Heart Mitochondria. *J Biol Chem* ;**266**:22028-34;1991

[34] Leopold J.A., Loscalzo J. Oxidative enzymopathies and vascular diseases. *Arterio Tromb Vasc Biol* ;**25**:1332-40;2005

[35] Ho Y., Xiong Y., Ma W., Spector A., Ho D.S. Mice Lacking Catalase Develop Normally but Show Differential Sensitivity to Oxidant Tissue Injury. *J Biol Chem* ;**279**:32804-12;2004

[36] Izawa S., Inoue Y., Kimura A. Importance of catalase in the adaptive response to hydrogen peroxide: analysis of acatalasaemic *Saccharomyces cerevisiae*. *Biochem J* ;**320 (Pt 1)**:61-7;1996

[37] Volkov A.G., Nicchols P., Worrall J.A.R. The complex of cytochrome *c* and cytochrome *c* peroxidase: The end of the road? *Biochim Biophys Acta* ;**1807**:1482-503;2011

[38] Kwon M., Chong S., Han S., Kin K. Oxidative stresses elevate the expression of cytochrome *c* peroxidase in *Saccharomyces cerevisiae*. *Biochim Biophys Acta* ;**1623**:1-5;2003

[39] Stadtman T.C. Selenocysteine. *Annu Rev Biochem* ;**65**:83-100;1996

[40] Khang S.W., Chae H.Z., Seo M.S., Kim K., Baines I.C., Rhee S.G. Mammalian peroxiredoxin isoforms can reduce hydrogen peroxide generated in response to growth factors and tumor necrosis factor-alpha. *J Biol Chem* ;**273**:6297-302;1998

[41] Jin D.Y., Chae H.Z., Rhee S.G., Jeang K.T. Regulatory role for anovel human thioredoxin peroxidase in NF-kappaB activation. *J Biol Chem* ;**272**:30952-61;1997

[42] Zhang P., Liu B., Kang S.W., Seo M.S., Rhee S.G., Obeid L.M. Thioredoxin peroxidase is a novel inhibitor of apoptosis with a mechanism distinct from that of Bcl-2. *J Biol Chem* ;**272**:30615-8;1997

[43] D'Autréaux B., Toledano M.B. ROS as signalling molecules: mechanisms that generate specificity in ROS homeostasis. *Mol Cell Biol* ;**8**:813-24;2007

[44] Lee J., Godon C., Lagniel S., Spector D., Garin J., Labarre J. et al. Yap1 and Skn7 control two specialized oxidative stress response regulons in yeast. *J Biol Chem* ;**274**:16040-6;1999

[45] Carmel-Harel O., Storz G. Roles of the glutathione- and thioredoxin-dependent reduction systems in the *Escherichia coli* and *Saccharomyces cerevisiae* responses to oxidative stress. *Annu Rev Microbiol* ;**54**:439-61;2000

[46] Delaunay A., Isnard A.D., Toledano M.B. H_2O_2 sensing through oxidation of the Yap1 transcription factor. *EMBO J* ;**19**:5157-66;2000

[47] Biochemistry of Oxidants and Antioxidants Group Website. http://cqb.fc.ul.pt/oxantiox/index.htm . 2011.

[48] Antunes F., Cadenas E. Estimation of H_2O_2 gradients across biomembranes. *FEBS Lett* ;**475**:121-6;2000

[49] Kim J.R., Yoon H.W., Kwon K.S., Lee S.R., Rhee S.G. Identification of proteins containing cysteine residues that are sensitive to oxidation by hydrogen peroxide at neutral pH. *Anal Biochem* ;**283**:214-21;2000

[50] Dixon J.E., Denu J.M. Protein tyrosine phosphatases: mechanisms of catalysis and regulation. *Curr Opin Chem Biol* ;**2**:633-41;1998

[51] Reth M. Hydrogen peroxide as second messenger in lymphocyte activation. *Nature Immunol* ;**12**:1129-34;2002

[52] Oliveira-Marques V., Cyrne L., Marinho H.S., Antunes F. A quantitative study of NF-kB activation by H_2O_2: relevance in inflammation and synergy with TNF-a. *J Immunol* ;**178**:3893-902;2007

[53] Kuge S., Jones N., Nomoto A. Regulation of yAP-1 nuclear localization in response to oxidative stress. *EMBO J* ;**16**:1710-20;1997

[54] Godon C., Lagniel G., Lee J., Buhler J.M., Kieffer S., Perrot M. et al. The H_2O_2 stimulon in Saccharomyces cerevisiae. *J Biol Chem* ;**273**:22480-9;1998

[55] Welch J.W., Burlingame A.L. Very long-chain fatty acids in yeast. *J Bacteriol* ;**115**:464-6;1973

[56] Farbiszewski R., Skrzydlewska E. [Adaptation mechanisms of cells and removal of damage due to oxidative stress]. *Postepy Hig Med Dosw* ;**50**:613-20;1996

[57] Branco M.R., Marinho H.S., Cyrne L., Antunes F. Decrease of H_2O_2 plasma membrane permeability during adaptation to H_2O_2 in *Saccharomyces cerevisiae*. *J Biol Chem* ;**279**:6501-6;2004

[58] Antunes F., Cadenas E. Cellular titration of apoptosis with steady state concentrations of H_2O_2: submicromolar levels of H_2O_2 induce apoptosis through Fenton chemistry independent of the cellular thiol state. *Free Radic Biol Med* ;**30**:1008-18;2001

[59] Davies J.M., Lowry C.V., Davies K.J. Transient adaptation to oxidative stress in yeast. *Arch Biochem Biophys* ;**317**:1-6;1995

[60] Kelley R., Ideker T. Genome-wide fitness and expression profiling implicate Mga2 in adaptation to hydrogen peroxide. *PLoS Genet* ;**5**:e1000488;2009

[61] Ouyang X., Tran Q.T., Goodwin S., Wible R.S., Sutter C.H., Sutter T.R. Yap1 activation by H2O2 or thiol-reactive chemicals elicits distinct adaptive gene responses. *Free Radic Biol Med* ;**50**:1-13;2011

[62] Hohmann S., Mager H. Yeast stress response. Heidelberg; 2003.

[63] Singer S.J., Nicolson G.L. The fluid mosaic model of the structure of cell membranes. *Science* ;**175**:720-31;1972

[64] Dowhan W. Molecular basis for membrane phospholipid diversity: why are there so many lipids? *Annu Rev Biochem* :199-232;1997

[65] van Meer G. Cellular lpidomics. *EMBO J* :3159-65;2005

[66] Pedroso N., Matias A.C., Cyrne L., Antunes F., Borges C., Malho R. et al. Modulation of plasma membrane lipid profile and microdomains by H_2O_2 in *Saccharomyces cerevisiae*. *Free Radic Biol Med* ;**46**:289-98;2009

[67] Tuller G., Nemec T., Hrastnik C., Daum G. Lipid composition of subcellular membranes of an FY1679-derived haploid yeast wild-type strain grown on different carbon sources. *Yeast* ;**15**:1555-64;1999

[68] Bossie M.A., Martin C.E. Nutritional regulation of yeast delta-9 fatty acid desaturase activity. *J Bacteriol* ;**171**:6409-13;1989

[69] Martin C.E., Oh C., Jiang Y. Regulation of long chain unsaturated fatty acid synthesis in yeast. *Biochim Biophys Acta* ;**1771**:271-86;2007

[70] Kunimoto M., Inoue K., Nojima S. Effect of ferrous ion and ascorbate-induced lipid peroxidation on liposomal membranes. *Biochim Biophys Acta* ;**646**:169-78;1981

[71] Cipak A., Hasslacher M., Tehlivets O., Collinson E.J., Zivkovic M., Matijevic T. et al. *Saccharomyces cerevisiae* strain expressing a plant fatty acid desaturase produces polyunsaturated fatty acids and is susceptible to oxidative stress induced by lipid peroxidation. *Free Radic Biol Med* ;**40**:897-906;2006

[72] van der Rest M.E., Kamminga A.H., Nakano A., Anraku Y., Poolman B., Konings W.N. The plasma membrane of Saccharomyces cerevisiae: structure, function, and biogenesis. *Microbiol Rev* ;**59**:304-22;1995

[73] Boumann H.A., Gubbens J., Koorengevel M.C., Oh C.S., Martin C.E., Heck A.J. et al. Depletion of phosphatidylcholine in yeast induces shortening and increased saturation of the lipid acyl chains: evidence for regulation of intrinsic membrane curvature in a eukaryote. *Mol Biol Cell* ;**17**:1006-17;2006

[74] Devaux P.S. Static and dynamic lipid asymmetry in cell membranes. *Biochemistry* ;**30**:1163-73;1991

[75] Tanaka K., Fujimura-Kamada K., Yamamoto T. Functions of phospholipid flippases. *J Biochem* ;**149**:131-43;2011

[76] Carman G.M., Han G. Regulation of phospholipid synthesis in the yeast *Saccharomyces cerevisiae*. *Annu Rev Biochem* ;**80**:859-83;2011

[77] Carman G.M., Han G.S. Regulation of phospholipid synthesis in Saccharomyces *cerevisiae* by zinc depletion. *Biochim Biophys Acta* ;**1771**:322-30;2007

[78] Ciesarová Z., Smogrovicova D., Domeny Z. Enhancement of yeast ethanol tolerance by calcium and magnesium. *Flia Microbiol* ;**41**:485-8;1996

[79] Janssen M.J.F.W., Koorengevel M.C., de Kruijff B., de Kroon A.I. The phosphatidylcholine to phosphatidylethanolamine ratio of *Saccharomyces cerevisiae* varies with the growth phase. *Yeast* ;**16**:650;2000

[80] Xia J.M., Yuan Y.J. Comparative lipidomics of four strains of *Saccharomyces cerevisiae* reveals different responses to furfural, phenol, and acetic acid. *J Agric Food Chem* ;**57**:99-108;2009

[81] Leandro M.J., Fonseca C., Goncalves P. Hexose and pentose transport in ascomycetous yeasts: An overview. *FEMS yeast Res* ;**9**:511-25;2009

[82] Guo Y., Au W.C., Shakoury-Elizeh M., Protchenko O., Basrai M., Prinz W.A. et al. Phosphatidylserine is involved in the ferrichrome-induced plasma membrane trafficking of Arn1 in *Saccharomyces cerevisiae*. *J Biol Chem* ;**285**:39564-73;2011

[83] Dickson R.C. New insights into sphingolipid metabolism and funtion in budding yeast. *J Lipid Res* ;**49**:909-21;2008

[84] van Meer G., Voelker D.R., Feigenson G.W. Membrane lipids: where they are and how they behave. *Nat REv Mol Cell Biol* ;**9**:112-24;2008

[85] Dickson R.C., Sumanasekera C., Lester R.L. Functions and metabolism of sphingolipids in *Saccharomyces cerevisiae*. *Prog Lipid Res* ;**45**:447-65;2006

[86] Obeid L.M., Okamoto Y., Mao C. Yeast sphingolipids: metabolism and biology. *Biochim Biophys Acta* ;**1585**:163-71;2002

[87] Sims K.J., Spassieva S.D., Voit E.O., Obeid L.M. Yeast sphingolipid metabolism: clues and connections. *Biochem Cell Biol* ;**82**:45-61;2004

[88] Oh C.S., Toke D.A., Mandala S., Martin C.E. ELO2 and ELO3 homolougues of the Saccharomyces cerevisiae ELO1 gene, function in fatty cid elongation and are required for sphingolipid formation. *J Biol Chem* ;**272**:17376-84;1997

[89] Smith S.W., Lester R.L. Inositol phosphorylceramide, a novel substance and the chief member of a major group of yeast sphingolipids containing a single inositol phosphate. *J Biol Chem* ;**249**:3395-405;1974

[90] Eisenkolb M., Zenzmaier C., Leitner E., Schneiter R. A specific structural requirement for ergosterol in long-chain fatty acid synthesis mutants important for maintaining raft domains in yeast. *Mol Biol Cell* ;**13**:4414-28;2002

[91] Rottem S., Yashouv J., Neeman Z., Razin S. Cholesterol in mycoplasma membranes. Composition, ultrastructure and biological properties of membranes from *Mycoplasma mycoides* var. capri cells adapted to grow with low cholesterol concentrations. *Biochim Biophys Acta* ;**323**:495-508;1973

[92] Mondal M., Mesmim B., Mukherjee S., Maxfield F.R. Sterols Are Mainly in the Cytoplasmic Leaflet of the Plasma Membrane and the Endocytic Recycling Compartment in CHO Cells. *Mol Biol Cell* ;**20**:581-8;2009

[93] Devaux P.F., Morris R. Transmembrane asymmetry and lateral domains in biological membranes. *Traffic* ;**5**:241-6;2004

[94] Abe F., Hiraki T. Mechanistic role of ergosterol in membrane rigidity and cycloheximide resistance in *Saccharomyces cerevisiae*. *Biochim Biophys Acta* ;**1788**:743-52;2009

[95] Folmer V., Pedroso N., Matias A.C., Lopes S.C., Antunes F., Cyrne L. et al. H_2O_2 induces rapid biophysical and permeability changes in the plasma membrane of *Saccharomyces cerevisiae*. *Biochim Biophys Acta* ;**1778**:1141-7;2008

[96] Róg T., Pasenkiewicz-Gierula M., Vattulainen I., Karttunen M. Ordering effects of cholesterol and its analogues. *Biochim Biophys Acta* ;**1788**:97-121;2009

[97] Hsueh Y.W., Chen M.T., Patty P.J., Code C., Cheng J., Frisken B.J. Ergosterol in POPC membranes: physical properties and comparison with structurally similar sterols. *Biophys J* ;**92**:1606-15;2007

[98] Bacia K., Schwille P., Kurzchalia T. Sterol structure determines the separation of phases and the curvature of the liquid-ordered phase in model membranes. *Proc Natl Acad Sci U S A* ;**102**:3272-7;2005

[99] Dupont S., Beney L., Ferreira T., Gervais P. Nature of sterols affects plasma membrane 1 behavior and yeast survival to dehydration. *Biochim Biophys Acta* ;**1808**:1520-8;2011

[100] Pichler H., Riezman H. Where sterols are required for endocytosis. *Biochim Biophys Acta* ;**1666**:51-61;2004

[101] Mukhopadhyay K., Kohli A., Prasad R. Drug susceptibilites of yeast cells are affected by membrane lipid composition. *Antimicrob Agents Chemother* ;**46**:3695-705;2002

[102] Walker-Caprioglio H., Casey M., Parks L.W. *Saccharomyces cerevisiae* membrane sterol modifications in response to growth in the presence of ethanol. *Appl Env Microbiol* ;**56**:2853-7;1990

[103] Darnet S., Rahier A. Plant sterol biosynthesis: identification of two distinct families of sterol 4a-methyl oxidases. *Biochem J* ;**378**:889-98;2004

[104] Marguet D., Lenne P., Rigneault H., He H. Dynamics in the plasma membrane:how to combine fluidity and order. *EMBO J* ;**25**:3446-57;2006

[105] Engelman D.M. Membranes are more mosaic that fluid. *Nature* ;**438**:578-80;2011

[106] Szopinska A., Degand H., Hochstenbach J., Nader J., Morsomme P. Rapid response of the yeast plasma membrane proteome to salt stress. *Mol Cell Proteomics* ;2011

[107] Pedroso N. Papel da membrana plasmática na adaptação de *Saccharomyces cerevisiae* ao H_2O_2. 2008. Universidade de Lisboa.

[108] Karnovsky M.J., Kleinfield A.M., Hoover R.L., Klausner R.D. The concept of lipid domains in membranes. *J Cell Biol* ;**94**:1-6;1982

[109] Hinderliter A., Biltonen R.L., Almeida P.F. Lipid modulation of protein induced membrane domains as a mechanism for controlling signal transduction. *Biochemistry* ;**43**:7102-10;2004

[110] Simons K., Ikonen E. Functional rafts in cell membranes. *Nature* ;**387**:569-72;1997

[111] Bagnat M., Keranen S., Shevchenko A., Shevchenko A., Simons K. Lipid rafts function in biosynthetic delivery of proteins to the cell surface in yeast. *Proc Natl Acad Sci U S A* ;**97**:3254-9;2000

[112] Pike L.J. Lipid rafts: bringing order to chaos. *J Lipid Res* ;**44**:655-67;2003

[113] Chazal N., Gerlier D. Virus Entry, Assembly, Budding, and Membrane Rafts. *Microbiol Mol Biol Rev* ;**67**:226-37;2003

[114] Stuart E.S., Webley W.C., Norkin L.N. Lipid rafts, Caveolae, Caveolin-1 and entry by Chlamydiae into host cells. *Exp Cell Res* ;**287**:67-78;2003

[115] Geisse N.A., Cover T.L., Henderson R.M., Edwardson J.M. Targeting of Helicobacter pylori vacuolating toxin to lipid raft membrane domains analysed by atomic force microscopy. *Biochem J* ;**381**:911-7;2011

[116] Brown D.A., London E. Structure and Origin of Ordered Lipid Domains in Biological Membranes. *J Membr Biol* ;**164**:103-14;1998

[117] Opekarova M., Malinska K., Novakova L., Tanner W. Differential effect of phosphatidylethanolamine depletion on raft proteins: further evidence for diversity of rafts in *Saccharomyces cerevisiae*. *Biochim Biophys Acta* ;**1711**:87-95;2005

[118] Aresta-Branco F., Cordeiro A.M., Marinho H.S., Cyrne L., Antunes F., de Almeida R.F. Gel domains in the plasma membrane of *Saccharomyces cerevisiae*: highly ordered, ergosterol-free, and sphingolipid-enriched lipid rafts. *J Biol Chem* ;**286**:5043-54;2011

[119] Anderson R.G.W. The caveolae membrane system. *Annu Rev Biochem* ;**67**:199-225;1998

[120] Fernandez I., Ying Y., Albanesi J., Anderson R.G. Mechanism of caveolin filament assembly. *Proc Natl Acad Sci U S A* ;**99**:11193-8;2002

[121] Thomsen P., Roepstorff K., Stahlhut M., van Deurs B. Caveolae are highly immobile plasma membrane microdomains, which are not involved in constitutive endocytic trafficking. *Mol Biol Cell* ;**13**:238-50;2002

[122] Yang B., Oo T.N., Rizzo V. Lipid rafts mediate H_2O_2 prosurvival effects in cultured endothelial cells. *The FASEB J* ;**20**:688-97;2006

[123] Lu S.P., Lin Feng M.H., Huang H.L., Huang Y.C., Tsou W.I., Lai M.Z. Reactive oxygen species promote raft formation in T lymphocytes. *Free Radic Biol Med* ;**42**:936-44;2007

[124] Davies A. Cells 101: Business basics. In. *Inside the cell*. EPUB: National Institutes of Health; 2005.

[125] Malinska K., Malinsky J., Opekarova M., Tanner W. Visualization of protein compartmentation within the plasma membrane of living yeast cells. *Mol Biol Cell* ;**14**:4427-36;2003

[126] Grossmann G., Opekarova M., Malinsky J., Weig-Meckl I., Tanner W. Membrane potential governs lateral segregation of plasma membrane proteins and lipids in yeast. *EMBO J* ;**26**:1-8;2007

[127] Malinsky J., Opekarova M., Tanner W. The lateral compartmentation of the yeast plasma membrane. *Yeast* ;**27**:473-8;2010

[128] Grossmann G., Malinsky J., Stahlschmidt W., Loibl M., Weig-Meckl I., Frommer W.B. et al. Plasma membrane microdomains regulate turnover of transport proteins in yeast. *J Cell Biol* ;**183**:1075-88;2008

[129] Lee M.C., Hamamoto R., Schekman R. Ceramide biosynthesis is required fo rthe oligomeric H+-ATPase Pma1p in the yeast endoplasmatic reticulum. *J Biol Chem* ;**277**:22395-401;2002

[130] François I.E.J.A., Bink A., Vandercappellen J., Ayscough K.R., Toulmay A., Schneiter R. et al. Membrane Rafts are involved in intracellular miconazole accumulation in yeast cells. *J Biol Chem* ;**284**:32680-5;2009

[131] Fröhlich F., Moreira K., Aguilar P.S., Hubner N.C., Mann M., Walter P. et al. A genome-wide screen for genes affecting eisosomes reveals Nce102 function in sphingolipid signaling. *J Cell Biol* ;**185**:1227-42;2009

[132] Berchtold D., Walther T.C. *TOR*C2 Plasma Membrane Localization Is Essential for Cell Viability and Restricted to a Distinct Domain. *Mol Biol Cell* ;**20**:1565-75;2009

[133] Walther T.C., Brickner J.H., Aguilar P.S., Bernales S., Pantoja C., Walter P. Eisosomes mark static sites of endocytosis. *Nature* ;**439**:998-1003;2006

[134] Seaver L.C., Imlay J.A. Hydrogen peroxide fluxes and compartmentalization inside growing Escherichia coli. *J Bacteriol* ;**183**:7182-9;2001

[135] Sousa-Lopes A., Antunes F., Cyrne L., Marinho H.S. Decreased cellular permeability to H_2O_2 protects *Saccharomyces cerevisiae* cells in stationary phase against oxidative stress. *FEBS Lett* ;**578**:152-6;2004

[136] Oliveira-Marques V. Redox Regulation of NF-kappaB activation by Hydrogen Peroxide and effects on gene expression. 2008. Universidade de Lisboa.

[137] Smith S. The animal fatty acid synthase: one gene, one polypeptide, seven enzymes. *FASEB J* ;**8**:1248-59;1994

[138] Jenni S., Leibundgut M., Maier T., Ban N. Architecture of a Fungal Fatty Acid Synthase at 5 Å Resolution. *Science* ;**311**:1263-7;2006

[139] Fichtlscherer F., Wellein C., Mittag M., Schweizer E. novel function of yeast fatty acid synthase. Subunit alpha is capable of self-pantetheinylation. *Eur J Biochem* ;**267**:2666-71;2000

[140] Mohamed A.H., Chirala S.S., Mody N.H., Huang W.Y., Wakil S.J. Primary structure of the multifunctional alpha subunit protein of yeast fatty acid synthase derived from *FAS2* gene sequence. *J Biol Chem* ;**263**:12315-25;1988

[141] Schweizer M., Roberts L.M., Holtke H.J., Takabayashi K., Hollerer E., Hoffmann B. et al. The pentafunctional *FAS1* gene of yeast: its nucleotide sequence and order of the catalytic domains. *Mol Gen Genet* ;**203**:479-86;1986

[142] Lomakin I.B., Xiong Y., Steitz T.A. The crystal structure of yeast fatty acid synthase, a cellular machine with eight active sites working together. *Cell* ;**129**:319-32;2007

[143] Schweizer E., Hofmann J. Microbial type I fatty acid synthases (FAS): major players in a network of cellular FAS systems. *Microbiol Mol Biol Rev* ;**68**:501-17;2004

[144] Leibundgut M., Maier T., Jenni S., Ban N. The multienzyme architecture of eukaryotic fatty acid synthases. *Curr Opin Struct Biol* ;**18**:714-25;2008

[145] Cronan J.E., Jr., Waldrop G.L. Multi-subunit acetyl-CoA carboxylases. *Prog Lipid Res* ;**41**:407-35;2002

[146] Chan D.I., Vogel H.J. Current understanding of fatty acid biosynthesis and the acyl carrier protein. *Biochem J* ;**430**:1-19;2010

[147] Leibundgut M., Jenni S., Frick C., Ban N. Structural basis for substrate delivery by acyl carrier protein in the yeast fatty acid synthase. *Science* ;**316**:288-90;2007

[148] Weiss L., Hoffman G.E., Schreiber R., Andres H., Fuchs E., Korber E. et al. Fatty acid biosynthesis in man, a pathway of minor importance: purification, optimal assay conditions and organ distribution of fatty acid synthase. *Biol Chem Hoppe-Seyer* ;**367**:905-12;1986

[149] Swinnen J.V., Veldhoven P.P.V., Timmermans L., de Schriver E., Brusselmans K., Vanderhoydonc F. et al. Fatty acid synthase drives the synthesis of phospholipids partitioning into detergent-resistant membrane microdomains. *Biochem Biophys Res Comm* ;**32**:898-903;2003

[150] Kuhadja F.P. Fatty acid synthase and human cancer: new perspectives on its role in tumor biology. *Nutrition* ;**16**:202-8;2000

[151] Rossler H., Rieck C., Delong T., Hoja U., Schweizer E. Functional differentiation and selective inactivation of multiple *Saccharomyces cerevisiae* genes involved in very-long-chain fatty acid synthesis. *Mol Genet Genomics* ;**269**:290-8;2003

[152] Schuller H.J., Hahn A., Troster F., Schutz A., Schweizer E. Coordinate genetic control of yeast fatty acid synthase genes *FAS1* and *FAS2* by an upstream activation site common to genes involved in membrane lipid biosynthesis. *EMBO J* ;**11**:107-14;1992

[153] Henry S.A., Patton-Vogt J. Genetic regulation of phospholipid metabolism: yeast as a model eukaryote. *Prog Nucleic Acid Res Mol Biol* ;**61**:133-79;1998

[154] Jesch S.A., Zhao X., Wells M.T., Henry S.A. Genome Wide Analysis Reveals Inositol, not Choline, as the Major Effector of Ino2p-Ino4p and Unfolded Protein Response Target Gene Expression in Yeast. *J Biol Chem* ;**10**:9106-18;2005

[155] Bailis A.M., Lopes J.M., Kohlwein S.D., Henry S.A. Cis and trans regulatory elements required for regulation of the CHO1 gene of *Saccharomyces cerevisiae*. *Nucleic Acids Res* ;**20**:1411-8;1992

[156] Lopes J.M., Hirsch J.P., Chorgo P.A., Schulze K.L., Henry S.A. Analysis of sequences in the INO1 promoter that are involved in its regulation by phospholipid percursors. *Nucleic Acids Res* ;**19**:1687-93;1991

[157] Ambroziak J., Henry S.A. *INO2* and *INO4* gene products, positive regulators of phospholipid biosynthesis in Saccharomyces cerevisiae, form a complex that binds to the *INO1* promoter. *J Biol Chem* ;**269**:15344-9;1994

[158] White M.J., Hirsch J.P., Henry S.A. The OPI1 gene of *Saccharomyces cerevisiae*, a negative regulator of phospholipid biosynthesis, encodes a protein containing polyglutamine tracts and a leucine zipper. *J Biol Chem* ;**266**:863-72;1991

[159] Wagner C., Dietz M., Wittman J., Albrecht A., Schuller H.J. The negative regulator Opi1 of phospholipid biosynthesis in yeast contacts the pleiotropic repressor Sin3 and the transcriptional activator Ino2. *Mol Microbiol* ;**41**:155-66;2001

[160] Nikawa J., Kamiuto J. The promoter of the yeast *OPI1* regulatory gene. *J Biosc Bioeng* ;**97**:369-73;2004

[161] Schuller H.J., Schutz A., Knab S., Hoffman B., Schweizer E. Importance of general regulatory factor Rap1p, Abf1p and Reb1p for the activation of yeast fatty acid synthase genes *FAS1* and *FAS2*. *Eur J Biochem* ;**225**:213-22;1994

[162] Wenz P., Schwank S., Hoja U., Schuller H.J. A downstream regulatory element located within the coding sequence mediates autoregulated expression of the yeast fatty acid synthase gene *FAS2* by the *FAS1* gene product. *Nucleic Acids Res* ;**29**:4625-32;2001

[163] Thumm M., Egner R., Koch B., Schlumpberger M., Straub M., Veenhuis M. et al. Isolation of autophagocytosis mutants of *Saccharomyces cerevisiae*. *FEBS Lett* ;**349**:275-80;1994

[164] Peng J., Schwartz D., Elias J.E., Thoreen C.C., Cheng D., Marsischky G. et al. A proteomics approach to understanding protein ubiquitination. *Nat Biotechnol* ;**21**:921-6;2003

[165] Souza J.M., Giasson B.I., Chen Q., Lee V.M., Ischiropolous H. Dityrosine cross-linking promotes formation of stable alpha -synuclein polymers. Implication of nitrative and oxidative stress in the pathogenesis of neurodegenerative synucleinopathies. *J Biol Chem* ;**275**:18344-9;2000

[166] Sere Y.Y., Regnacq M., Colas J., Berges T. A *Saccharomyces cerevisiae* strain unable to store neutral lipids is tolerant to oxidative stress induced by α-synuclein. *Free Radic Biol Med* ;**49**:1755-64;2010

[167] Wright H.T., Reynolds K.A. Antibacterial Targets in Fatty Acid Biosynthesis. *Curr Opin Microbiol* ;**10**:447-53;2007

[168] Kusakabe T., Maeda M., Hoshi N., Sugino T., Watanabe K., Fukuda T. et al. Fatty acid synthase is expressed mainly in adult hormone-sensitive cells or cells with high lipid metabolism and in proliferating fetal cells. *J Histochem Cytochem* ;**48**:613-22;2000

[169] Menendez J.A., Lupo R. Fatty acid synthase and the lipogenic phenotype in cancer pathogenesis. *Nat Rev Cancer* ;**7**:763-77;2007

[170] Menendez J.A., Decker J.P., Lupo R. In support of fatty acid synthase (FAS) as a metabolic oncogene: extracellular acidosis acts in an epigenetic fashion activating FAS gene expression in cancer cells. *J Cell Biochem* ;**94**:1-4;2005

[171] Graner E., Tang D., Rossi S., Baron A., Migita T., Weinstein L.J. et al. The isopeptidase USP2a regulates the stability of fatty acid synthase in prostate cancer. *Cancer Cell* ;**5**:253-61;2004

[172] Liu H., Liu J., Wu X., Zhang J. Biochemistry, molecular biology, and pharmacology of fatty acid synthase, an emerging therapeutic target and diagnosis/prognosis marker. *Int J Biochem Mol Biol* ;**1**:69-89;2010

[173] Johnston J.R. Molecular Genetics of Yeast. A Practical Approach. New York; 1994, p. 261-5.

[174] Peterson G.L. A simplification of the protein assay method of Lowry et al. which is more generally applicable. *Anal Biochem* ;**83**:346-56;1977

[175] Lynen F. Yeast Fatty Acid Synthetase. *Methods Enzymology* ;**14**:17-33;1969

[176] Aebi H.E. Methods of Enzymatic Analysis. Weinheim: Verlag Chemie; 1983, p. 273-84.

[177] Yonetani T., Ray G.S. Studies on cytochrome *c* peroxidase. I. Purification and some properties. *J Biol Chem* ;**240**:4503-8;1965

[178] Laemmli U.K. Cleavage of structural proteins during the assembly of the head of bacteriophage T4. *Nature* ;**227**:680-5;1970

[179] Rasband WS. ImageJ. 1997. U. S. National Institutes of Health, Bethesda, Maryland, USA.

[180] Sambrook J.R.D. Molecular cloning: a laboratory manual. 2001.

[181] Ausubel F.M., Brent R., Kingston R.E., Moore D.D., Seidman J.G., Smith J.A. et al. Current Protocols in Molecular Biology. New York: Wiley-Interscience; 1989.

[182] Gietz D., St Jean A., Woods R.A., Schiestl R.H. Improved method for high efficiency transformation of intact yeast cells. *Nucleic Acids Res* ;**20**:1425;1992

[183] Belli G., Gari E., Piedrafita L., Aldea M., Herrero E. An activator/repressor dual system allows tight tetracycline-regulated gene expression in budding yeast. *Nucleic Acids Res* ;**26**:942-7;1998

[184] Gari E., Piedrafita L., Aldea M., Herrero E. A set of vectors with a tetracycline-regulatable promoter system for modulated gene expression in *Saccharomyces cerevisiae*. *Yeast* ;**13**:837-48;1997

[185] Bicle M., Delley P.A., Schmidt A., Hall M.N. Cell wall integrity modulates RHO1 activity via the exchange factor ROM2. *EMBO J* :2235-4225;1998

[186] Vilella F., Herrero E., Torres J., Torre-Ruiz M.A. Pkc1 and the upstream elements of the cell integrity pathway in *Saccharomyces cerevisiae*, Rom2 and Mtl1, are required for cellular responses to oxidative stress. *J Biol Chem* ;**280**:9149-59;2005

[187] Panaretou B., Piper P. Isolation of yeast plasma membranes. *Methods Mol Biol* ;**313**:27-32;2006

[188] Folch J., Lees M., Sloane, Stanley G.H. A simple method for the isolation and purification of total lipides from animal tissues. *J Biol Chem* ;**226**:497-509;1957

[189] Broekhuyse R.M. Phospholipids in tissues of the eye. I. Isolation, characterization and quantitative analysis by two-dimensional thin-layer chromatography of diacyl and vinyl-ether phospholipids. *Biochim Biophys Acta* ;**152**:307-15;1968

[190] Christie W.W. Gas Chromatography and Lipids: a Practical Guide. Ayr.: The Oily Press; 1989.

[191] MORRISON W.R., SMITH L.M. Preparation of Fatty Acid Methyl Esters And Dimethylacetals From Lipids With Boron Fluoride-Methanol. *J Lipid Res* ;**5**:600-8;1964

[192] Aresta-Branco F. Caracterização biofísica da membrana plasmática da levedura. 2009. Universidade de Lisboa.

[193] Lakowicz J.R. Principles of Fluorescence Spectroscopy. New York; 1999.

[194] Silva L.C., de Almeida R.F., Castro B.M., Fedorov A., Prieto M. Ceramide-domain formation and collapse in lipid rafts: membrane reorganization by an apoptotic lipid. *Biophys J* ;**92**:502-16;2007

[195] Schweizer E., Bolling H. A Saccharomyces cerevisiae mutant defective in saturated fatty acid biosynthesis. *Proc Natl Acad Sci U S A* ;**67**:660-6;1970

[196] Fernandes A. Estudo da importancia das proteinas Asc1p e Scs7p na adaptacao das celulas de *Saccharomyces cerevisiae* ao H_2O_2. 2009. Universidade de Lisboa.

[197] Li B.Z., Cheng J.S., Ding M.Z., Yuan Y.J. Transcriptome analysis of differential responses of diploid and haploid yeast to ethanol stress. *J Biotechnol* ;**148**:194-203;2010

[198] Matias A.C., Pedroso N., Teodoro N., Marinho H.S., Antunes F., Nogueira J.M. et al. Down-regulation of fatty acid synthase increases the resistance of *Saccharomyces cerevisiae* cells to H_2O_2. *Free Radic Biol Med* ;**43**:1458-65;2007

[199] Cyrne L., Martins L., Fernandes L., Marinho H.S. Regulation of antioxidant enzymes gene expression in the yeast Saccharomyces cerevisiae during stationary phase. *Free Radic Biol Med* ;**34**:385-93;2003

[200] Shenton D., Smirnova J.B., Selley J.N., Carroll K., Hubbard S.J., Pavitt G.D. et al. Global translational responses to oxidative stress impact upon multiple levels of protein synthesis. *J Biol Chem* ;**281**:29011-21;2006

[201] Nurminen T., Suomalainen H. Occurrence of long-chain fatty acids and glycolipids in the cell envelope fractions of baker's yeast. *Biochem J* ;**125**:963-9;1971

[202] De Nobel J.G., Klis F.M., Ram A., Van Unen H., Priem J., Munnik T. et al. Cyclic variations in the permeability of the cell wall of *Saccharomyces cerevisiae*. *Yeast* ;**7**:589-98;1991

[203] Ovalle R., Lim S.T., Holder B., Jue C.K., Moore C.W., Lipke P.N. A spheroplast rate assay for determination of cell wall integrity in yeast. *Yeast* ;**14**:1159-66;1998

[204] Belli G., Gari E., Aldea M., Herrero E. Functional analysis of yeast essential genes using a promoter-substitution cassette and the tetracycline-regulatable dual expression system. *Yeast* ;**14**:1127-38;1998

[205] Plessis A., Dujon B. Multiple tandem integrations of transforming DNA sequences in yeast chromosomes suggest a mechanism for integrative transformation by homologous recombination. *Gene* ;**134**:41-50;1993

[206] Feddersen S., Neergaard T.B., Knudsen J., Faergeman N.J. Transcriptional regulation of phospholipid biosynthesis is linked to fatty acid metabolism by an acyl-

CoA-binding-protein-dependent mechanism in Saccharomyces cerevisiae. *Biochem J* ;**407**:219-30;2007

[207] Wishart J.A., Hayes A., Wardleworth L., Zhang N., Oliver S.G. Doxycycline, the drug used to control the tet-regulatable promoter system, has no effect on global gene expression in *Saccharomyces cerevisiae*. *Yeast* ;**22**:565-9;2005

[208] Angrave F.E., Avery S.V. Antioxidant functions required for insusceptibility of Saccharomyces cerevisiae to tetracycline antibiotics. *Antimicrob Agents Chemother* ;**45**:2939-42;2001

[209] Kroon A.M., Dontje B.H., Holtrop M., Van den B.C. The mitochondrial genetic system as a target for chemotherapy: tetracyclines as cytostatics. *Cancer Lett* ;**25**:33-40;1984

[210] Daum G., Lees N.D., Bard M., Dickson R. Biochemistry, cell biology and molecular biology of lipids of *Saccharomyces cerevisiae*. *Yeast* ;**14**:1471-510;1998

[211] Patton J.L., Lester R.L. The phosphoinositol sphingolipids of *Saccharomyces cerevisiae* are highly localized in the plasma membrane. *J Bacteriol* ;**173**:3101-8;1991

[212] de Kroon A.I. Metabolism of phosphatidylcholine and its implications for lipid acyl chain composition in Saccharomyces cerevisiae. *Biochim Biophys Acta* ;**1771**:343-52;2007

[213] Paula S., Volkov A.G., van Hoek A.N., Haines T.H., Deamer D.W. Permeation of protons, potassium ions and smaller polar molecules through phospholipid bilayers as a function of membrane thickness. *Biophys J* ;**70**:339-48;1996

[214] Trotter P.J. The genetics of fatty acid metabolism in *Saccharomyces cerevisiae*. *Annu Rev Nutr* ;**21**:97-119;2001

[215] Morrow M.R., Singh D., Lu D., Grant C.W. Glycosphingolipid fatty acid arrangement in phospholipid bilayers: cholesterol effects. *Biophys J* ;**68**:179-86;1995

[216] Brown D.A., Rose J.K. Sorting of GPI-anchored proteins to glycolipid-enriched membrane subdomains during transport to the apical cell surface. *Cell* ;**68**:533-44;1992

[217] Ferreira T., Mason A.B., Slayman C.W. The yeast Pma1 proton pump: a model for understanding the biogenesis of plasma membrane proteins. *J Biol Chem* ;**276**:29613-6;2001

[218] Chamberlain L.H. Detergents as tools for the purification and classification of lipid rafts. *FEBS Lett* ;**559**:1-5;2004

[219] Lagerholm B.C., Weinreb G.E., Jacobson K., Thompson N.L. Detecting microdomains in intact cell membranes. *Annu Rev Phys Chem* ;**56**:309-36;2005

[220] Wahle K.W. Fatty acid modification and membrane lipids. *Proc Nutr Soc* ;**42**:273-87;1983

[221] Shinitzky M., Barenholz Y. Fluidity Parameters of lipid regions determined by fluorescence polarization. *Biochim Biophys Acta* ;**515**:367-94;1978

[222] Gallegos A.M., McIntosh A.L., Atshaves B.P., Schroeder F. Structure and cholesterol domain dynamics of an enriched caveolae/raft isolate. *Biochem J* ;**382**:451-61;2004

[223] Mateo A.R., Brochon J., Lillo M.P., Acuña A.U. Lipid Clustering in Bilayers Detected by the Fluorescent Kinetics and Anisotropy of Trans-Parinaric Acid. *Biophys J* ;**65**:2237-47;1993

[224] Malinska K., Malinsky J., Opekarova M., Tanner W. Distribution of Can1p into stable domains reflects lateral protein segregation within the plasma membrane of living *S. cerevisiae* cells. *J Cell Sci* ;**117**:6031-41;2004

[225] Norman A.W., Demel R.A., de Kruyff B., van Deenen L.L. Studies on the biological properties of polyene antibiotics. Evidence for the direct interaction of filipin with cholesterol. *J Biol Chem* ;**247**:1918-29;1972

[226] Castanho M., Prieto M. Filipin fluorescence quenching by spin-labeled probes: studies in aqueous solution and in a membrane model system. *Biophys J* ;**69**:155-68;1995

[227] Bagnat M., Simons K. Cell surface polarization during yeast mating. *Proc Natl Acad Sci U S A* ;**99**:14183-8;2002

[228] Martin S.W., Konopka J.B. Lipid raft polarization contributes to hyphal growth in Candida albicans. *Eukaryot Cell* ;**3**:675-84;2004

[229] Parks L.W., Casey W.M. Physiological implications of sterol biosynthesis in yeast. *Annu Rev Microbiol* ;**49**:95-116;1995

[230] Veen M., Lang C. Interactions of the ergosterol biosynthetic pathway with other lipid pathways. *Biochem Soc Trans* ;**33**:1178-81;2005

[231] Gaigg B., Toulmay A., Schneiter R. Very long-chain fatty acid-containing lipids rather than sphingolipids per se are required for raft association and stable surface transport of newly synthesized plasma membrane ATPase in yeast. *J Biol Chem* ;**281**:34135-45;2006

[232] Chatterjee S.N., Agarwal S. Liposomes as membrane model for study of lipid peroxidation. *Free Radic Biol Med* ;**4**:51-72;1988

[233] Nuclear Function and Structure. In: Berrios M., editor. *Methods in Cell Biology*: Academic Press; 1998.

[234] Schulz I. Permeabilizing cells: some methods and applications for the study of intracellular processes. *Methods Enzymol* ;**192**:280-300;1990

[235] Adam S.A., Sterne-Marr R., Gerace L. Nuclear protein import using digitonin-permeabilized cells. *Methods Enzymol* ;**219**:97-110;1992

[236] Alberts e.al. Molecular Biology of the Cell. New York: Garland Science; 2002.

[237] Blank N., Gabler C., Schiller M., Kriegel M., Kalden J.R., Lorenz H.M. A fast, simple and sensitive method for the detection and quantification of detergent-resistant membranes. *J Immunol Methods* ;**271**:25-35;2002

[238] Boesze-Battaglia K. Isolation of Membrane Rafts and Signaling Complexes . In. *Transmembrane Signaling Protocols*: Humana Press; 2006.

[239] Parton R.G. Ultrastructural localization of gangliosides; GM1 is concentrated in caveolae. *J Histochem Cytochem* ;**42**:155-66;1994

[240] Chen S., Periasamy A., Yang B., Herman B., Jacobson K., Sulik K.K. Differential sensitivity of mouse neural crest cells to ethanol-induced toxicity. *Alchool* ;**20**:75-81;2000

[241] Pei B., Chen J. More Ordered, Convex Ganglioside-Enriched Membrane Domains: The Effects of GM_1 on Sphingomyelin Bilayers Containing a Low Level of Cholesterol . *J Biochem* ;**134**:575-81;2003

[242] Wang Y., Kuhajda F.P., Li J.N., Pizer E.S., Han W.F., Sokoll L.J. et al. Fatty acid synthase (FAS) expression in human breast cancer cell culture supernatants and in breast cancer patients. *Cancer Lett* ;**167**:99-104;2001

[243] Nyholm T.K., Ozdirekcan S., Killian J.A. How protein transmembrane segments sense the lipid environment. *Biochemistry* ;**46**:1457-65;2007

[244] Berglund A.H., Quartacci M.F., Calucci L., Navari-Izzo F., Pinzino C., Liljenberg C. Alterations of wheat root plasma membrane lipid composition induced by copper stress result in changed physicochemical properties of plasma membrane lipid vesicles. *Biochim Biophys Acta* ;**1564**:466-72;2002

[245] Berglund A.H., Larsson K.E., Liljenberg C.S. Permeability behaviour of lipid vesicles prepared from plant plasma membranes--impact of compositional changes. *Biochim Biophys Acta* ;**1682**:11-7;2004

[246] Atkinson K., Fogel S., Henry S.A. Yeast Mutant Defective in Phosphatidylserine Synthesis. *J Biol Chem* ;**255**:6653-61;1980

[247] Tehlivets O., Scheuringer K., Kohlwein S.D. Fatty acid synthesis and elongation in yeast. *Biochim Biophys Acta* ;2006

[248] Lingwood D., Simons K. Lipid rafts as a membrane-organizing principle. *Science* :46-50;2010

[249] Ewers H., Römer W., Smith A.E., Bacia K., Dmitrieff S., Chai W. et al. GM1 structure determines SV40-induced membrane invagination and infection. *Nat Cell Biology* ;**12**:11-8;2010

[250] Römer W., Pontani L.L., Sorre B., Rentero C., Berland L., Chambon V. et al. Actin dynamics drive membrane reorganization and scission in clathrin-independent endocytosis. *Cell* ;**140**:550-3;2010

[251] Tam C., Idone V., Devlin C., Fernandes M.C., Flannery A., He X. et al. Exocytosis of acid sphingomyelinase by wounded cells promotes endocytosis and plasma membrane repair. *The Journal of Cell Biology* ;2010

[252] Brach T., Specht T., Kaksonen M. Reassessment of the role of plasma membrane domains in the regulation of vesicular traffic in yeast. *J Cell Sci* ;**124**:328-37;2011

[253] Wang Q., Chang A. Sphingoid base synthesis is required for oligomerization and cell surface stability of the yeast plasma membrane ATPase Pma1. *Proc Natl Acad Sci U S A* ;**99**:12853-8;2002

[254] Olivera-Couto A., Graña M., Harispe L., Aguilar P.S. The eisosome core is composed of BAR domain proteins. *Mol Biol Cell* ;**22**:2360-72;2011

[255] Suetsugu S., Toyooka K., Senju Y. Subcellular membrane curvature mediated by the BAR domain superfamily proteins. *Sem Cell Dev Biol* ;**21**:340-9;2009

[256] Deng X., Yin X., Allan R., Lu D., Maurer C., Haimovitz-Friedman A. et al. Ceramide biogenesis is required for radiation-induced apoptosis in the germ line of C. elegans. *Science* ;**322**:110-5;2010

[257] Breslow D.K., Weissman J.S. Membranes in Balance: Mechanisms of Sphingolipid Homeostasis. *Mol Cell* ;**40**:267-79;2010

[258] Cowart L., Hannum Y. Selective substrate supply in the regulation of yeast de novo sphingolipid synthesis. *J Biol Chem* ;**282**:12330-40;2007

[259] Zou Z., Tong F., Færgeman N.J., Børsting C., Black P.N., DiRusso C.C. Fat1p And fatty acyl-CoA synthetase are interacting components of a fatty acid import complex. *J Biol Chem* ;**278**:16414-22;2003

[260] Oliveira-Marques V., Marinho H.S., Cyrne L., Antunes F. Role of hydrogen peroxide in NF-kappaB activation: from inducer to modulator. *Antioxid Redox Signal* ;**11**:2223-43;2009

[261] Quinn J., Findlay V.J., Dawson K., Millar J.B., Jones N., Morgan B.A. et al. Distinct regulatory proteins control the graded transcriptional response to increasing H(2)O(2) levels in fission yeast *Schizosaccharomyces pombe*. *Mol Biol Cell* ;**13**:805-16;2002

[262] Sergent O., Pereira M., Belhomme C., Chevanne M., Huc L., Lagadic-Gossman D. Role for membrane fluidity in ethanol-induced oxidative stress of primary rat hepatocytes. *J Pharmacol Exp Ther* ;**313**:104-11;2005